

MASTER THESIS

Term paper submitted in partial fulfillment of the requirements for the degree of Master of Science in Engineering at the University of Applied Sciences Technikum Wien - Degree Program Tissue Engineering and Regenerative Medicine

Zinc and Calcium define ATP levels and innate immune readiness in human blood

By: Mark-Josef Elevado, BSc
Student Number: 2010692043

Supervisor 1: Mag. Dr. Heidemarie Fuchs-Eitel
Supervisor 2: Prof. Wolfgang G. Junger, Ph.D
Cologne, 7 December 2022

Declaration of Authenticity

“As author and creator of this work to hand, I confirm with my signature knowledge of the relevant copyright regulations governed by higher education acts (see Urheberrechtsgesetz/ Austrian copyright law as amended as well as the Statute on Studies Act Provisions / Examination Regulations of the UAS Technikum Wien as amended).

I hereby declare that I completed the present work independently and that any ideas, whether written by others or by myself, have been fully sourced and referenced. I am aware of any consequences I may face on the part of the degree program director if there should be evidence of missing autonomy and independence or evidence of any intent to fraudulently achieve a pass mark for this work (see Statute on Studies Act Provisions / Examination Regulations of the UAS Technikum Wien as amended).

I further declare that up to this date I have not published the work to hand nor have I presented it to another examination board in the same or similar form. I affirm that the version submitted matches the version in the upload tool.”

Cologne, 12-07-2022

Place, Date

Signature

Kurzfassung

Die Anregung praktisch aller Säugetierzelltypen führt zur Freisetzung von Adenosin-5'-triphosphat (ATP). Seit Geoffrey Burnstock in den späten 1970er Jahren den Begriff purinergen Signaltransduktion (Purinergic Signaling) vorschlug, wurde die Aufmerksamkeit auf ATP als extrazelluläres Signalmolekül gelenkt, das mit autokrinen Feedback Mechanismen einhergeht, die Immunreaktionen und andere physiologische Funktionen regulieren. Neuere Studien zeigen, dass eine übermäßige ATP-Anreicherung im Blut zu einer unangemessen hohen Aktivierung von Neutrophilen führt, die wiederum Organschäden und Lungenkomplikationen verursachen, indem sie lebenswichtiges Gewebe des Körpers bei infizierten Patienten zerstören. Der Mechanismus, durch den sich ATP im menschlichen Blut anreichert, ist jedoch noch unbekannt. Unsere Studie untersucht die zellulären und molekularen Mechanismen, die den extrazellulären ATP-Level regulieren, und wie diese Mechanismen zu Entzündungen und Gewebeschäden bei schwerkranken Patienten beitragen. ATP wurde dem Blut von Menschen oder Mäusen zugesetzt. HPLC misst den ATP-Rest und seine Abbauprodukte in verschiedenen Blutbestandteilen, wo hingegen Durchflusszytometrie analysiert die neutrophilen Funktionen. Wir fanden heraus, dass ATPase extrazelluläres ATP zu seinen Abbauprodukten Adenosin-5'-diphosphat (ADP), Adenosin-5'-monophosphat (AMP), Adenosin (ADO) und desaminierten Produkten abbaut. Außerdem trägt das Plasma mehr zum ATP-Abbau bei als die Blutzellen. Wir haben die Beteiligung von löslichem und zellgebundenem CD39 und löslichem ENPP1 als Regulator für den ATP-Level und von löslichem und zellgebundenem CD73 für den AMP-Level festgestellt. Coenzyme sind wichtig für die Ektonukleotidase und entscheidend für den ATP-Abbau. Umgekehrt stellten physiologisches Ca^{2+} und Mg^{2+} die ATP-Abbauaktivität in mit EDTA behandelte menschliche Blutzellen teilweise wieder her. Für die teilweise Wiederherstellung des ATP-Abbaus im Plasma, war jedoch zusätzlich Zn^{2+} erforderlich. In Bezug auf den klinischen Aspekt konnten wir zeigen, dass Sepsis die Ektonukleotidase Aktivität in menschlichem und Mausplasma beeinträchtigt. Zn^{2+} in Kombination mit physiologischem Ca^{2+} und Mg^{2+} stellt den ATP-Abbau im Plasma von Menschen und Mäusen *in vitro* teilweise wieder her. Zusammenfassend lässt sich sagen, dass unsere Ergebnisse die Suche nach neuen therapeutischen Strategien zur Verhinderung von Immundysfunktionen bei Patienten mit viralen und bakteriellen Infektionen unterstützen können.

Schlagwörter: ATP, purinerge Signaltransduktion, Coenzyme, Sepsis, Neutrophile

Abstract

Stimulation of virtually all mammalian cell types induce the release of adenosine 5'-triphosphate (ATP). Since the proposal of purinergic signaling by Geoffrey Burnstock in the late 1970s, attention was drawn on ATP as extracellular signaling molecule, concomitant with autocrine feedback mechanisms regulating immune responses and other physiological functions. Recent studies show that excessive ATP accumulation in blood leads to inappropriate activation of neutrophils that further cause organ damage and pulmonary complications by destroying vital tissues of the body seen in infected patients. However, the mechanism by which ATP excessively yield in human blood remains unknown. Our study examines cellular and molecular mechanisms that regulate extracellular ATP levels and how these mechanisms contribute to inflammation and tissue damage in critically ill patients. ATP was added into human or mouse blood and HPLC analysis measures ATP remain and its breakdown products in distinct blood compartments and flow cytometry neutrophil functions. We found that ATPase catalyzes extracellular ATP to its breakdown products adenosine 5'-diphosphate (ADP), adenosine 5'- monophosphate (AMP), adenosine (ADO) and deaminated products. Moreover, plasma contributes mostly to ATP breakdown than blood cells. We identified the involvement of soluble and cell bound CD39 and soluble ENPP1 as regulator for ATP level and soluble and cell bound CD73 for AMP level. Coenzymes are crucial for ectonucleotidase to perform ATP breakdown activity. Conversely, physiological Ca^{2+} and Mg^{2+} partially restored ATP breakdown activity in human EDTA treated blood cells. However, Zn^{2+} was additionally needed for partial replenishment of ATP breakdown in plasma. Translating into clinical aspect, we could reveal that sepsis impairs ectonucleotidase activity in human and mouse plasma. Zn^{2+} , in combination with physiological Ca^{2+} and Mg^{2+} partially restores ATP breakdown of human and mouse plasma *in vitro*. In sum, our findings may support searching for novel therapeutic strategies that prevent immune dysfunction in patients with viral and bacterial infections.

Keywords: ATP, purinergic signaling, coenzymes, sepsis, neutrophils

Acknowledgements

Special thanks goes to my research supervisor and principal investigator Wolfgang Junger, Ph.D and Harvard University who provides me the opportunity to work as research assistant at his laboratory in Boston, Massachusetts, USA. Dr. Junger was really dedicated and supportive during my research project. There, I could apply my existing knowledge from previous work and UAS Technikum Vienna and learn more about being a scientist.

Also, a special thanks goes to Austrian Marshallplan Foundation that provides me scholarship covering most of my living costs in Boston. I would like to thank my co-workers Carola Ledderose, Eleftheria Valsami and Alix Han for technical support during my research project. Overall, it was a pleasure working at Harvard Medical School, Beth Israel Deaconess Medical Center and living in an amazing city like Boston, Massachusetts.

Kurzfassung	1
Abstract.....	1
Acknowledgements.....	2
1 Introduction.....	7
1.1 Purinergic signaling.....	7
1.1.1 History of purinergic signaling.....	7
1.1.2 Intracellular roles of ATP	7
1.1.3 ATP as an extracellular signaling molecule	8
1.1.4 ATP release mechanism.....	9
1.1.5 Purinergic receptors	10
1.1.5.1 P1 receptor.....	11
1.1.5.2 P2X receptor	12
1.1.5.3 P2Y receptor	12
1.1.6 ATP metabolism in the extracellular space.....	13
1.1.6.1 ENTPDases (Ectonucleoside triphosphate diphosphohydrolases)	14
1.1.6.2 ENPPs (Ectonucleotide pyrophosphatase/phosphodiesterase).....	15
1.1.6.3 CD73.....	17
1.1.6.4 Alkaline phosphatase.....	18
1.1.7 Adenosine breakdown and uptake.....	18
1.2 Purinergic Regulation of neutrophil function	18
1.2.1 Neutrophil function.....	18
1.2.2 Rolling, adhesion, transmigration	19
1.2.3 Chemotaxis.....	20
1.2.4 Phagocytosis	21
1.2.5 Oxidative burst	21
1.2.6 Degranulation	22
1.2.7 NET and NETosis.....	22
1.2.8 Elimination of activated neutrophils.....	22
1.2.9 Regulation of neutrophils	23
1.3 Change in extracellular ATP and adenosine levels under pathological conditions	23
1.3.1 Cancer.....	23
1.3.2 Inflammation and sepsis	24
1.4 Aim of the study	25
2 Materials and Methods.....	26
2.1 Human Subjects	26
2.2 ATP breakdown in human blood.....	26
2.2.1 Time course of ATP breakdown in human whole blood.....	26
2.2.2 Time course of ATP breakdown in human blood cells (washed).....	26
2.2.3 Time course of ATP breakdown in human plasma	27
2.2.4 ATP breakdown to study inhibitors.....	27
2.2.5 Effect of Zn ²⁺ in ATP breakdown	27
2.2.5.1 EDTA blood cells and plasma	27
2.2.5.2 sepsis patients	28
2.3 Mouse model.....	28
2.3.1 Mice	28
2.3.2 Ethical Statement.....	28

2.3.3	Sepsis model	28
2.3.3.1	Preparation of Cecal Slurry (CS).....	28
2.3.3.2	Sepsis induction and monitoring	29
2.3.4	ATP breakdown in mice	30
2.3.4.1	Cardiac puncture and blood sampling.....	30
2.3.4.2	Time dependent ATP breakdown in mice whole blood.....	30
2.3.4.3	Time dependent ATP breakdown in mice plasma	30
2.3.4.4	Inhibitor in whole blood and plasma	30
2.3.4.5	Effect of Zn ²⁺ in mouse plasma	30
2.4	High Performance Liquid Chromatography (HPLC)	31
2.4.1	Buffer preparation	31
2.4.2	Sample preparation (regular ATP)	31
2.4.2.1	Protein precipitation	31
2.4.2.2	Ethno-derivatization	31
2.4.2.3	Solid-phase extraction (SPE)	32
2.4.3	Sample preparation (ϵ -ATP).....	32
2.4.3.1	Ethno-derivatization of AMPCP.....	32
2.4.3.2	Protein precipitation	33
2.4.3.3	Solid-phase extraction (SPE)	33
2.4.4	HPLC analysis.....	33
2.5	Flow cytometry	34
2.5.1	Polymorphonuclear neutrophils (PMN) activation.....	34
2.5.2	Flow cytometry and analysis	34
2.6	Statistical Analysis.....	34
3	Results.....	35
3.1	Extracellular ATP in human whole blood	35
3.1.1	Extracellular ATP is rapidly broken down in whole blood, but cells also release ATP	35
3.1.2	ATP is rapidly hydrolyzed in human plasma	36
3.1.3	Ethno-ATP (ϵ -ATP) can be used to distinguish between ATP breakdown and ATP release in human blood.....	37
3.1.4	Plasma contributes more to ATP hydrolysis than cells in human blood	40
3.2	Enzymes involved in ATP breakdown in human blood.....	41
3.2.1	CD39 contributes to ATP breakdown in human blood	41
3.2.2	Soluble ENPP1 in plasma contributes to ATP breakdown in human blood	45
3.2.3	CD73 and other mechanisms regulate AMP levels in human blood	48
3.3	The role of co-enzymes in ATP breakdown in human blood.....	51
3.3.1	Ca ²⁺ and other metal-ions are crucial for ATP hydrolysis.....	51
3.3.2	Calcium cannot restore ATP breakdown in EDTA-treated human plasma but in blood cells	54
3.3.3	Zinc can partially restore ATP breakdown in human plasma	57
3.3.4	Zinc induces minor changes in ATP breakdown in blood cells	58
3.4	Mice vs Human blood	59
3.4.1	ATP breakdown in mouse blood, but not plasma is more rapid than in human blood	59
3.4.2	ATPase and CD73 inhibitors cause ATP accumulation and ADO decrease in mouse plasma	62
3.5	Clinical relevance of ATP breakdown	64
3.5.1	Patient demographics.....	64
3.5.2	Sepsis impair ATP breakdown in human plasma	65
3.5.3	Zinc can partially restore ATP breakdown in sepsis patient.....	66

3.5.4	Sepsis impairs ATP hydrolysis in mouse plasma.....	68
3.5.5	Extracellular ATP and CD39 cause elevated PMN activation.....	71
4	<i>Discussion</i>	73
5	<i>Conclusion</i>	78
	<i>Bibliography</i>	79
	<i>List of Figures</i>	87
	<i>List of Tables</i>	89
	<i>List of Abbreviations</i>	90
	<i>A: HPLC chromatogram (example)</i>	93
	<i>B: Flow cytometry (unstimulated vs fMLP)</i>	95
	<i>C: Flow cytometry (raw data)</i>	97

1 Introduction

1.1 Purinergic signaling

1.1.1 History of purinergic signaling

For almost four decades, the role of purine and pyrimidines as chemical transmitters has been observed and discovered. In the late 1920s, Albert Szent-Györgyi and Alan Drury showed the perturbation of cardiac rhythm in guinea-pigs upon intravenous injection of extracted adenine [1]. In another study, Pamela Holton reported adenosine 5'-triphosphate (ATP) release upon antidromic stimulation of sensory nerves in the rabbit [2].

Nevertheless, the importance of ATP as a signaling molecule in the extracellular milieu was first described by Geoffrey Burnstock in the early 1970s. Burnstock found out that smooth muscles of guineapig continued to transmit single pulses and were able to relax even when stimulated in the presence of atropine and bretylium, inhibitors of the classical neurotransmitter acetylcholine and noradrenaline, respectively. Based on this finding and his subsequent studies, he proposed a so-called 'purinergic' neurotransmission hypothesis rendering ATP as the non-adrenergic, non-cholinergic (NANC) neurotransmitter [3]–[5]. Moreover, Burnstock suggested a concept for differentiating two types of purinoreceptors, one that recognizes adenosine (P1 receptor) and is antagonized by methylxanthines, and a second one that recognizes ATP/ADP (P2 receptor) [6]. This established theory was met with doubt among scientists until receptors for purine and pyrimidines were characterized and identified in the early 1990s [7]. Since then, the number of published papers has been increased exponentially [3].

1.1.2 Intracellular roles of ATP

ATP, an organic compound structurally consisting of the purine base adenine, ribose sugar and three consecutive phosphate groups, refers as the main energy currency of all living organisms (Figure 1) [8], [9]. Compared to plants, animals are dependent on mitochondria as "powerhouse" of cell driving ATP production. A healthy adult generates daily 50 kg (110 lbs) ATP which is in a great extent [10], [11].

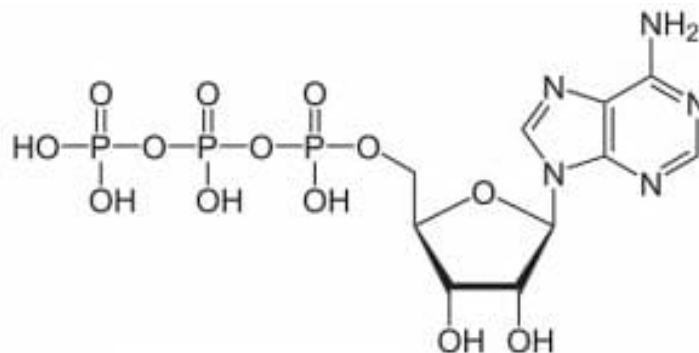


Figure 1: **Structure of Adenosine 5'-Triphosphate.** An adenine ring (nitrogenous base), ribose sugar and three phosphate groups constitute ATP structure. Taken from [12].

Hydrolysis of ATP generates adenosine 5'-diphosphate (ADP) and inorganic phosphate (p_i) resulting in free energy. Cells require this free energy to drive energy-consuming process, including membrane transport, muscle transport, mechanical movement. ATP is also essential as building block of nucleic acids and other biomolecules (e.g. nicotinamide adenine dinucleotide + hydrogen, NADH) [11], [13]–[15].

Glucose is the major “metabolic fuel” for ATP production delivered by carbohydrates, lipids, or proteins [15]. Mammals requires both glycolysis and oxidative phosphorylation process for ATP synthesis that perform under aerobe and anaerobe conditions, respectively. Under oxygen-independent conditions in cytoplasm, glycolysis involves the catalysis of glucose to pyruvate [16], [17]. The latter enters the mitochondria and is further processed to acetyl coenzyme A (acetyl-CoA) that is involved into tricarboxylic acid (TCA) cycle for generating NADH. NADH, in combination with oxygen (O_2) is required to perform oxidative phosphorylation and F_1F_0 ATP synthase catalyze ADP and p_i into large amount of ATP [10], [15], [18].

1.1.3 ATP as an extracellular signaling molecule

ATP has emerged as an essential molecule in the intracellular milieu driving energy-required processes, but it acts also as a powerful extracellular signaling molecule once released into the extracellular space [9]. Purinergic signaling is a form of extracellular signaling, arbitrated by ATP and other purine nucleotides and nucleosides, such as its breakdown products ADP and adenosine [19]. It involves the activation of purinergic receptors, thereby exerting cellular functions, including proliferation, differentiation, death and motility in development, regeneration and wound healing [19]–[21]. This mechanism can act through autocrine signaling to regulate certain downstream signaling processes within the same cell. Purinergic signaling can also be performed in a paracrine fashion to appear as a danger signal to immune cells, such as neutrophils (Figure 2) [22], [23].

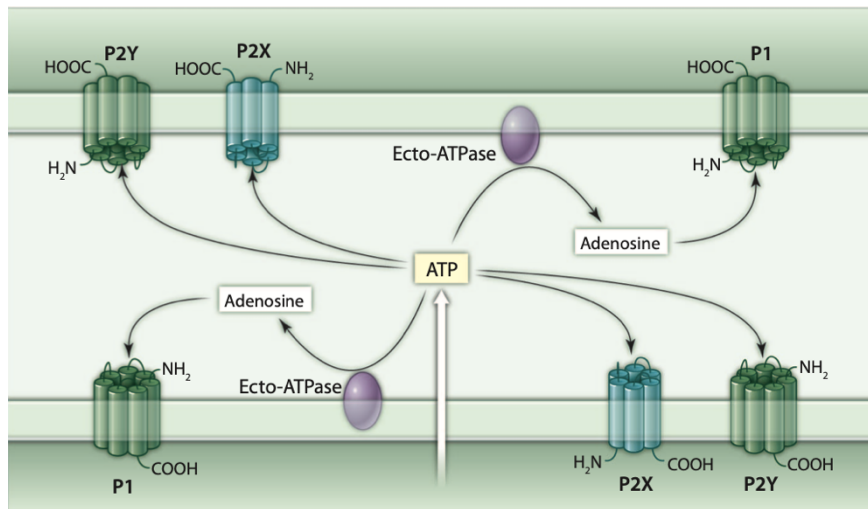


Figure 2: ATP release from cells appears as autocrine or paracrine messenger. Cellular lysis, cell damage or inflammatory stimuli induces the release of ATP and stimulates purinergic receptor (P2X, P2Y receptor) to stimulate further downstream signals. Taken from [23].

1.1.4 ATP release mechanism

As it was revealed and proven that ATP act as a co-transmitter in neuronal synapses, scientific interest has been exponentially gained in neurotransmission and neuromodulation associated with purinergic signaling [3]. Meanwhile, it is also crucial in virtually all other fields, including cardiovascular or immune system [24]–[26].

In general, ATP release can be performed in a passive, non-specific or active form. Moreover, the latter can be further divided in vesicular and conductive mechanism [27]. Vesicular ATP release occurs in specialized exocytic vesicles served as storage for ATP. Vesicular nucleotide transporter (VNUT) is the secondary active transporter ensuring the influx and accumulation of ATP into the specialized cytosolic granules in a chloride-dependent fashion. Driving force is mediated by V-ATPase. Stimulation of nerve or secretory cells induce the release of ATP via merging with the plasma membrane [28]–[30]. Harada *et al.* [31] propose VNUT as mediator for driving additionally ATP release in neutrophils.

However, many immune cell types select the conductive pathway via plasma membrane channels [25], [27]. Multiple types of membranes have been reported that perform the active release of ATP into the extracellular space, including trimeric ion-gated channel P2X7 receptors, connexin (C_x) and pannexin (PANX) hemichannels, calcium homeostasis modulator-1 (CALHM1), volume-regulated anion channel (VRAC), and maxi-anion channel (MAC) [20], [29]. ATP release through CALHM1, a pore-forming Ca²⁺ - semipermeable channel, was reported to play a crucial role in taste receptor cells in buds to perceive bitter, sweet and umami [29], [32], [33]. VRAC regulates the volume decrease by efflux of Cl⁻ and various organic osmolytes, mainly during cell proliferation and migration [34]. MACs are large conductance anion channels that are dependent on voltage and are activated upon certain

stimuli, such as osmotic cell swelling, salt stress, high glucose level, hypoxia or excision of a patch membrane [29], [35], [36]. Hemichannels are plasma membrane channels with a hexameric structure and high conductance that release molecules, such as ATP, prostaglandins, or glutamate [37], [38]. Connexins and pannexin form gap junctions bridging a gap between cells. Connexin serve as a communication basis on the intracellular level whereas pannexin primarily concentrate in performing intracellular molecules to the extracellular space [39]. The pannexin family entails 3 members (PANX1-3); the connexin family 21 subtypes. Human neutrophils release ATP through PANX1 in response to formyl-peptide-receptors (FPRs), $Fc\gamma$, interleukin (IL)-8, complement C5a and LBT_4 [20], [40].

For many years, it was believed that trigger of purinoreceptors by ATP was derived from dying, damaged or stressed cells [3]. In addition to proteolytic enzymes, necrotic cells secrete, large amount of ATP into surrounding tissues [30]. Moreover, extreme conditions such as trauma, ischemia or infection elicit large amount of ATP from the storage [8], [41]. It is more likely that this role attracts monocytes and neutrophils as "find-me signal" to ease their navigation through the chemotactic gradient to the inflammatory site. Once arrived at their "destination", they promote proinflammatory function to damaged and apoptotic cells in response to damage-associated molecular pattern (DAMP) leading to their death [42]. ATP release has been shown to play additionally a crucial role in assembling inflammasomes, such as caspase-1 activated cryopyrin, also known as NLRP3 inflammasome. The latter release ATP through PANX1 that further involves further P2X7 receptor as proinflammatory purinergic receptor. NLRP3-mediated inflammasomes modulate the release of IL-1b and its corresponding cytokines [43], [44]. However, the mechanism by which NLRP3 drives P2X7 activation, remains unknown and needs to be further elucidated [20].

Meanwhile, knowledge has been enlarged and many mammalian intact cells, including endothelial cells, urothelial cells, astrocytes, monocytes, osteoblasts release ATP under physiological conditions [3], [45]. Gentle disruption in mechanical and chemical stimulations, e.g., shrinking, or even washing, and splitting the cells, or biological cues such as hypoxia or osmotic swelling facilitate ATP release [23]. These mechanisms of ATP release can change cell physiology or regulate immune functions, in particular chemotaxis of neutrophils and monocytes [25].

1.1.5 Purinergic receptors

Five years after Burnstock had coined the term purinergic signaling, he also suggested a basis to differentiate 2 purinergic receptors families into P1 and P2 receptor recognizing adenosine and nucleotides like ATP or ADP, respectively and appearing as crucial short-term co-transmitter in both central and peripheral nervous system [6]. To date, 19 subtypes are well-known and have been characterized which can be subdivided into 3 main classes: P1, P2X and P2Y receptor (Table 1). P2 receptor has been divided into P2X and P2Y receptor because of different receptor types [41], [46]. Purinergic receptors, mediated by purines and pyrimidines

regulate many physiological functions, in particular cell growth, differentiation, and death and also a regulator of release of hormones, neurotransmitter and cytokines. Immune cells express all three purinergic receptor classes that influence their immune functions such as migration, secretion, phagocytosis and chemotaxis [19].

Table 1: **Overview purinergic receptor subtypes.** 19 subfamilies of purinergic receptor have been characterized that are further divided into P1, P2X and P2Y receptor. ND = not detected. Information gathered from [25].

Purinergic receptor isoforms	Ligands	Downstream signaling events	Expression in neutrophils
P2X receptor			
P2X1	ATP	Ca ²⁺ and Na ²⁺ influx	+
P2X2	ATP	Ca ²⁺ influx	ND
P2X3	ATP	Cation influx	ND
P2X4	ATP	Ca ²⁺ influx	+
P2X5	ATP	Ion influx	+
P2X6	ATP	Ion influx	ND
P2X7	ATP	Cation influx and pore formation	+
P2Y receptor			
P2Y1	ADP	PLC β activation	+
P2Y2	ATP, UTO	PLC β activation, cAMP inhibition	+
P2Y4	UTP (ATP, UDP)	PLC β activation, cAMP inhibition	ND
P2Y6	UDP, UTP	PLC β activation	+
P2Y11	ATP	cAMP production, PLC β activation	ND
P2Y12	ADP	cAMP inhibition	+
P2Y13	ADP, ATP	cAMP inhibition	+
P2Y14	UDP-glucose	PLC β activation	+
P1 receptor			
A1	Adenosine	cAMP inhibition	+
A2a	Adenosine	cAMP production	+
A2b	Adenosine	cAMP production	+
A3	adenosine	cAMP inhibition	+

1.1.5.1 P1 receptor

P1 receptors, also known as adenosine receptors, are G protein-coupled receptors (GPCR) recognizing adenosine as endogenous ligand. Since the early 1990s, four different subtypes of P1 receptors have been identified, namely adenosine A1, A2a, A2b, and A3 receptors [47]. All four subtypes that modulate mitogen-activated protein kinases (MAPK) pathways, including extracellular signal-regulated kinase 1 and 2 (ERK1 and 2) and p38 MAPK. A1 and A3 receptors are coupled to G_q and G_o family of G_i G-proteins whereas A2a and A2b receptors couple to G_s protein, thereby exerting an inhibitory or stimulatory effect on adenylyl cyclase (AC) activity and cyclic AMP (cAMP) production, respectively. Moreover, the release of intracellular Ca²⁺ can be elicited upon A1 and A3 receptor activation [46], [48], [49].

1.1.5.2 P2X receptor

Ionotropic P2X receptors are ATP-gated trimeric ion channels, mainly activated by ATP as exogenous ligand [50]. Seven subtypes of P2X receptors have been cloned and characterized, P2X1-7, so far. These seven subtypes differ in terms of their gating features, pharmacology and cellular distribution that gives members of P2X receptor family a unique appearance [51]. P2X receptors are mainly expressed in the nervous system with P2X2, P2X4 and P2X6 as the most abundant ones [53], [54]. P2X7 has been known as a channel to allow release of certain molecules, e.g. ATP [29].

P2X receptors compose of six transmembrane helices and small extracellular domain bearing three ATP-binding binding portions [54]. On the molecular level, P2X receptors share joint topology with intracellular NH₂, elongated COOH terminus and transmembrane (TM) 1 and TM 2 as hydrophobic, putative membrane-spanning regions. TM1 is required for channel gating whereas TM 2 for channel pore formation [41], [55]. Binding of ATP to these portions favors channel opening that renders extracellular cations such as Ca²⁺, Na⁺ and K⁺ entering semi permeably into the cell leading to membrane depolarization. Recent studies propose that Ca²⁺ activates further signaling cascades, such as p38 MAPK or phospholipase A2 activation [8].

1.1.5.3 P2Y receptor

Metabotropic P2Y receptors are GPCRs that belong to δ -branch of class A [41]. Till now, 8 distinct subunits have been identified: P2Y1, 2, 4, 6, 11- 14 [56], [57]. Other P2Y subunits (P2Y3, 5, 7-10) are found in non-mammalian orthologs or do not respond to pyrimidines or purines. Depending on the subunit, P2Y receptors are mainly activated by mononucleotides such as ADP, ATP, UTP, UDP, by dinucleotides or nucleotide sugars [41], [46], [57]. By contrast, P2Y1,12 and 13 prefer ADP as agonist for the activation [8]. Three extracellular carboxy termini and three intracellular amino termini, linked to seven transmembrane spanning-motifs constitute the structure of P2Y receptor [44], [49]. P2Y receptors are widely expressed in many systems, including cardiovascular, musculoskeletal system and also regulate many functions, such as immune, pulmonary, or endocrine/exocrine function [56].

Several studies propose the above-mentioned P2Y receptors subunits to subdivide into 2 main groups due to their phylogenetic and sequence divergence and corresponding coupling to G proteins. The first group, P2Y 1/2/4/6/11, referred to as G_q-coupled P2Y1 receptor-like, exhibit a sequence homology of 35-52% in amino acid composition and a Y- Q/K-X-X-R defining motif in the transmembrane α -helix 7. By contrast, the other group, P2Y12-14, defined as G_i-coupled P2Y12 receptor-like) entails a sequence homology of 47-48% and the presence of K-E-X-X-L motif in transmembrane α -helix 7 [8]. G_q-coupled P2Y11 receptor-like tend to couple to G_q/G₁ mediating phospholipase C signaling pathway and Ca²⁺ influx. G_i-coupled P2Y12 receptor-like couple to G_i/0 proteins that decrease AC and increase cAMP production[41].

1.1.6 ATP metabolism in the extracellular space

To abrogate P2 receptor desensitization and terminate signaling, extracellular ATP needs to be hydrolyzed by certain ectoenzymes so-called ectonucleotidases once released into the pericellular environment [58]. Four main groups of ectonucleotidases have been identified in mammalian cells that can be distinguished in terms of structure and substrate preferences and expression pattern, including ectonucleoside triphosphate diphosphohydrolases (ENTPD) family, the ectonucleotide pyrophosphatase/phosphodiesterase (ENPP) family, ecto-5'-nucleotidase (NT5E or CD73) or alkaline phosphatase [60], [61], [62]. Ectonucleotidases are expressed virtually in all mammalian cell types. They also mark the beginning of a rapid and repeated purinergic signaling with its associated receptors [25]. Among ENTPD families, ENTPD1, known as CD39 has been the most widely studied enzyme that catalyze step-wisely ATP to ADP and AMP, followed by CD73 that further process AMP to adenosine (Figure 3) [13], [63], [64].

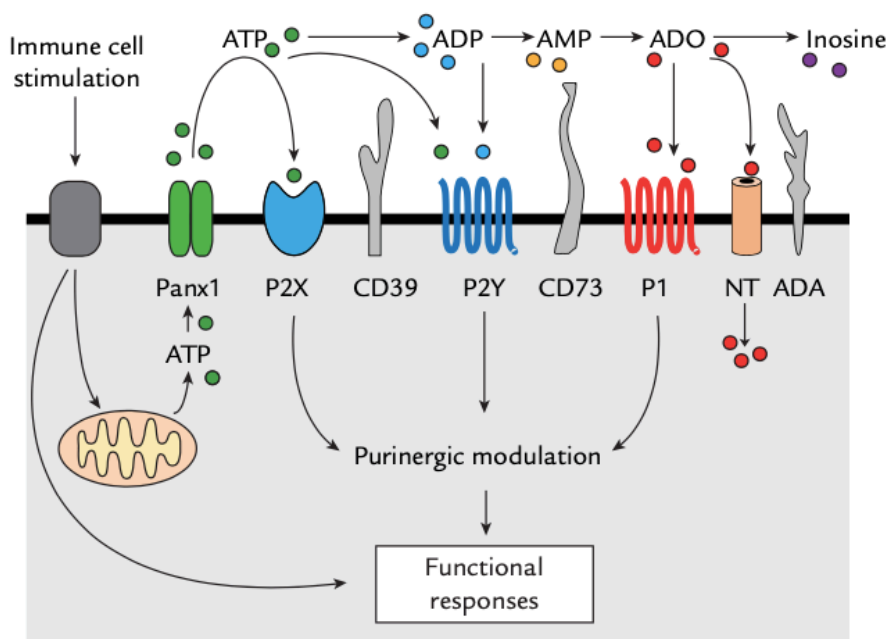


Figure 3: **Purinergic signaling system in immune cells.** In response to certain stimuli, pericellular ATP is released from mitochondria via pannexin1 (PANX) channel. Once released in the extracellular space, ATP triggers the stimulation of P2X or P2Y receptor. Ectoenzymes such as CD39 catalyze ATP step-wisely to ADP, then to AMP. CD73 degrades AMP to adenosine that activates P1 receptor. Adenosine deaminase (ADA) convert adenosine to inosine or adenosine can be removed via cellular uptake through nucleoside transporter (NT). Image taken from [20].

Recent studies have pointed out that the traditional paradigm through CD39 – CD73 is not the only pathway to inactivate ATP effluxed in the extracellular space. Thus, other families such as ENPP and alkaline phosphatase also participate in breaking also down extracellular ATP, following the “non-canonical” ectoenzymatic pathway [9]. In particular, ENPP1 or ENPP3 hydrolyze ATP directly to AMP and p_i and adenosine is generated by CD73 [64]. This ENPP-

CD73 axis is considered as an alternative pathway to CD39 by-passing the production of ADP in the vascular system and other tissues [9]. Another family, tissue non-specific alkaline phosphatases (TNAP), anchored to the plasma membrane via glycosylphosphatidylinositol (GPI), hydrolyze not only ATP, but also diphosphates, monophosphates, polyphosphates and other phosphate- compounds [65]. Regardless of which ectonucleotidase breaks down ATP, the balance between ATP and adenosine must be sustained. Therefore, ATP and adenosine appear as opposing signaling molecules modulating pro-inflammatory or immunosuppressive functions, respectively. Distortion of homeostasis might cause local and system inflammation on tissue that influence on the regulation of immune cells [20], [41].

1.1.6.1 ENTPDases (Ectonucleoside triphosphate diphosphohydrolases)

The family of ectonucleoside triphosphate diphosphohydrolases (ENTPD) comprise of seven different isoforms, ENTPD1-6 and ENTPD 8 in mammals [20], [63]. Among the ENTPD family, ENTPD 1-3 and 8 are cell-bound transmembrane proteins and ENTPD 4-6 has been found intracellular, but ENTPD 5-6 has been reported as soluble form [65], [66]. ENTPD1-3 and 8 utilize ATP and other nucleotide phosphates as substrates. Only ENTPD 1,2,3 and 8 are expressed on the cell surface and hydrolyze ATP and other nucleoside tri- and diphosphates as substrate in a Mg^{2+} and Ca^{2+} dependent fashion [48], [59], [66]. ENTPD1, also known as CD39 has been the most widely studied ectoenzyme and preferably utilize ATP as substrate (substrate affinity, $K_m = 10-200 \mu M$) [65]. CD39 catalyzes the conversion of ATP to ADP and subsequently to AMP [20], [61], [62]. Structurally, two transmembrane domains with N- and C-terminal domain, a large extracellular hydrophobic domain constitutes CD39 as transmembrane protein (Figure 4). Moreover, CD39 entails 510 amino acid (aa) protein with seven N-linked glycosylation sites, 11 Cysteine residues and two TM regions [67].

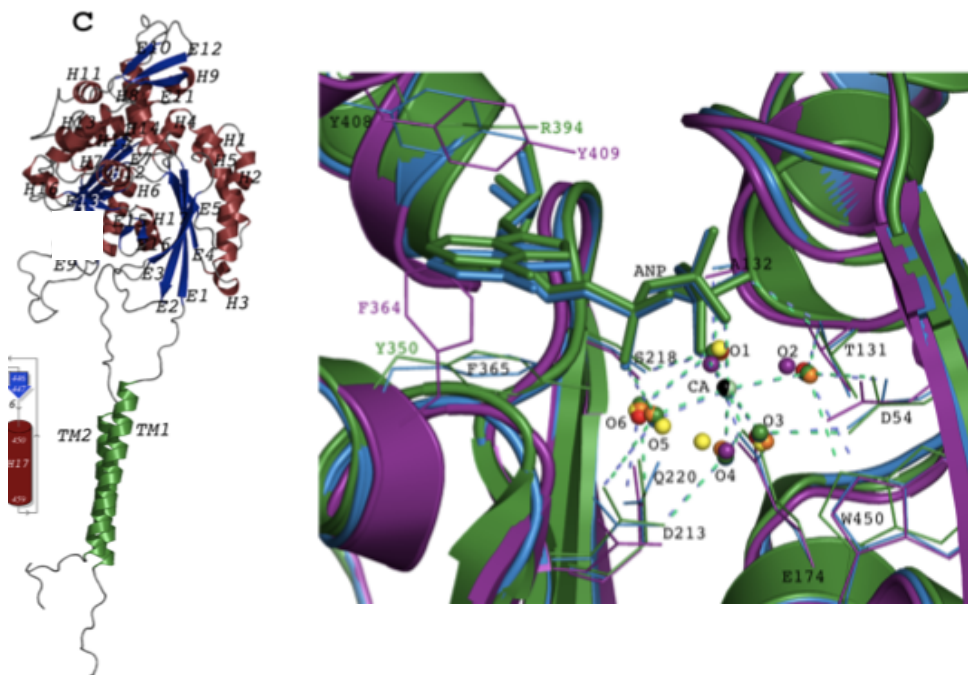


Figure 4: (A) 3D model of CD39: Two transmembrane domain (TMD) and extracellular domain constitute the CD39 as protein. (B) Structural arrangement of CD39 model and templates in the active site region. The ligand (ANP), catalytic residues (black), conserved waters (O1, O2, O3, O4, O5 and O6) and the calcium ion from structures (black) are illustrated. Image taken from [68]

CD39 is expressed abundantly in many cell types such as vascular endothelial, smooth muscle cells, immune cells, and other hematopoietic cells. In immune cells, CD39 is present in B lymphocytes and monocytes/macrophages but is also found in T lymphocytes (20-30% CD4 effector and regulatory cells, 2-5% natural killer (NK) cells and less than 5% in CD8) [62], [66], [69]. Mostly, CD39 is located as transmembrane protein on the cell surface, but recent studies have shown that this protein can also be found as soluble enzyme in the extracellular space [70].

1.1.6.2 ENPPs (Ectonucleotide pyrophosphatase/phosphodiesterase)

Another family of ecto-nucleotidase are ectonucleotide pyrophosphatase/phosphodiesterase (ENPPs). In general, ENPP family entails five isoforms, ENPP1-5; ENPP6 and 7 was added to the list in 2006. ENPP6 was identified as choline-specific PLC and ENPP7 as an alkaline sphingomyelinase [71]. More than 50 years ago, Takashi *et al.* identified ENPP1 for the first time as plasma cell-differentiation antigen (PC-1), together with ENPP2 and ENPP3 [72].

On the structural level, ENPP members have a phosphodiesterase (PDE) domain as catalytic core in common that harbors the activity of pyrophosphatase/phosphodiesterase. Based on the structure and domain constitution, isoforms are divided into two subgroups: ENPP1-3 and ENPP4-7. ENPP1-3 exhibit two tandem N-terminal somatomedin B-like domains (SMB 1 and

SMB 2), two linker region L1 and L2, catalytic domain and a C-terminal nuclease-like domain (NUC, Figure 4). ENPP1 and ENPP3 are single-pass type II membrane, whereas ENPP4,5, and 7 single-pass type I membrane. ENPP2, or autaxin (ATX) is a secreted protein and ENPP6 is anchored to the plasma membrane via GPI [71], [73].

Among ENPP members, ENPP1 has been widely studied and is a type II transmembrane glycoprotein. ENPP1 exhibit a strong affinity for ATP with a K_m value of 46 μM [74]. Besides, ATP, it utilizes UTP and other polyphosphates as substrate (Guanosine triphosphate (GTP), cytosine triphosphate (CTP) and UTP > 1 mM) [71]. ENPP1 can be found mainly on plasma membranes and endoplasmic reticulum (ER) and is expressed in many tissues, in particular on the cell surface of osteoblasts and chondrocytes. It is known for regulating calcification processes in the bone area [74]. They also play a role as a regulatory function in immune cells, such as neutrophils, macrophages, dendritic cells, natural killer cells and B lymphocytes [64]. ENPP1 hydrolyzes ATP or GTP to AMP or guanosine monophosphate (UMP) generating additionally inorganic pyrophosphate, respectively [64], [65]. It is known that hydrolysis of ATP by ENPP1 regulates calcification in bones. Also, ENPP1 has some regulatory functions in immune cells to prevent P2-receptor mediated inflammatory damage and adenosine-mediated immunosuppression. Its catalytic activity is strongly dependent on Ca^{2+} and Zn^{2+} . The PDE catalytic domain chelates two Zn^{2+} ions that is crucial for ENPP1 to catalyze pyrophosphatase/phosphodiesterase activities. The two Zn^{2+} ions are located in the active site, forming a shallow groove and are synchronized by seven highly conserved amino acids, including histidines, aspartate and catalytic nucleophile, respectively. By contrast, NUC domain that encompasses a so-called EF hand-like motif, linked with a Ca^{2+} -ion, contributes to the stability of the enzyme and acts as a “helping hand” for catalytic PDE domain to catalyze enzymatic activity (Figure 5) [71], [73].

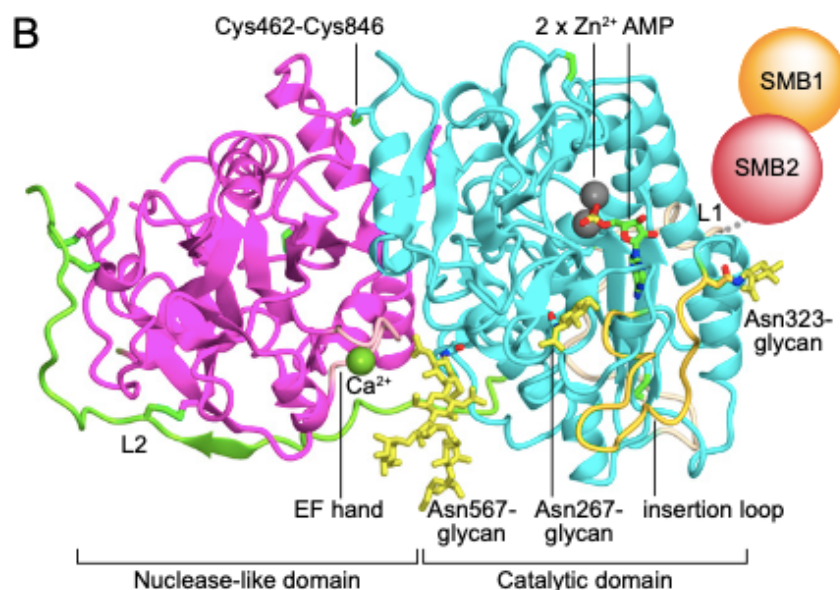


Figure 5: **Crystal structure of ENPP1**. Catalytic domain, cyan; nuclease-like domain (NUC), magenta; L1, wheat; L2, yellow- green; EF hand-like motif, pink; insertion loop, gold. AMP and N-glycans are depicted as green and yellow, respectively. The bound zinc and calcium ions are illustrated as gray and yellow-green spheres. Disulfide linkages are shown as sticks. The two somatomedin B-like (SMB) domains are indicated by circles. Image taken from [74]

1.1.6.3 CD73

Human ecto 5'-nucleotidase (NT5E), also known as CD73, is a non-covalent homodimer anchored via GPI to the plasma membrane [75], [76]. CD73 utilizes preferably AMP as substrate with K_m value of 1-50 μM . AMP is hydrolyzed to adenosine, thereby acting as a "control checkpoint" for adenosine [75]. Tumor growth is dependent from adenosine and inhibiting effect on CD73 might be considered as a potential target to cancer immunotherapy[48], [75], [77]. It has been reported that CD73 can also hydrolyze other nucleoside monophosphate and utilize NAD^+ [78].

On the structural level, CD73 comprise of two domains: N-terminal domain (residues 26-317) with a metal-binding site chelating divalent Zn^{2+} ions, and C-terminal domain (residues 337-549) harboring the substrate binding site. A-helices connects the two domains (Figure 6) [78].

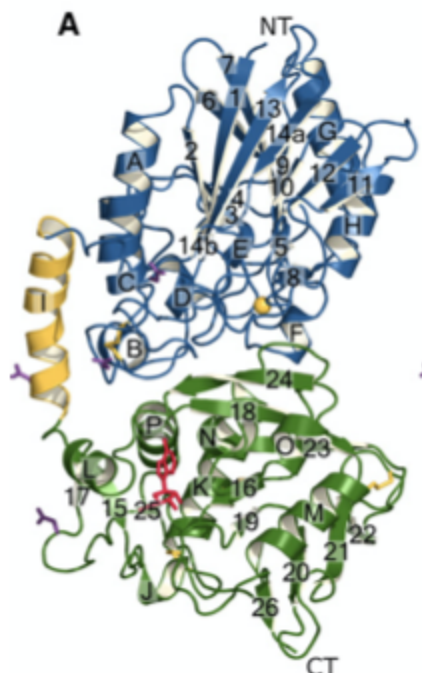


Figure 6: **Crystal structure of CD73**. The N- and C-terminal domains are shown in blue and green respectively, whereas the connecting a helix is shown in yellow. The adenosine ligand is depicted as red sticks. Zn^{2+} ion is illustrated as a yellow sphere. Disulfide bonds (yellow sticks) and N-glycosylation sites (purple sticks) are highlighted, and the N and C termini, b strands (1–26), and helices (A–P) are labeled. Images taken from [79].

1.1.6.4 Alkaline phosphatase

Alkaline phosphatase (AP) are glycoproteins anchored to the plasma membranes and are ubiquitous. As metalloenzyme, AP hydrolyses phosphate monoester at alkaline milieu. To ensure functionality, AP need three metal ions on the active site, including two Zn^{2+} and Mg^{2+} . Huizinga *et al.* could show that AP treatment contributes to inactivation of ATP and furthermore, mitigate the severity in encephalomyelitis (EAE) [80].

1.1.7 Adenosine breakdown and uptake

Extracellular adenosine appears as intermediate purine metabolite that needs to be removed to prevent inflammatory damage or adenosine-mediated immunosuppression. In a coordinated fashion, adenosine is either degraded or re-up taken by cells [9], [25]. Catabolic enzyme adenosine deaminase (ADA) degrades extracellular adenosine to inosine and hypoxanthine (Figure 3) [81]. Two isoenzymes of ADA (ADA1 and ADA2) have been found in the cytoplasm, but also on the surface of cells, including lymphocytes, dendritic cells and other lymphoid and non-lymphoid tissues [9]. By contrast, cellular re-uptake was completed through two families of nucleoside transporters (NT), namely concentrative nucleoside transporters (CNTs) or equilibrative nucleoside transporters (ENTs, Figure 3).

Three subtypes of CNT, CNT1-3 that differ in regard to their substrate selectivity execute a passive transport of adenosine into the cell with a simultaneous influx of sodium ions. Four ENTs have been identified from which ENT4 has been disregarded as conventional nucleoside transporter. Generally, ENT family members exhibit a lower ENT-to-substrate affinity than the CNT family members. They facilitate an active transport of nucleoside, in particular adenosine [82], [83]. It is believed that cellular reuptake of adenosine serves as a recycling mechanism to obtain intracellular ATP and re-start the purinergic signaling system [25].

1.2 Purinergic Regulation of neutrophil function

1.2.1 Neutrophil function

Neutrophils, also known as polymorphonuclear leukocytes (PMN), are in addition to eosinophils, basophils, and mast cells another type of granulocytes and appears as the first line of defense upon infiltration of microorganisms and fungi in the innate immune system [84]. Neutrophils are terminally differentiated and short-lived cells with a limited life span less than 24h [85], [86]. They also have two to four lobed nucleus and granular content filled in the cytoplasm (Figure 7) [87].

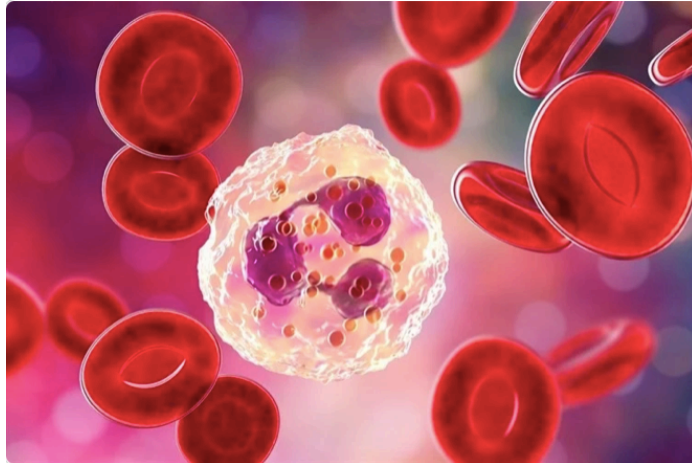


Figure 7: **Polymorphonuclear leukocytes (PMN) and red blood cells (RBC)**. Nucleus of PMN cell is multi-lobed and cytoplasm contains granules, specifically for its antimicrobial function. Image was taken from [88].

The population of neutrophils is the most abundant (50-70%) among leukocytes in the peripheral blood of humans [86], [89]. They are constantly renewed in the bone marrow with approximately 10¹¹ neutrophils daily and have their origin from pluripotent hematopoietic stem cells (HSC). Committing to the myeloid lineage, multipotent progenitor cells (MPPs) are formed from HSC which then differentiate into lymphoid-primed multipotent progenitors (LMPPs) and subsequently, to granulocyte-monocyte progenitors (GMPs). By upregulating granulocyte colony-stimulatory factor (G-CSF), GMPs give rise to myeloblasts. The latter follow maturation stages, including promyelocyte, myelocyte, metamyelocyte, band cell and mature neutrophil [84], [86].

1.2.2 Rolling, adhesion, transmigration

In response to an inflammatory event (e.g., microorganisms invading through the human skin), tissue-resident macrophages secrete cytokines, such as tumor necrosis factor (TNF- α), IL-1, 6, 8 and 12 that attract mostly neutrophils, but also other monocytes and activate endothelial cells. Neutrophils exit the circulating blood stream and are navigated to the infection site deploying some effector mechanisms. Neutrophils and endothelial cells express distinct families of adhesion molecules so that “rolling” as cellular movement of neutrophils along the endothelium is facilitated (extravasation) [86],[89].

Extravasation process can be divided in four sequential, but partially overlapping categories (Figure 8). Cytokines and exposure of LTB₄, C5a complement component and histamine triggers endothelial cells to express P-selectin, then subsequently E-selectin on the surface [86]. These selectins recognize sulfated sialyl- Lewis^x fraction on the glycoprotein of neutrophils, allowing the neutrophils to reversibly adhere on the vessel wall and “roll” along the endothelium. Neutrophil’s β -integrins such as lymphocyte function-associated antigen (LFA1) or Macrophage-1 antigen (MAC1) induce permanent adhesion, interacting with receptors on

the surface of endothelium, intercellular adhesion molecule (ICAM) 1 and 2. This is followed then by crawling through the endothelial wall and thereby infiltrating the basement membrane of endothelium. This so-called diapedesis is mediated by interactions of LFA-1 and MAC1 in neutrophils and platelet endothelial cell adhesion molecule (PECAM) or CD31 in endothelial cells [89], [90]. It has been reported that pericytes function as guide for the neutrophils crossing the subendothelial barrier [91].

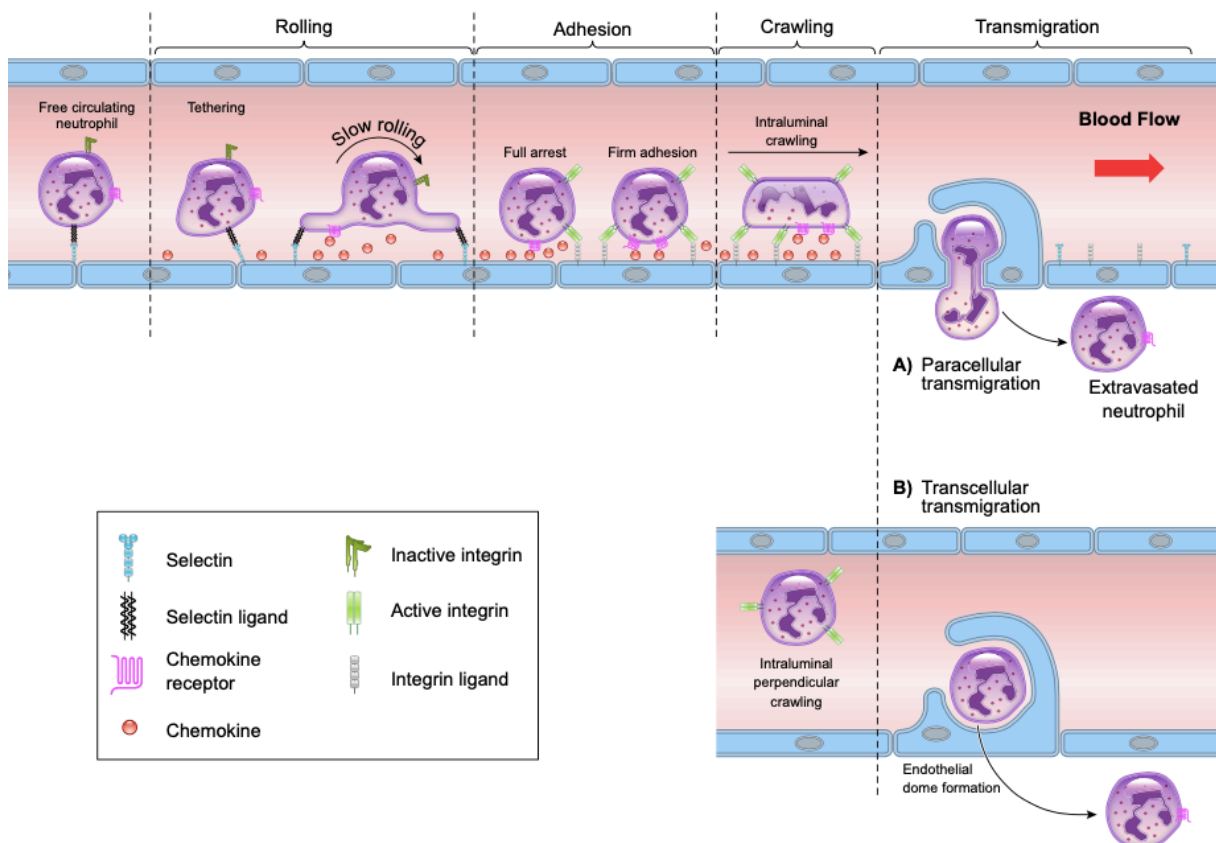


Figure 8: **Neutrophil recruitment to the infection site (extravasation)**. Steps of extravasation include attachment of neutrophils to the endothelium, rolling, permanent adhesion intraluminal crawling and transmigration (diapedesis). Rolling process is selectin dependent whereas adhesion, crawling and transmigration depends on interactions between integrin molecules. Image was taken from [87].

1.2.3 Chemotaxis

Once reaching the interstitial space, chemoattractant navigate neutrophils to the infection site and thereby exert effector mechanisms to eliminate pathogen or promote inflammatory response. This chemotaxis encompasses three sequential steps, including gradient sensing, cell polarization and directed migration (Figure 9). Gradient sensing is defined as an immune cell, in particular neutrophils sensing distinct concentrations of chemoattractant in the extracellular space. This is followed by cell polarization in which cells form an elongated shape arranged within the gradient field of chemoattractant. Finally, neutrophils migrate forwardly along the chemoattractant gradient [25]. In humans, these chemoattractant substances can be

divided into four families, including chemotactic lipids, (LTB₄, e.g.) chemokines (CXCL8), complement anaphylatoxins (C5a, e.g.), and formyl peptides (N-formyl-Met-Leu-Phe or fMLP, e.g.) [92].

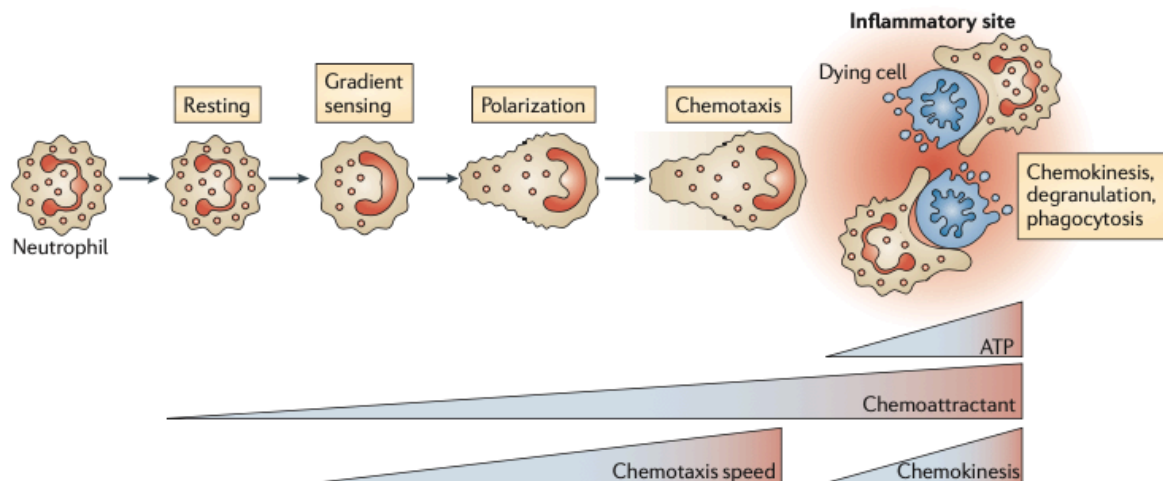


Figure 9: **Purinergic signaling mechanism regulate chemotaxis of neutrophils.** Chemoattractants like interleukin (IL)-8 drives recruitment of neutrophils to the inflammatory site (gradient sensing) and. Polarization and chemotaxis support neutrophils to reach the site where they perform antimicrobial function. Image taken from [25].

1.2.4 Phagocytosis

Phagocytosis is defined as the physical ingestion and elimination of a microbe $> 0.5 \mu\text{m}$ diameter [93], [94]. Macrophages, neutrophils, monocytes, dendritic cells are considered as those cells that displays high phagocytosis efficiency [94]. Several processes describe phagocytosis, including detection of target particle (microbial or apoptotic), activation of internalization and formation and maturation of phagosome. Recognition and binding to pathogen-associated molecular pattern (PAMP) can be performed directly by Pattern recognition receptors (PRRs) such as Dectin-1, Mincle, macrophage C-type lectin (MCL) or CD14 or indirectly, such as Fc γ receptors with opsonic features [86]. Interacting of receptor with microbe particles results in alteration of membrane remodeling and the actin cytoskeleton. This leads to the generation of pseudopods that internalize microbes in large membrane-enclosed endocytic vesicle, called phagosome (endocytosis). Once internalized, lysosomal content merge with phagosome membrane and the resulting phagolysosome induces ingested particle degradation [94], [95].

1.2.5 Oxidative burst

Simulation of PMNs modulate intracellular signaling pathways, which among of them are the rapid release of reactive oxygen species (ROS). This so-called oxidative burst, also known as

respiratory burst, is one of the important hallmarks in neutrophil function. It is considered as the “weapon” to eliminate microbial invaders at the infection site [96], [97]. NADPH oxidase (NOX2) is the driving force of oxidative burst, recruited by phagolysosome. Normally, NOX2 are found in quiescent and segregated state in cell compartments [98]. Stimuli of neutrophils induce the assembly of NOX2, that transfers electron (e^-) across the plasma membrane to O_2 , producing superoxide anion (O_2^-). Dismutation of superoxide anion further induce the generation of hydrogen peroxide (H_2O_2) and hydroxyl radicals ($OH\bullet$) [99]. Moreover, the release of granule-derived myeloperoxidase (MPO) catalyzes formed hydrogen peroxide H_2O_2 to hypochlorous acid, a substance effective against microbes [86]. It has been reported that impairment of ROS increases the survival in bacteria and may cause bacterial infection or sepsis [97].

1.2.6 Degranulation

Neutrophil degranulation involves the mobilization of so-called granules, packaged within intracellular vesicles. Degranulation and the resulting killing of microbe can be performed in either extracellular or intracellular milieu [100]. These granules can be divided into four main types: secretory, tertiary, secondary and primary. Tertiary granules (e.g., cathepsin, gelatinase) are firstly released, followed by secondary granules (e.g. lactoferrin, alkaline phosphatase, lysozyme, cathelicidin, NADPH oxidase and collagenase). Primary granules are secreted after the secondary granules that encompasses proinflammatory and antimicrobial functions, such as elastase, MPO, cathepsin G. To prevent tissue harm, primary and secondary granules are secreted into the phagosome in neutrophils [101].

1.2.7 NET and NETosis

Neutrophil extracellular traps (NETs) display another crucial strategy from neutrophils to immobilize and combat microbial pathogens and firstly described by Takei *et al.* [102], [103]. Neutrophils extrude forming web-like structures that entail DNA-histone complex. This scaffold, (15-17 nm diameter) surrounded by granule-derived peptide and enzymes such as elastase, cathepsin G and MPO, exhibit sticky properties that catch and kill pathogens [103], [104]. NETs are also known as “double edge swords” of innate immune system because of its ability to induce also programmed cell death, apoptosis [103]. In contrast to the other model, neutrophils release decondensed chromatin and antimicrobial proteins to the extracellular space, thereby leads to nuclear de-lobulation, dissolving of granular membrane, releasing of nuclear content into cytoplasm and rupturing of plasma membrane and chromatin de-condensation [105], [106].

1.2.8 Elimination of activated neutrophils

These hallmarks of neutrophils function ensure the death of microbial pathogen and prevent additionally the spreading. When inflammatory event has been finished, neutrophils induce

cell death and were removed mainly from macrophages [86]. Primarily, neutrophils undergo programmed cell death, but other types such as pyroptosis, necrosis, NETosis have been reported [105], [107].

1.2.9 Regulation of neutrophils

As previously described, chemotaxis involves orienting and driving neutrophils towards the chemoattractant to reach the infection or inflammation site, associated with gradient sensing, cell polarization and directed migration [86]. Over the past years, ATP and adenosine appear as regulatory function to PMN activation, in particular oxidative burst, phagocytosis, adherence and chemotaxis [20], [25]. Recent studies have pointed out the necessity of autocrine purinergic signaling in neutrophils that drives the chemotaxis process from recognizing the chemotactic gradient, cell polarization and directed migration. Neutrophils are stimulated upon exposure to a chemoattractant substance, releasing rapidly mitochondria-derived ATP via P2X1 channel into the extracellular space. Our laboratory could show that ATP release and purinergic signaling via P2Y2 receptors drive mitochondrial ATP production in neutrophils [108]. Both receptor subgroups elicit Mammalian target of rapamycin (mTOR2) signaling and the influx of Ca^{2+} , respectively [109], [110]. These autocrine feedback mechanism enables the amplification of excitatory signals (more ATP production and release) that helps neutrophils to sense gradient and orient in a chemotactic field at the edge front [25]. CD39, ENPP1, CD73 catalyze ATP to adenosine that activates P1 receptors [9], [46], [65]. Specifically, A2a and A3 are other purinergic receptors essential in chemotaxis model of neutrophils. Accumulation of A3 receptor at leading edge cause neutrophils to enhance and control its migration speed and constitute a second mechanism of autocrine amplification [74]. Stimulation of the A2a receptors in response to ADO at the back of the cell elicits cAMP signaling in neutrophils and shuts down neutrophil functions. Together, the opposing signaling mechanisms downstream of P2Y2, A3 and A2a receptors fine-tune the complex functional responses in a chemotaxis model [20], [25], [111].

1.3 Change in extracellular ATP and adenosine levels under pathological conditions

1.3.1 Cancer

ATP and adenosine as “pull-push” mechanism are tightly regulated by the ectonucleotidase under normal, physiological conditions [20]. However, pathological conditions such as cancer alters completely regulatory mechanisms, associated with purinergic signaling [112]. Therefore, elevated ATP occurs, secreted by tumor cells [112]. Recently, attention has been gained in tumor microenvironment (TME) due to incremented ATP and adenosine level. TME entails the interchange between tumor and non-malignant cells, including endothelial, fibroblast and immune cells[113]. Additionally, TME appears as an dynamic environment that

tumor cells are in proximity to healthy host cells [114]. The ATP release in TME by cancerous function as auto-paracrine cues that induce the activation of cell proliferation and tumor growth as well as epithelial-to-mesenchymal transition (EMT) and migration of tumor cells [113], [114]. Among purinergic receptors, P2X7 has been widely studied in breast, thyroid, pancreas and liver cancer with possible regulatory functions on cancer cell physiology [113]. Based on these findings, interest has been sparked on finding therapeutic potential with the involvement of purinergic signaling on cancer treatment [115].

1.3.2 Inflammation and sepsis

Sepsis is a life-threatening medical emergency in which overwhelming inflammatory response causes sudden functional alteration of immune system (IS). This further leads to the harm of subtle texture of tissue and to organ dysfunction [86], [116], [117]. Bacterial infection, as well as viral infection such as coronavirus disease 2019 (COVID-19) could be the trigger for severe systemic infection and inflammation and subsequently to the underlying complex disease [86], [118]. Despite improvements on the management, sepsis remains one of the leading causes of immediate death and intensive care units (ICU) worldwide, surpassing the mortality rate of myocardial infarction and progressive cancer. In the United States (U.S.), 1.7 million people are confronted with sepsis yearly, with an in-hospitality rate up to 30% [119], [120]. Nevertheless, no specific treatment has been discovered yet or were met with failure in clinical trials that cure or restrain septic activity. Hence, more effective strategies are required to counteract against major global health problem [20].

Neutrophil are the first line of host defense of the immune system, patrolling through the peripheral blood and respond to the infection or inflammation event [86]. Additionally, the counterplay between P2Y2, A3 and A2a renders neutrophils to perform appropriately antimicrobial function [25], [111]. Studies have shown that chemotaxis model was impaired during systemic infection and concomitant sepsis manifestation. Neutrophils exhibit lower response to chemoattractant substances and other agonist, providing therefore insufficient clearance against bacterial pathogens [121]. Sumi *et al.* [122] could reveal that plasma ATP, ADP and AMP was elevated after 8 hours of introducing cecal ligation and puncture (CLP) sepsis model. This elevated plasma ATP showed a correlation with neutrophil stimulation, assessed *in vitro* via CD11b expression. This study could emphasize the interconnectivity between ATP release and neutrophil activation, needed to provide orientation in a chemotactic field and eliminate pathogen [122]. However, too much circulating ATP profoundly leads to collateral damage in host and further to organ dysfunction, as observed in critical care and trauma patients experiencing septic shock [20]. Li *et al.* [123] could point out in our laboratory that elevated plasma ATP interfered autocrine feedback mechanism, neutrophils require to regulate chemotaxis. Excessive P2Y2 receptor activation by systemic ATP increases neutrophil degranulation and cause tissue harm on host [123]. This dilemma might be the

reason for low progress in terms of searching for the effective therapy against severe infection and sepsis [20]. Interestingly, recent findings have found apyrase as an essential enzyme that can hydrolyze systemic ATP. This clearance could re-establish chemotaxis, alleviate systemic inflammation and altogether, improve survival in CLP-subjected mice[123].

1.4 Aim of the study

Key goals of this master thesis are to define mechanistic links between cellular adenosine triphosphate (ATP) concentrations, purinergic signaling, and inflammatory response that leads to poor outcome in patients with bacterial and viral infections such as influenza and sepsis. Specifically, we studied how immune cells and other physiological processes regulate purinergic signaling system and which enzymes and its corresponding coenzymes are involved. Excessive ATP levels have been shown that contributes to excessive neutrophil activation and the fatal outcome in patients with sepsis and other infections, but the mechanisms behind this ATP elevation have not been fully understood. Therefore, we hypothesize that dysregulated ATPase level elevated extracellular ATP levels and promote the inflammatory cascade that contributes to excessive neutrophil activation and the fatal outcome in patients with COVID-19 and other infections.

2 Materials and Methods

2.1 Human Subjects

All studies performed with human subjects were approved by the Institutional Review Board of Beth Israel Deaconess Medical Center (BIDMC) and Urayasu Hospital with international ethical standards. Prior to blood draws, written informed consent was obtained from healthy volunteers or patients. Blood draw from healthy volunteers and sepsis patients were performed at BIDMC and Urayasu Hospital, respectively. 14 male and five female subjects, aged between 38 and 89 and diagnosed with sepsis and other diseases, were participated in this study.

2.2 ATP breakdown in human blood

2.2.1 Time course of ATP breakdown in human whole blood

Human blood was collected by venipuncture in lithium heparin vacutainer tubes (Becton Dickinson #367,874, Franklin Lakes, NJ) and was aliquoted in Eppendorf tubes. Blood samples were diluted 1:4 in Hank's Balanced Salt Solution (HBSS, HyClone, Logan, UT) and pre-incubated in a water bath at 37°C for 10min. 2 μM ϵ -ATP (etheno-ATP, Jena Bioscience, #NU-1103S, Jena, Germany) was added and incubated for 5, 15 and 30 min at 37°C. At each timepoint, the reaction was ceased by cooling blood sample on ice for at least 10 min. Blood samples were then centrifuged at 400 x g, 10min, 0°C and plasma was collected in new Eppendorf tubes. To remove remaining platelets, plasma was centrifuged the second time at 2,300 x g, 5 min and 0°C and collected in new Eppendorf tubes. To prevent further ATP breakdown, 400 mM perchloric acid (PCA, Millipore Sigma, #244,252, Burlington, MA) was added to the samples as "stop solution" and stored at -80°C until further use.

2.2.2 Time course of ATP breakdown in human blood cells (washed)

Human blood was drawn in lithium heparin vacutainer. To separate plasma from blood cells, whole blood was aliquoted in Eppendorf tubes and diluted 15-fold in HBSS. Blood samples were then centrifuged at 400 x g, 10min and 25°C. Equal amount of supernatant, including plasma was discarded. Washed blood cells were then flicked on the bottom of Eppendorf tube and gently resuspended in HBSS.

Human washed blood cells were preincubated at 37°C for 10min. 2 μM ϵ -ATP was added and incubated for 5, 15, and 30 min. At each timepoint, blood cells were transferred on ice to halt the reaction. Washed blood cells were further processed, as previously described with the whole blood. Briefly, two centrifugation steps were performed to obtain the culture medium from blood cells. 400 mM PCA was added to the samples and stored at -80°C until further use.

2.2.3 Time course of ATP breakdown in human plasma

To also study the rapidity of ATP degradation in human plasma, blood was drawn by venipuncture in lithium heparin vacutainer, and immediately chilled on ice for at least 10min. Blood samples were then processed, as previously described with the whole blood. Briefly, two centrifugation steps were conducted to obtain the human plasma. Human plasma was diluted 1:4 with HBSS and preincubated at 37°C for 10min. 2 μM ATP (Millipore Sigma, #A6,419, Burlington, MA) or ε-ATP was pipetted into the plasma and incubated 5, 15 and 30 min. PCA as “stop solution” was added to the plasma after each timepoint and stored at -80°C until further use.

2.2.4 ATP breakdown to study inhibitors

To examine the importance of enzymes and co-enzymes related to purinergic signaling in whole blood, blood cells and plasma, inhibitors against enzymes with ATPase activity or that scavenge Ca²⁺ and other metal-ions were applied in ATP breakdown experimental design.

POM-1 (Tocris Bioscience, #2,689, Minneapolis, MN) is a sodium polyoxometalates that selectively inhibits NTPDase activity. ENPP1 inhibitor C (Cayman Chemicals, #29809, Ann Arbor, MI) inhibits ENPP1 activity. PSB12379 disodium (Tocris Bioscience, #6083, Minneapolis, MN) is a nucleotide analogue that suppresses CD73 activity. EDTA (Sigma-Aldrich, E9,884, Sigma-Aldrich, St. Louis, MO) and ethylene glycol tetra acetic acid (EGTA, Sigma-Aldrich, 324,626, St. Louis, MO) as chelating agents were used to scavenge Ca²⁺ and other metal ions.

Unless stated otherwise, whole blood, washed blood cells or plasma were diluted 1:4 with 80 μM POM-1, 50 μM NPP1 inhibitor C and 10 μM PSB12379 and pre-incubated for 10 min. Procedure was repeated with 2 μM ε-ATP or ATP, 5- or 10-min incubation at 37°C, plasma extraction and PCA treatment, respectively.

2.2.5 Effect of Zn²⁺ in ATP breakdown

2.2.5.1 EDTA blood cells and plasma

To study the effect of Zn²⁺, human blood was drawn by venipuncture in ethylenediamine tetra acetic acid (EDTA)- containing (Becton Dickinson, #367,835, Franklin Lakes, NJ) or lithium-heparin vacutainer tubes. One part was aliquoted for blood cells, the other part for plasma.

Blood cells were washed, as previously described on 2.2.1, diluted 1:2 in 10-fold ZnCl₂/HBSS concentration (Sigma-Aldrich, #E1644, St. Louis, MO) and preincubated in 30 min. ATP breakdown experiment was conducted with 2 μM ε-ATP and 10 min incubation time and

processed, as previously described on 2.2.2. Plasma extractions were processed, as previously described on 2.2.3 Samples were then diluted 1:50 with 10-fold ZnCl₂ concentration or HBSS and pre-incubated for 30min. 2 μM ATP was added and incubated for 10 min. After 10 min, plasma was treated with 400mM PCA to precipitate plasma proteins and cease the reaction.

2.2.5.2 sepsis patients

To study the effect of Zn²⁺ in critical care patients, heparinized blood from sepsis patient or healthy control subjects was drawn and processed to obtain the plasma. The latter was diluted 1:10 in either 5 μM ZnCl₂ or HBSS and pre-incubated for 30 min. 2 μM ε-ATP was added and incubated for 25 min. Plasma was treated with 400 mM PCA and stored at -80°C until further use.

2.3 Mouse model

2.3.1 Mice

Groups of 2-5 animals were housed in type III cages and had free access to rodent food and water *ad libitum* throughout the study. These mice were sustained in a 12-hour light-dark diurnal cycle and 22-24°C standard room temperature.

2.3.2 Ethical Statement

The use of laboratory animals was authorized by Institutional Animal Care and Use Committee (IACUC) of BIDMC and in compliance with guidelines of the National Institutes of Health (NIH). All in vitro experiments and used biological materials were in accordance with international ethical standards. C57BL/6 wildtype (wt) mice strain were used in this study (Jackson Laboratories, Bar Harbor, ME).

2.3.3 Sepsis model

2.3.3.1 Preparation of Cecal Slurry (CS)

Six healthy female C57BL/6 mice (n = 6) aged 17 to 22 weeks were used for cecal slurry preparation. Mice were anaesthetized with Pivotal® isoflurane (Aspen Veterinary Resources, LTD, #21,295,098, Liberty, MO) in an induction chamber and euthanized by cervical dislocation. Cecae from mice were dissected and then, distal end of the cecum cut with a blade. The entire cecal contents were collected with sterile forceps and spatula. These cecal content were weighed and mixed with sterile saline (200 mg/ml). Suspension was filtered through 70 μm cell strainer and mixed with equal volume of 30% glycerol in phosphate buffered saline (PBS; Cytiva HyClone, Logan, UT). While mixing, aliquots were transferred into Eppendorf tubes and stored at -80°C.

2.3.3.2 Sepsis induction and monitoring

Six female and six male C57BL/6 mice (n = 12) aged 10 weeks, were selected for subjecting bacterial infection using CS infection model [124]. CS stock was rapidly thawed on 37°C water bath and diluted 1:2 in saline. Mice were anaesthetized in induction chamber, covered with isoflurane. Tail of the mice was marked, followed by temperature measurement and weight. CS (0.3mg/g) was administered with 27G needle intraperitoneally into the lower right abdomen of the mice. Buprenorphine (1.2 mg/kg) SR-LAB (ZooPharma, Fort Collins, CO) was injected subcutaneously for pain control. All mice were evaluated after 10 hours and then every 2 hours based on our own-developed mouse clinical assessment scoring system (M-CASS) to identify and sacrifice moribund animals. Parameters, in particular overall appearance, activity, response to external stimulus, body temperature, respiration, and eyes were recorded and scored from 0 (normal) to 4 (severely impaired). Mice were euthanized if any parameter reached a score of 4 (Table 2). All other mice were euthanized after 18-20 hours by cardiac puncture and exsanguination. To ensure death, cervical dislocation was performed.

Table 2: Sepsis severity score of mice.

1	Overall appearance
0	Coat is smooth
1	Patches of hair piloerected
2	Majority of back is piloerected, hunched posture
3	Piloerection may or may not be present, mouse appears “puffy”
4	Piloerection may or may not be present, mouse appears emaciated
2	Consciousness/activity
0	Mouse is, alert, involved in activities like eating, drinking, running, climbing, fighting, grooming
1	Active but slightly suppressed, avoids standing upright
2	Activity noticeably slowed, mouse still ambulant, does not try to escape when lifted up
3	Activity impaired, stationary; only moves when provoked, impaired movement, possibly tremor
4	Severely impaired, no reaction to stimulus, cannot right itself up if pushed over, possibly tremor
3	Response to stimulus
0	Mouse responds immediately to auditory stimulus or touch
1	Slow or no response to auditory stimulus, strong response to touch (moves to escape)
2	No response to auditory stimulus, moderate response to touch (moves a few steps)
3	No response to auditory stimulus, mild response to touch (no locomotion)
4	No response to auditory stimulus, little or no response to touch.
4	Eyes
0	Open
1	Not fully open, possibly with secretion
2	Half closed, possibly with secretion
3	More than half closed, possibly with secretion
4	Closed or milky
5	Respiration, rate and quality
0	Normal, rapid mouse respiration
1	Slightly decreased (rate not quantifiable by eye)
2	Moderately reduced respiration rate (rate at the upper range of quantifiable by eye), labored
3	Respiration rate easily countable by eye (0.5 s between breaths); labored, intermittent gasping
4	Extremely reduced respiration (>1s between breaths), gasping

2.3.4 ATP breakdown in mice

2.3.4.1 Cardiac puncture and blood sampling

To collect blood, mice were anaesthetized with isoflurane in the induction chamber and placed in a surgery table. Abdominal cavity of mice was opened, followed by puncturing the heart through the diaphragm. Blood was drawn with a needle, pre-covered with heparin and released in new microcentrifuge tube.

2.3.4.2 Time dependent ATP breakdown in mice whole blood

To examine the quantity of ATP breakdown products over time, heparinized healthy control mice blood (n = 4) was diluted 1:4 with HBSS and pre-incubated for 10min at 37°C. 2 µM ε-ATP was added and incubated for 5, 15, 30 and 60 min under the same condition. Reaction was ceased after each timepoint by transferring the blood sample on ice. Blood was centrifuged twice to obtain the plasma, as previously described on 2.2.1.

2.3.4.3 Time dependent ATP breakdown in mice plasma

To also investigate the rapidity of ATP breakdown in plasma, heparinized healthy control mice blood (n = 3) was cooled immediately on ice after blood draw by cardiac puncture. Blood samples were centrifuged twice to obtain the plasma, as previously described on 2.2.3. Plasma samples were then diluted 1:4 with HBSS and pre-incubated for 10 min at 37°C. 2 µM ATP was added to the plasma and incubated for 5, 15, 30 and 60 min under the same condition. At each timepoint, plasma was treated with 400 mM PCA and stored at -80°C until further use.

2.3.4.4 Inhibitor in whole blood and plasma

To study the role of enzymes in whole blood and plasma, heparinized healthy control mice blood (n = 3) or plasma was diluted 1:4 with 80 µM POM-1, 50 µM NPP1 inhibitor C, 50 µM TNAP inhibitor or 10 µM PSB12379 in HBSS and procedure was repeated with 2 µM ε-ATP or 2 µM and 10 min incubation time, respectively.

2.3.4.5 Effect of Zn²⁺ in mouse plasma

To investigate Zn²⁺, 10 weeks-old sepsis mice (n =12) and 8 to 12 weeks-old healthy mice control (n = 19) were used for the study. Therefore, heparinized mice blood, obtained by cardiac puncture method, were cooled down on ice and prepared to plasma, as described on 2.2.3. Mice Plasma was diluted 1:10 in either 5 µM ZnCl₂ or HBSS and preincubated for 10min. 2 µM ATP was added and incubated for another 25 min. Reaction was stopped by precipitating the plasma proteins with 400 mM PCA and stored at -80°C until further use.

2.4 High Performance Liquid Chromatography (HPLC)

ATP and its derivatives and adenosine were identified and quantified with High Performance Liquid Chromatography (HPLC) in human and mouse. Solvents, reagents, and chemical compounds used in this study reached High Performance Liquid Chromatography (HPLC)-grade quality. Therefore, HPLC grade methanol (Sigma Aldrich, # 11199435209) and water (Sigma Aldrich, # 62222) were used. Sample preparation and HPLC analysis were proceed and followed, as described, and optimized by [125].

2.4.1 Buffer preparation

All laboratory equipment were designated, rinsed properly with chromic sulfuric acid (Fisher Chemical, #171,637, Waltham, MA) and distilled water (dH₂O) and exclusively used for HPLC purposes. For analyzing samples on HPLC, buffer A as equilibration buffer and buffer B as elution buffer were prepared and used. Buffer A consists of 100 mM KH₂PO₄, (Millipore Sigma, #104,873, Burlington, MA) and 4 mM ion-pairing tetrabutylammonium (TBA) bisulfate (Millipore Sigma, #86,853, Burlington, MA) with pH 6.0. For buffer preparation of HPLC buffer A, 100 mM KH₂PO₄ and 4 mM TBA bisulfate were dissolved in HPLC grade water and adjusted to pH 6.0 with HPLC grade potassium hydroxide (45% KOH, Fluka, #03,564 Honeywell, NC). To remove impurities, HPLC buffer A was then sterile- filtered (25 mm diameter, 0.2 μM pore size, Millipore Sigma, Burlington, MA) and kept in 500 ml flasks until further use. To obtain HPLC buffer B, 70% of sterile-filtered buffer A was mixed with methanol and stored in 500ml flasks. Both buffers were kept on 4°C fridge.

2.4.2 Sample preparation (regular ATP)

2.4.2.1 Protein precipitation

To prepare for HPLC analysis, plasma samples treated with perchloric acid (PCA) were thawed from -80°C on ice and 5 μM α, β-Methyleneadenosine 5'-diphosphate monosodium salt (AMPCP, final concentration: 500 nM) as internal standard was added (R&D system #3633, Minneapolis, MN). These plasma samples were then centrifuged at 16,000 x g, for 10 min and 0°C. Supernatants were collected and treated with 4 M K₂HPO₄ (400 mM final, Fluka, #60,347, Honeywell, Charlotte, NC). To remove lipids and cell debris, samples were centrifuged secondly at 16,000 x g, for 10 min and 0°C. Supernatants were collected in fresh Eppendorf tubes.

2.4.2.2 Etheno-derivatization

Etheno-derivatization involves conversion of ATP, ADP, AMP and ADO into 1,N⁶ – etheno-derivatives making the analytes visible on scanning fluorescence detector. Based on the collected supernatants, samples were treated with 250 mM Na₂HPO₄ solution pH 4.0 (25 mM final, Fluka, #71,629, Honeywell, NC) and 1 M chloroacetaldehyde solution (158 mM final,

Millipore Sigma, #317,276, Burlington, MA), then vortexed, and spined briefly on centrifuge at 0°C. Samples were incubated at 72°C for 30 min to convert ATP, ADP, AMP and ADO into 1,N6 – etheno-derivatives. After 30 min, samples were cooled on ice and spined briefly the second time on centrifuge at 0°C to collect everything vaporized within Eppendorf tube. pH was neutralized with 500 nM NH₄HCO₃ pH 8.5 (100 mM final, Fluka, #09,830, Honeywell, NC).

2.4.2.3 Solid-phase extraction (SPE)

For solid-phase extraction (SPE), Sep-Pak® C18 Vac cartridges (Waters™ #054,955, Milford, MA) were used to remove lipids and soluble compounds and achieve separation efficiency. These SPE cartridges consists of hydrophobic, silica-based bonded phase, served as separation technique for analytes from aqueous solution.

SPE columns were firstly positioned in vacuum manifold (Kinesis TELOS Column Sample processing manifold, Cole-Parmer, Vernon Hills, IL). Pressure of this manifold was set to 0.25” Hg to ensure a steady and slowly flow-through. Columns were primed with 200 µl HPLC-grade methanol, followed by 200 µl HPLC-grade water, 1 ml HPLC buffer A. Samples undergone etheno-derivatization were diluted 3:1 with HPLC buffer A and loaded onto the activated SPE column. The latter containing the sample were washed with 200 µl HPLC buffer A. Sample were then eluted with 400 µl HPLC buffer B consisting of 70% HPLC buffer A and 30% HPLC-grade methanol (v/v) in fresh microcentrifuge tubes. The resulting eluates were frozen in liquid nitrogen (LN) for at least 5 min. Rapidly frozen samples were lyophilized using a SpeedVac concentrator (Savant SPD111V, Thermo Scientific, Waltham, MA) and Cooled Vapor Trap (Savant RT 5105, Thermo Scientific, Waltham, MA).

Freeze-dried samples were reconstituted in 50 mM KOH and 30 µl of HPLC-grade buffer A, vortexed and centrifuged at 16,000 x g, 3 min and 0°C. Samples were then filtered through a syringe filter with a 0.2 µm pore size and 4 mm diameter (PTFE, Thermo Scientific, Rockwood, TN), centrifuged briefly and loaded into 384-well plates for HPLC analysis.

2.4.3 Sample preparation (ε-ATP)

2.4.3.1 Etheno-derivatization of AMPCP

Compared to ATP, preparation of samples with ε-ATP allows to circumvent etheno-derivatization procedure. Still, AMPCP needs to be etheno-derivatized. 5 µM AMPCP was treated with 8 M PCA and 4 M KH₂PO₄ that result in precipitation. AMPCP solution was centrifuged at 16,000 x g, 10 min and 0°C. Pellet was discarded, and supernatant put in fresh Eppendorf tubes. Etheno-derivatization of AMPCP was performed, as previously described with plasma samples treated with ATP. Briefly, AMPCP was subjected to 250 mM Na₂HPO₄ and 1 M chloroacetaldehyde and incubated for 30 min at 72 °C. To neutralize pH, 500 mM

NH₄HCO₃ pH 8.5 were added and vortexed for 10 seconds. Freshly etheno-derivatized AMPCP (3 μM) can be stored at -80°C until further use.

2.4.3.2 Protein precipitation

Plasma samples treated with perchloric acid (PCA) were thawed from -80°C on ice and already etheno-derivatized AMPCP (3 μM) was added. These plasma samples were then centrifuged and treated with KH₂PO₄, as previously described in 2.4.2.1.

2.4.3.3 Solid-phase extraction (SPE)

Samples undergone the precipitation process were diluted 3-fold with HPLC buffer A and follows the same procedure, as previously described in 2.4.2.3. Briefly, samples retained in SPE column were rinsed with 200 μl HPLC buffer A and then eluted with 400 μl HPLC buffer B. Eluates were then rapidly frozen in LN and freeze-dried to remove liquid and methanol.

2.4.4 HPLC analysis

Separation of etheno-derivatized samples were performed using Ion-pairing reverse phase liquid chromatography. HPLC system (Agilent 1260 Infinity HPLC system, Santa Clara, CA) was equipped with a micro vacuum degasser (G1379B), a binary pump (G1312B), a temperature-controlled column compartment (G1316A) and a thermostatted autosampler (G1367C), Atlantis dC18 analytical column (3 mm x 150 mm, 3-μm particle size, #186,001,307; Waters, Milford, MA) as separation column, and scanning fluorescence detector which emission and excitation wavelength was set to 254nm and 410nm, respectively. (A Waters 474, Milford, MA).

Prior to injecting samples, HPLC system was rinsed for at least 10 min with HPLC grade water, then 5 min with HPLC buffer B. The column was equilibrated with HPLC buffer A. Temperature of the column was set to 40 °C and flow rate to 0.3 ml/min. 10 μl of sample was injected into the HPLC system, allowing them with HPLC buffer A to migrate the etheno-derivatized samples to the column. Linear gradient was applied during analysis, from 100% HPLC buffer A to 100% HPLC buffer B over 13 min to separate ATP, ADP, AMP and ADO based on their retention time. After the linear gradient, column was washed with 100% HPLC buffer B for 12 min, then re-equilibrated with 100% HPLC buffer A for 8 min before the following sample could be injected. After sample analysis, column was automatically rinsed with HPLC grade water for 30min before shutting down the system and immerse the tubes into 70% methanol. To control the instrument online and analyze the outcome offline, ChemStation software was used.

As standard, known concentration (500nM) of ATP(#A6,419), ADP (#A5285), AMP (#A1752) and adenosine (#A9251), obtained from Millipore Sigma (Burlington, MA) and AMPCP or as ε-standard, known concentration (500nM) of ε-ATP, ε-ADP (#NU-1140S), ε-AMP (#NU-1141S),

obtained from Jena Bioscience (Jena, Germany), ϵ -ADO (Biosynth, #NE01669, Gardner, MA) and AMPCP were used and treated, similar to the plasma samples, respectively. Peak height of these four identified purinergic compounds were normalized to AMPCP and sample concentration are calculated based on known concentration of standard or ϵ -standard mixture.

2.5 Flow cytometry

2.5.1 Polymorphonuclear neutrophils (PMN) activation

Heparinized human blood was aliquoted in Eppendorf tubes and preincubated for 10 min at 37°C. Then, blood samples were mixed 1:1 with POM-1, NPP1 inhibitor C or PSB12379 and incubated for another 10 min. 1 μ M ATP and 5 nM N-formylmethionyl-leucyl-phenylalanine (fMLP, Sigma-Aldrich, #F3,506, St. Louis, MO) were simultaneously added to the blood sample by pipetting both substances at the interior of the lid, followed by closing the lid and converting the rack. Blood samples were incubated for 15 min at 37°C. Reaction was ceased by cooling on ice for at least 5 min. Blood samples were stained with anti-CD11b APC (clone M1/70), anti-CD66b (clone: G10F5) or anti-CD62L PE (clone: DREG-56) antibodies, diluted with 0.1% bovine serum albumin (BSA, #A3294, Millipore Sigma, Burlington, MA) or HBSS and obtained from BioLegend, San Diego, CA. These samples were then incubated for 20 min under dark conditions. After staining, blood samples were treated with red blood cell (RBC) lysis buffer (BioLegend, 420,301, San Diego, CA) and incubated for 10min at 25°C under dark conditions. Lysed samples were centrifuged at 400 x g, 5 min and 25°C and supernatant was aspirated down to the pellet. The latter with the remaining liquid were resuspended in 200 μ l HBSS.

2.5.2 Flow cytometry and analysis

Analysis was performed with a NovoCyte 3000 flow cytometer (Agilent, Santa Clara, CA). PMN population were identified, based on forward (FSC) and side scatter properties (SSC). For the analysis, another gating was defined selecting CD11+ - stimulated PMN populations.

2.6 Statistical Analysis

Unless otherwise stated, results were reported as mean values \pm standard deviation (SD). Differences between groups were tested for statistical significance using a two-tailed t test if comparing two groups and one-way or two-way ANOVA followed by the Dunn's multiple comparison test for multiple group comparison. Graph Pad Prism 9.0.0 were used to perform statistical analysis. Differences were considered statistically significant at * $p < 0.05$.

3 Results

3.1 Extracellular ATP in human whole blood

3.1.1 Extracellular ATP is rapidly broken down in whole blood, but cells also release ATP

To investigate ATP breakdown in whole blood, ATP was pipetted into blood of a healthy volunteer and concentrations of remaining ATP and its breakdown products ADP, AMP, adenosine and deaminated products were determined at specific timepoints (0, 0.5, 1, 2, 3 and 5 min). Results were depicted as scatter plots in Figure 10. Only seconds after adding ATP, it was already degraded by about 40%, and based on the amount of added ATP, 12% ADP, 38% AMP and 7% adenosine were obtained. After 5 min, ATP leftover of 36% was achieved. 24% of ADP, 49% AMP and 12%

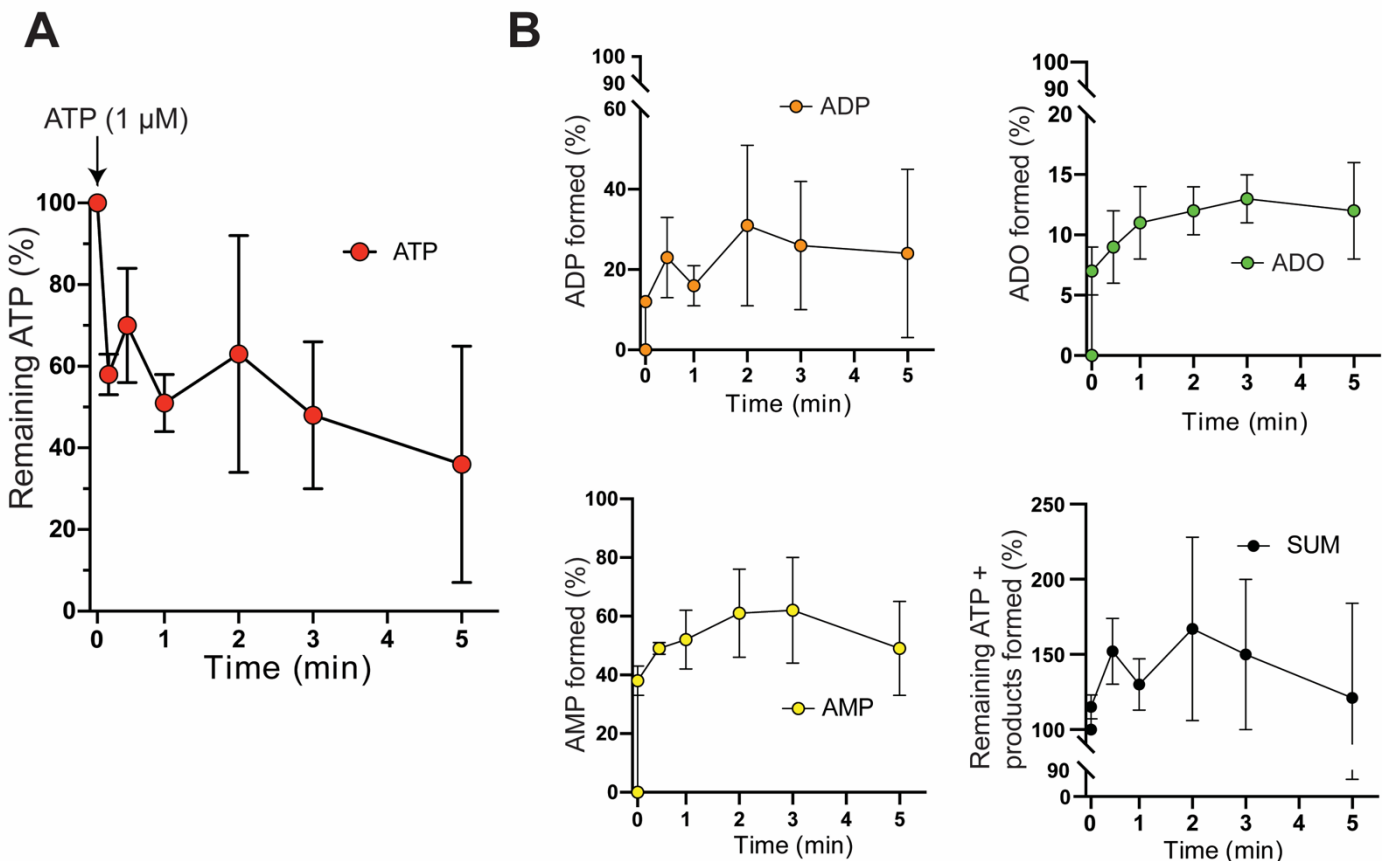


Figure 10: **ATP added into human whole blood is rapidly hydrolyzed but can also cause ATP release from cells.** Equal amounts of blood from a healthy volunteer were aliquoted in Eppendorf tubes and pre-incubated for 10 min at 37°C. 1 μ M ATP was pipetted into the blood and incubated up to 5 min. At respective timepoints (0, 0.5, 1, 2, 3 and 5 min), reactions were stopped by transferring the samples into ice. Blood was then centrifuged twice at 0°C (1st run: 400 x g, 10 min, 2nd run: 2,300 x g, 5 min). The resulting plasma was treated with PCA and processed for HPLC analysis. Concentrations of ATP

(A), ADP, AMP, and ADO (B) were assessed and expressed as % of the ATP amount added. The sum of the ATP remaining, and the ATP breakdown products formed at each timepoint is shown in E. Data show mean values \pm SD (n = 3 different donors).

However, when calculating the sum of remaining ATP and its breakdown products ADP, AMP, and adenosine, we obtained values over 100%. This could be explained by blood cells experiencing a so-called positive feed-forward response that results in the release of additional ATP [126]. Due to this positive enhancement on blood cells, we could not study ATP breakdown with this experimental set-up. Therefore, we performed the following experiments with blood cells with commercially fluorescently labeled ϵ -ATP.

3.1.2 ATP is rapidly hydrolyzed in human plasma

We also studied ATP hydrolysis in human plasma. Plasma was obtained from blood of healthy volunteers and incubated with ATP. At certain timepoints (0, 5, 10, 15, 30 and 60 min), concentration of ATP, ADP, AMP, and adenosine as well as adenosine breakdown products were determined and depicted as scatter plot (Figure 11). Our results showed that ATP degradation was complete within 30 min and simultaneously, adenosine production increased up to 60% of added ATP after 30 min and remained at this level until the 60 min timepoint. ADP production peaked at a low level of about 6% seconds after addition of ATP and decreased thereafter. AMP production reached its highest peak at 25% after 10 min before being degraded to adenosine. The amount of inosine and further deaminated products was calculated and increased gradually over time. This ATP breakdown pattern suggests the prevalence of ENPP1, CD73 and ADA activity in the plasma as ENPP1 grasps ATP converting it directly to AMP and therefore by-passing ADP production [9], [64].

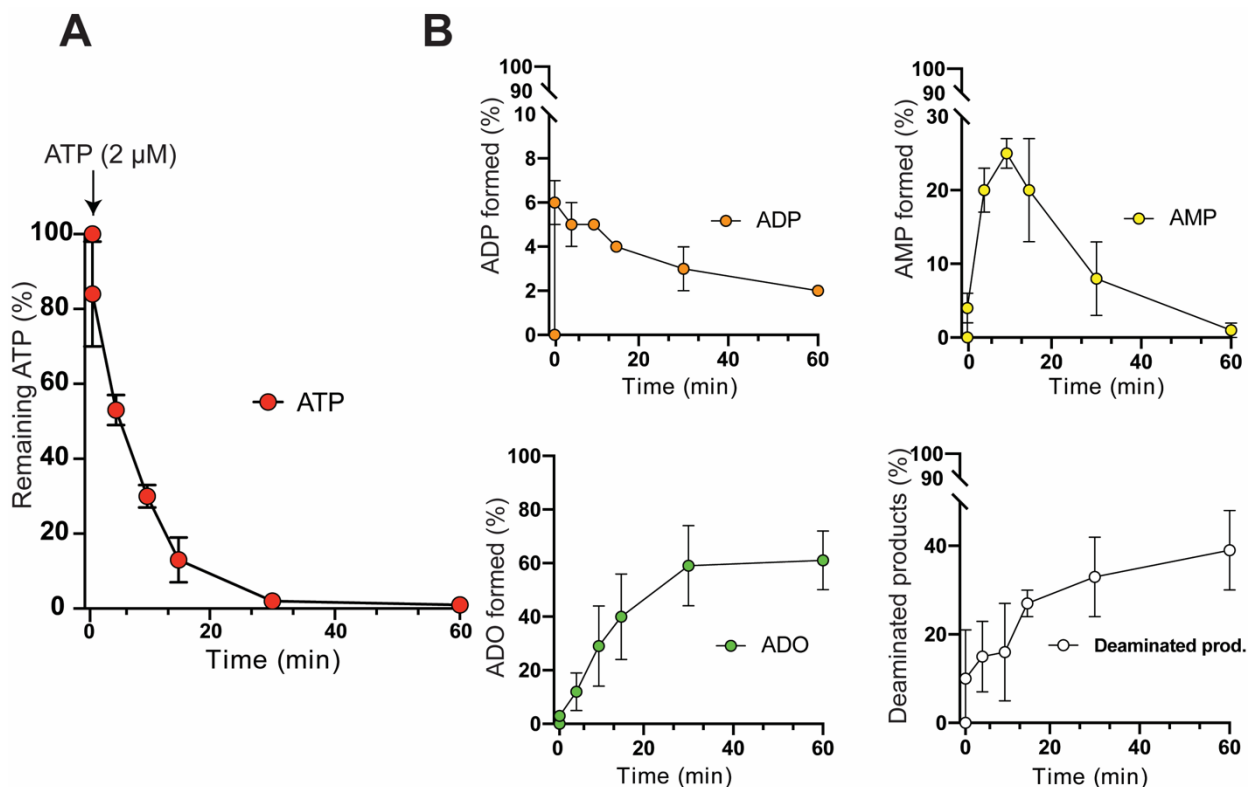


Figure 11: **ATP added to human plasma is rapidly converted to adenosine and adenosine breakdown products.** Healthy volunteer's blood was centrifuged twice (1st run: 400 x g, 10min, 0°C; 2nd run: 2,300 x g, 5 min, 0°C) to obtain the plasma. The latter was diluted 1:4 and pre-incubated for 10 min at 37°C. 2 μ M ATP was pipetted into the plasma and incubated for up to 60 min. To stop the reaction, plasma was treated with PCA at each respective timepoint (0, 5, 10, 15, 30 and 60 min) and processed for HPLC analysis. ATP remain (A), ADP, AMP, adenosine and deamination production (B) were determined, normalized to added ATP. Results were depicted separately as scatter plot (mean \pm SD, n = 3).

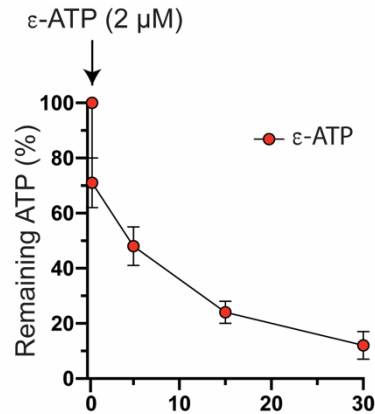
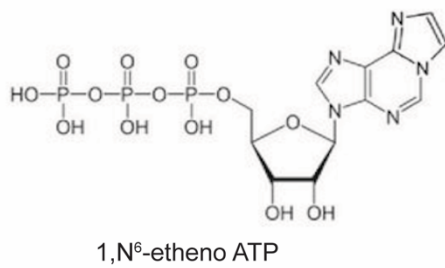
3.1.3 Etheno-ATP (ϵ -ATP) can be used to distinguish between ATP breakdown and ATP release in human blood

The results described in 3.1.1. demonstrate that regular ATP cannot be used to study ATP hydrolysis in whole blood as addition of ATP triggers ATP release from blood cells. To ensure that we measured only the breakdown products from added ATP, we used a commercially available etheno derivative of ATP (ϵ -ATP, Figure 12A) to study the ATP breakdown profile over time in both the cellular and extracellular compartments of human blood. Unlike natural ATP, ϵ -ATP can be detected by a fluorescent detector. Since the etheno group is retained after dephosphorylation, it is also possible to measure the production of ADP, AMP and adenosine.

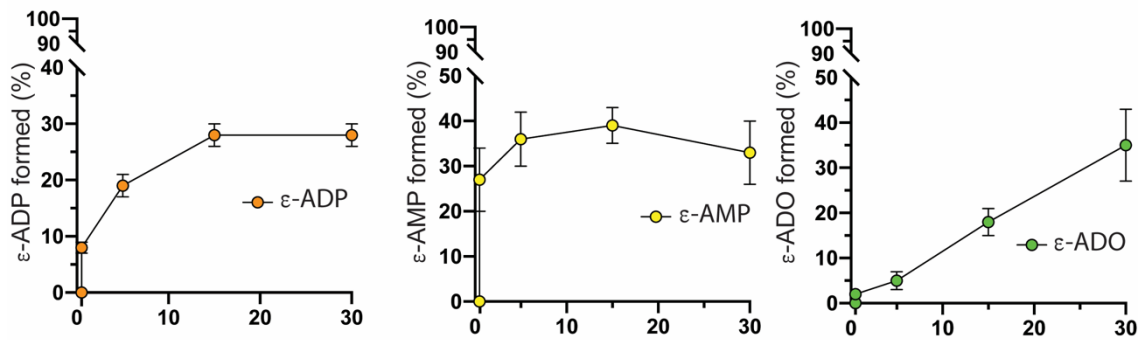
Therefore, human whole blood or plasma, diluted with HBSS was incubated with ϵ -ATP. As ATP was entirely degraded in plasma after 30 min, we chose timepoints up to 30 min, including 0, 5 and 15 min. On each respective timepoint, concentrations of remaining ϵ -ATP and its breakdown products were determined via HPLC analysis.

In general, we found that enzymes in whole blood and plasma were also able to catalyze the breakdown of ϵ -ATP to ϵ -ADP, ϵ -AMP and ϵ -ADO. In blood as well as plasma, about 12% of the initially added ϵ -ATP was left after 30 min. Both ϵ -ADP and ϵ -AMP increased rapidly in blood and plasma. However, while the amount of ϵ -AMP measured after 30 min was similar in both compartment (about 30%), more ϵ -ADP was produced in blood than in plasma (28% vs. 10%). ϵ -ADO accumulated over time in plasma, about twice as much in whole blood. Interestingly, ϵ -ATP and its breakdown products sum up of a value of approximately 100% in whole blood and plasma (Figure 12, Figure 13). Hence, no inosine and further deaminated products were produced. This is consistent with the loss of the ADA cleavage site in ϵ -ADO (Figure 12C). Nevertheless, ϵ -ATP is suitable to study ATP, ADP and AMP converting enzymes in both compartments.

A Human Whole Blood



B



C

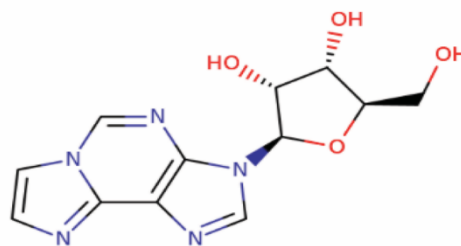


Figure 12: **ATPase and CD73, but not ADA catalyze ε-ATP and ε-ADP to ε-AMP and ε-ADO, in whole blood.** To examine ATP breakdown pattern with commercially available etheno derivative of ATP, whole blood was drawn by healthy volunteers and aliquoted in Eppendorf tubes. Whole blood was diluted with 1:4 HBSS and preincubated for 10 min. 2 μM ε-ATP was pipetted into the whole blood or plasma and incubated up to 30 min. At each respective timepoints (0, 5, 15, and 30min), reaction was stopped by putting whole blood on ice. 2 centrifugation steps were conducted (1st run: 400 x g, 10min, 0°C; 2nd run: 2,300 x g, 5 min, 0°C). Plasma was obtained and incubated with PCA. ε-ATP remain (A) as well as ε-ADP, ε-AMP ε-adenosine products (B) were determined in both compartments, normalized to added ATP. Structure of ε-ATP [127] (A) and ε-adenosine [128] was shown to demonstrate the deprivation of ADA cleavage site (B). Results were depicted separately as scatter plot (mean ± SD, n = 3)

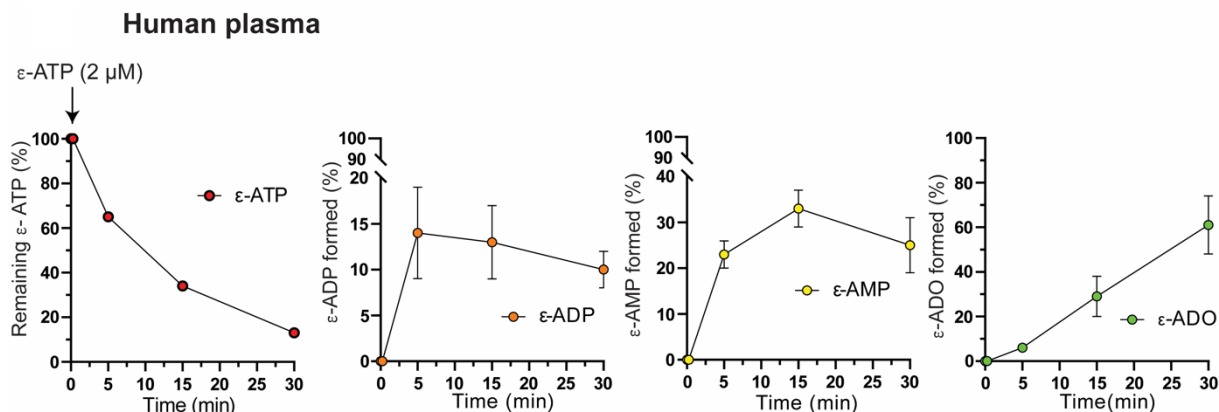


Figure 13: ATPase and CD73, but not ADA catalyze ϵ -ATP to ϵ -ADP, ϵ -AMP and ϵ -ADO in plasma. To examine ATP breakdown pattern with commercially available etheno derivative of ATP [127], whole blood was drawn by healthy volunteers processed to human plasma (2 centrifugation steps: 1st run: 400 x g, 10 min, 0°C; 2nd run: 2,300 x g, 5 min, 0°C). Obtained plasma were then diluted 1:4 with HBSS and preincubated for 10 min. 2 μ M ϵ -ATP was pipetted into the plasma and incubated up to 30 min. At each respective timepoints (0, 5, 15, and 30min), reaction was ceased by treating plasma with PCA. Remaining ϵ -ATP, ϵ -ADP, ϵ -AMP ϵ -adenosine products were determined, normalized to added ATP. Results were depicted as scatter plot (mean \pm SD, n = 3)

3.1.4 Plasma contributes more to ATP hydrolysis than cells in human blood

Above, we have demonstrated that enzymes can breakdown ϵ -ATP in both human whole blood and plasma. This observation facilitates the traceability of added ATP, which is particularly useful when working with whole blood.

We next investigated to what extent enzymes expressed on the surface of blood cells and soluble enzymes in the plasma contribute to the breakdown of ATP in human blood, respectively. Therefore, we repeated the ϵ -ATP experiment with the same donor. Whole blood was separated from plasma by centrifugation and the cell pellet was washed once with HBSS to remove remaining plasma from blood cells and then resuspended in an equal amount of HBSS. ϵ -ATP was pipetted into the blood cells and remaining ϵ -ATP and its breakdown products were assessed via HPLC and compared with those obtained from whole blood and plasma from the same donor (Figure 14).

We found that 3.7 times more ϵ -ATP remain in washed blood cells than in human plasma after 30 min. Blood cells (washed) exhibited higher ϵ -ADP production than plasma after 30 min (10% vs 43%). During the first 15 min, more ϵ -AMP is more produced in human plasma than in blood cells (washed). Also, human plasma generates more ϵ -ADO than human blood cells. These findings suggest that soluble enzymes contribute more to ATP hydrolysis in human blood than cell-bound enzymes.

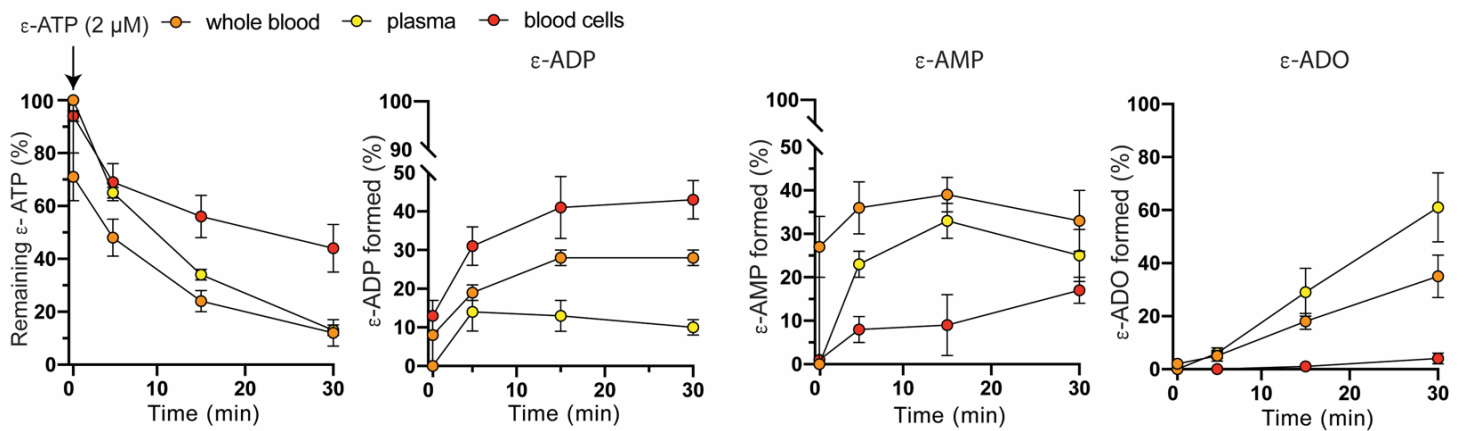


Figure 14: **Cell-free plasma breaks down added ATP more than blood cells (washed).** Whole blood was drawn by healthy volunteer and washed 1:15 with equal amount of HBSS. Whole blood was drawn by healthy volunteer and washed 1:15 with equal amount of HBSS. This is followed by centrifugation (400 x g, 10 min, 25°C). Supernatant, including the plasma was discarded. The remaining blood cells were then gently flicked on the Eppendorf tube side, resuspended 1:4 with HBSS and preincubated for 10min. 2 μ M ϵ -ATP was pipetted into the blood cells and incubated for up to 30 min on 37°C. At each respective timepoints (0, 5, 15 and 30 min), blood cells were transferred on ice for at least 5 min and centrifuged twice (1st run: 400 x g, 10min, 0°C; 2nd run: 2,300 x g, 5 min, 0°C). The resulting culture medium were treated with PCA and processed for HPLC analysis. Remaining ϵ -ATP, ϵ -ADP, ϵ -AMP, ϵ -adenosine products were determined, normalized to added ϵ -ATP and compared with the outcome from whole blood and plasma. Results were depicted separately as scatter plot (mean \pm SD, n = 3)

3.2 Enzymes involved in ATP breakdown in human blood

Our findings described above showed that plasma without blood cells is capable of hydrolyzing extracellular ATP and that it contributes more to ATP breakdown than blood cells. Here, we investigated which enzymes were involved in this breakdown. It is known that ENTPD1 (CD39) catalyzes the hydrolyzation of extracellular ATP to ADP and AMP in a stepwise manner[25], [59]. AMP is then converted to ADO by CD73, following the “classical” CD39-CD73 pathway. Also, ENPP1 utilize ATP as substrate to catalyze its breakdown to AMP and then to ADO by CD73, which is the “non-canonical” pathway (ENPP1-CD73 axis) [9].

3.2.1 CD39 contributes to ATP breakdown in human blood

To examine whether CD39 might be present in different blood compartments, we used a CD39 inhibitor, polyoxotungstate ($\text{Na}_6[\text{H}_2\text{W}_{12}\text{O}_{40}]$ POM-1). POM-1 is an anion complex containing the transition metal ion tungsten and is reported to suppress CD39 activity more vigorously than ARL 67156, another commonly used inhibitor of CD39 [129], [130]. Prior to that, our laboratory performed some pilot dose-dependent ATP breakdown experiments with human plasma with POM-1 to find out POM-1 concentration with the strongest inhibitory effect. Therefore, whole blood, drawn from healthy volunteer was first preincubated with different POM-1

concentrations, then with ATP. After 10 min, ATP and its breakdown products were measured via HPLC (Figure 15).

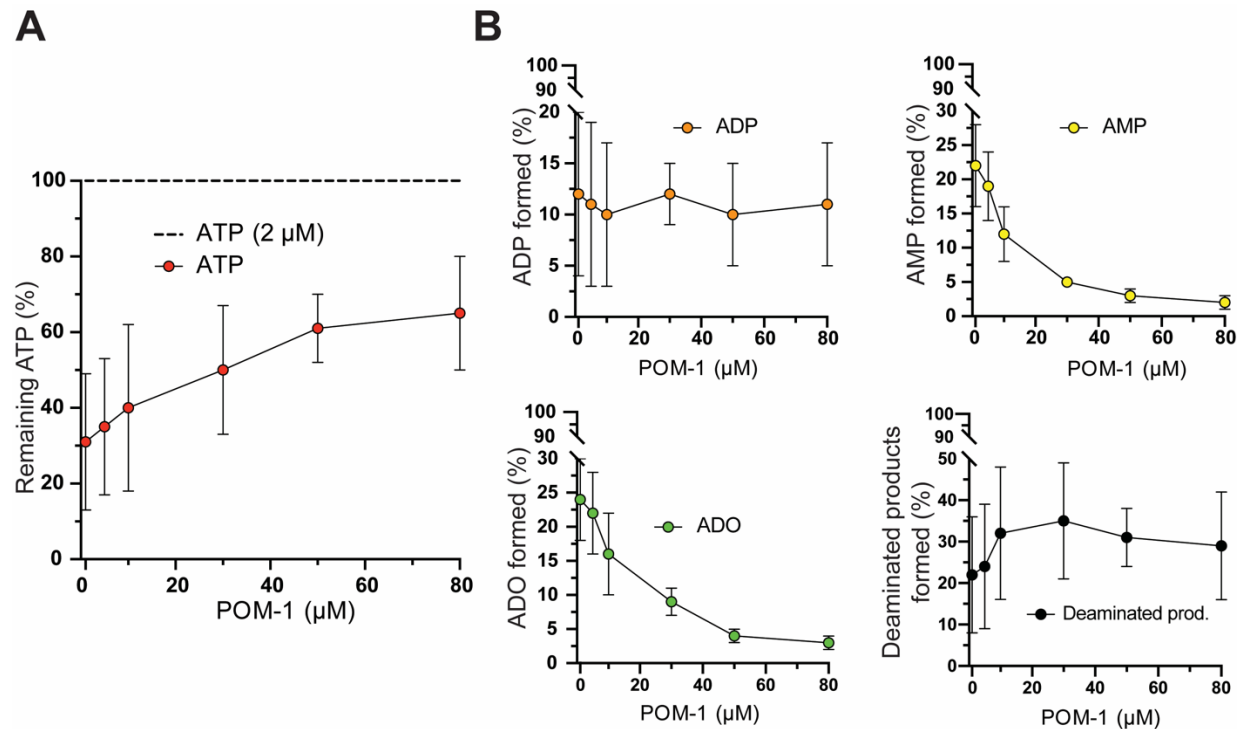


Figure 15: **Blocking CD39 with POM-1 dose-dependently reduces ATP breakdown in human plasma.** To test ENTPD1 on human plasma, blood was drawn from healthy donor and process to plasma via centrifugation (1st run: 400 x g, 10min, 0°C; 2nd run: 2,300 x g, 5 min, 0°C). The resulting plasma was preincubated dose-dependent POM-1 concentration. Then, 2 μM ATP was pipetted into the plasma and incubated for 10 min. To cease the metabolism, plasma was treated with PCA and further processed to HPLC analysis. Concentration of ATP remaining (A), ADP, AMP, ADO (B) and deaminated products were assessed and normalized to added ATP. Scatterplot showed mean ± SD with error bars as SD (n = 3).

HPLC analysis showed that POM-1 dose-dependently inhibited the breakdown of ATP up to a maximum of 65% remaining ATP. Moreover, ADP remained constant, and AMP and ADO production decreased. Under our experimental conditions, 80 μM POM-1 showed already the highest inhibitory effect on CD39, which is similar to the concentration of 100 μM POM-1 used by Wall *et. al* used to study the effect of CD39 in the central nervous system (CNS) of Wiscar rats [129].

Based on these results, we decided to use 80 μM POM-1 for further studying the presence of CD39 in blood cells and whole blood. Therefore, we collected blood from healthy donors and prepared aliquots of diluted whole blood, plasma, and washed blood cells as described above. All samples were preincubated with 80 μM POM-1 prior to the addition of 2 μM ε-ATP (blood, blood cells) or ATP (plasma). After 10 min, reactions were stopped in an ice water bath, supernatants were collected by centrifugation, and ATP leftover and its breakdown products

were assessed (Figure 16A-C). Whole blood exhibits a 3-fold increase of ATP and decrease of AMP and ADO level with the highest POM-1 concentration. When investigating the blood cells (washed), ATP accumulation from 45 to 65% was observed and accordingly, partial inhibition of ADP and AMP production. As ATP accumulation was shown in both blood compartments, we conclude that CD39 is present, as protein anchored to the transmembrane protein and as soluble enzyme.

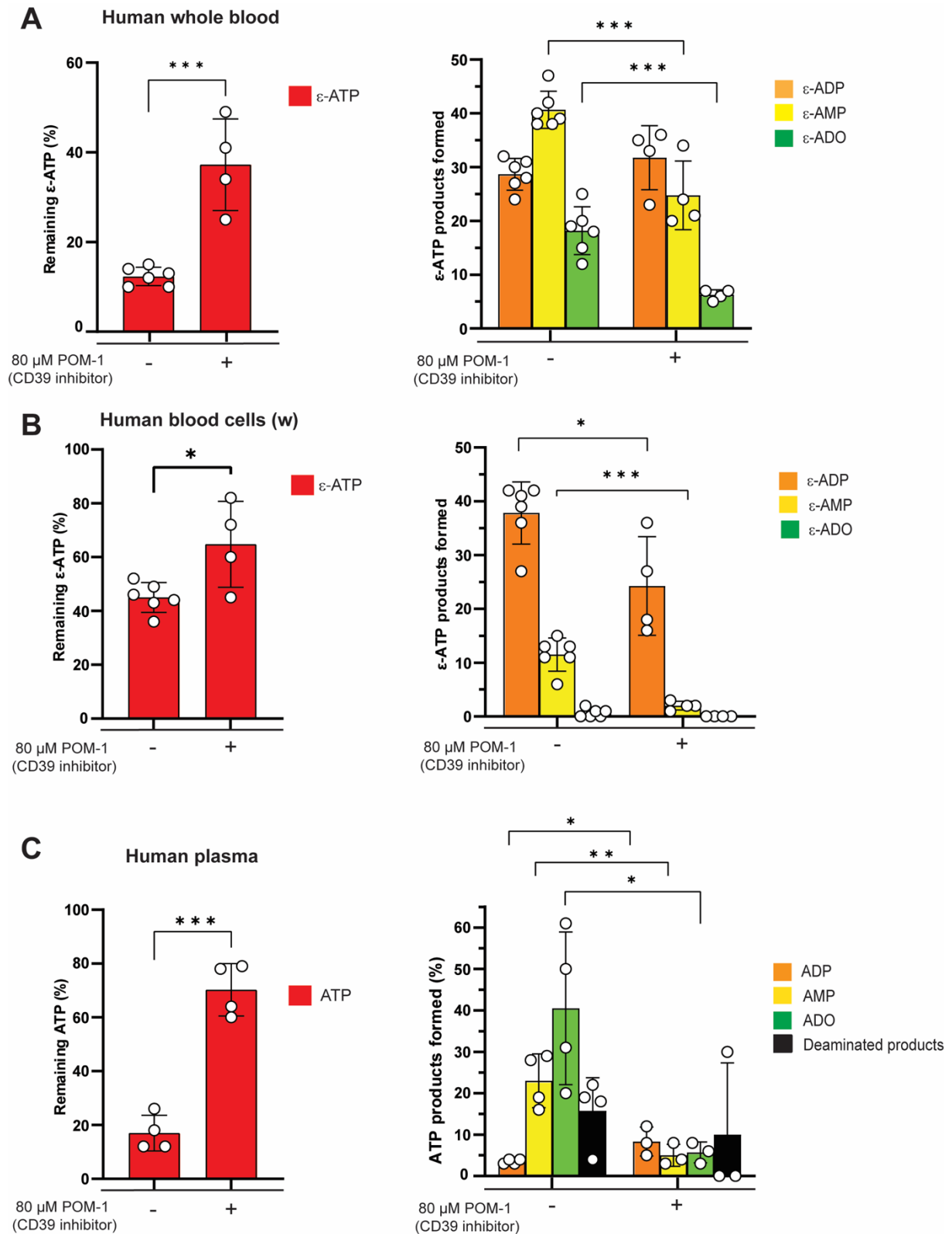


Figure 16: Soluble CD39 in plasma contributes more to ATP breakdown in human blood than cell-bound CD39. (A) Human whole Blood: Blood from healthy volunteer was drawn and preincubated with highest POM-1 concentration for 10 min. 2 μM ε-ATP was pipetted into the blood and incubated for 5 min. Reaction was stopped by putting whole blood on ice and plasma was obtained by two

centrifugation steps (1st run: 400 x g, 10min, 0°C; 2nd run: 2,300 x g, 5 min, 0°C). Then, plasma was treated with PCA and prepared for the HPLC analysis. (B) **Human blood cells:** Blood, drawn from healthy donor, were washed with HBSS to remove the plasma. Blood cells were then flicked on the bottom of Eppendorf tube and gently resuspended with HBSS or highest concentration of POM-1. These samples were preincubated for 10 min on 37 °C, then incubated with 2 μM ε-ATP for 5 min at 37 °C. To cease the reaction, washed blood cells were transferred on ice and processed, similar to whole blood. (C) **Human plasma:** Blood, drawn from healthy donor, were immediately cooled down and centrifuged, as described in (A) with the whole blood. The resulting plasma were pre-incubated with highest concentration of POM-1, then with 2 μM ATP for another 10min, both at 37 °C. PCA was added to cease the reaction and prepared for HPLC analysis. Purinergic compounds were measured in all three distinct blood compartments and normalized to the input ε-ATP or ATP, respectively. Bar graphs were shown as mean ± SD; with error bars as SD. n ≥ 3. Statistically significant differences are indicated with asterisks (*p<0.05 vs. control with HBSS/without POM-1; unpaired t-test)

3.2.2 Soluble ENPP1 in plasma contributes to ATP breakdown in human blood

ENPP1 also utilize extracellular ATP as a substrate to prevent P2 receptors from desensitization. To investigate this enzyme in the different blood compartments, we used the NPP1 inhibitor C to block the activity of ENPP1 or 3. Like CD39 inhibitor, we did some preliminary ATP breakdown experiments with NPP1 inhibitor C in a dose-dependent manner. The experimental set-up was similar to the experiment with POM-1 described above (3.2.1). ATP leftover and its breakdown products were depicted separately as scatter plots (Figure 17). Compared to the CD39 inhibitor POM-1, lower NPP1 inhibitor C concentrations were needed to inhibit ATP breakdown in human plasma. Moreover, ADP production remained constant, whereas AMP and ADO production was reduced with increasing NPP1 inhibitor C concentrations. In accordance with the study of Kawaguchi *et al.*[131], we could show 50 μM as the NPP1 inhibitor C concentration that yields the most inhibitory effect with about 78% of added ATP remaining.

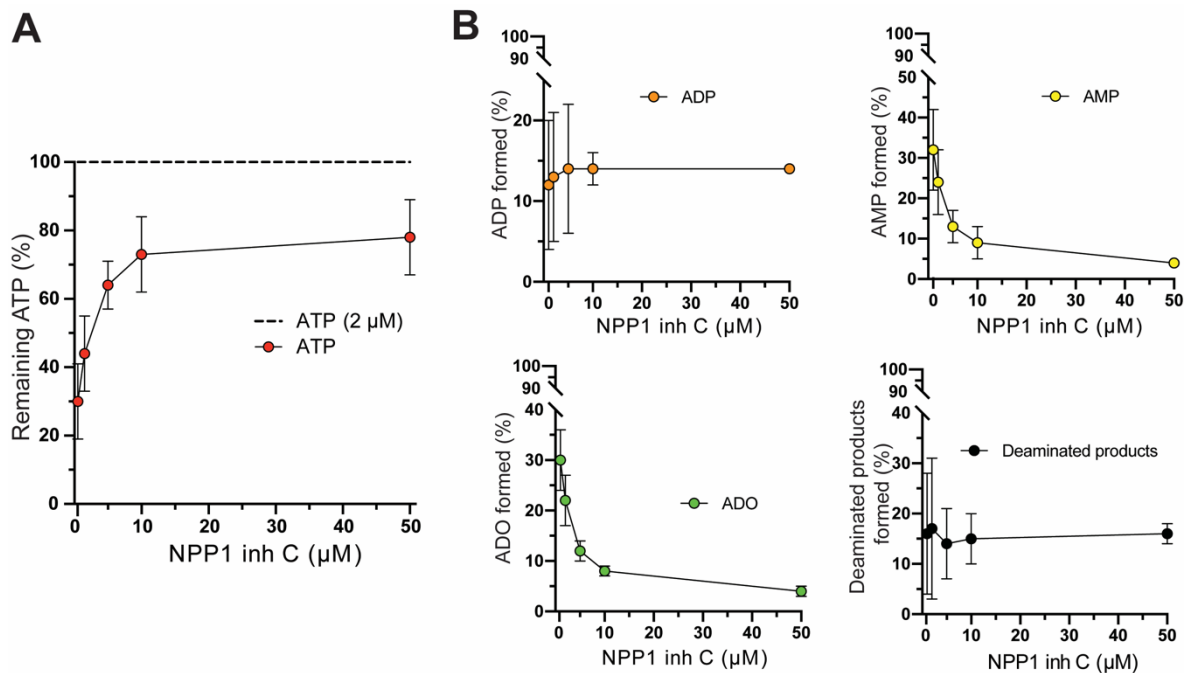


Figure 17: **Blocking ENPP1 with ENPP1 inhibitor C dose-dependently reduces ATP breakdown in human plasma.** Blood from healthy donor was drawn and processed to plasma via centrifugation (1st run: 400 x g, 10 min, 0°C; 2nd run: 2,300 x g, 5 min, 0°C). Plasma was then preincubated with dose-dependent concentrations of NPP1 inhibitor C. Then, 2 μM ATP was pipetted into the plasma and incubated for 10 min. Plasma was treated with PCA to precipitate proteins and further processed to HPLC analysis. Concentration of ATP remaining (A), ADP, AMP, ADO and deaminated products (B) were assessed and normalized to added ATP. Scatterplot showed mean ± SD with error bars as SD. (n = 3)

We investigated subsequently the presence of ENPP1 in whole blood and blood cells. We used the same experimental set-up, as already described when performing ATP breakdown experiment with POM-1. Whole blood, blood cell and plasma samples were preincubated with 50 μM NPP1 inhibitor C for 10 min before adding ε-ATP or ATP (plasma). ATP leftover as well as breakdown products were assessed and depicted as bar graphs (Figure 18). In whole blood, ATP levels increased 3-fold, accompanied by a significant decrease in AMP and ADO production whereas ADP did not change significantly. By contrast, no difference was observed between inhibitor-treated and untreated human blood cells. As described above, NPP1 inhibitor C significantly inhibited the breakdown of ATP resulting in a reduction of the amounts of AMP and adenosine formed while the formation of ADP slightly but significantly increased compared to plasma without inhibitor treatment. Based on this result, enzymatic activity of ENPP1 in human blood is restricted to soluble ENPP1 in the plasma.

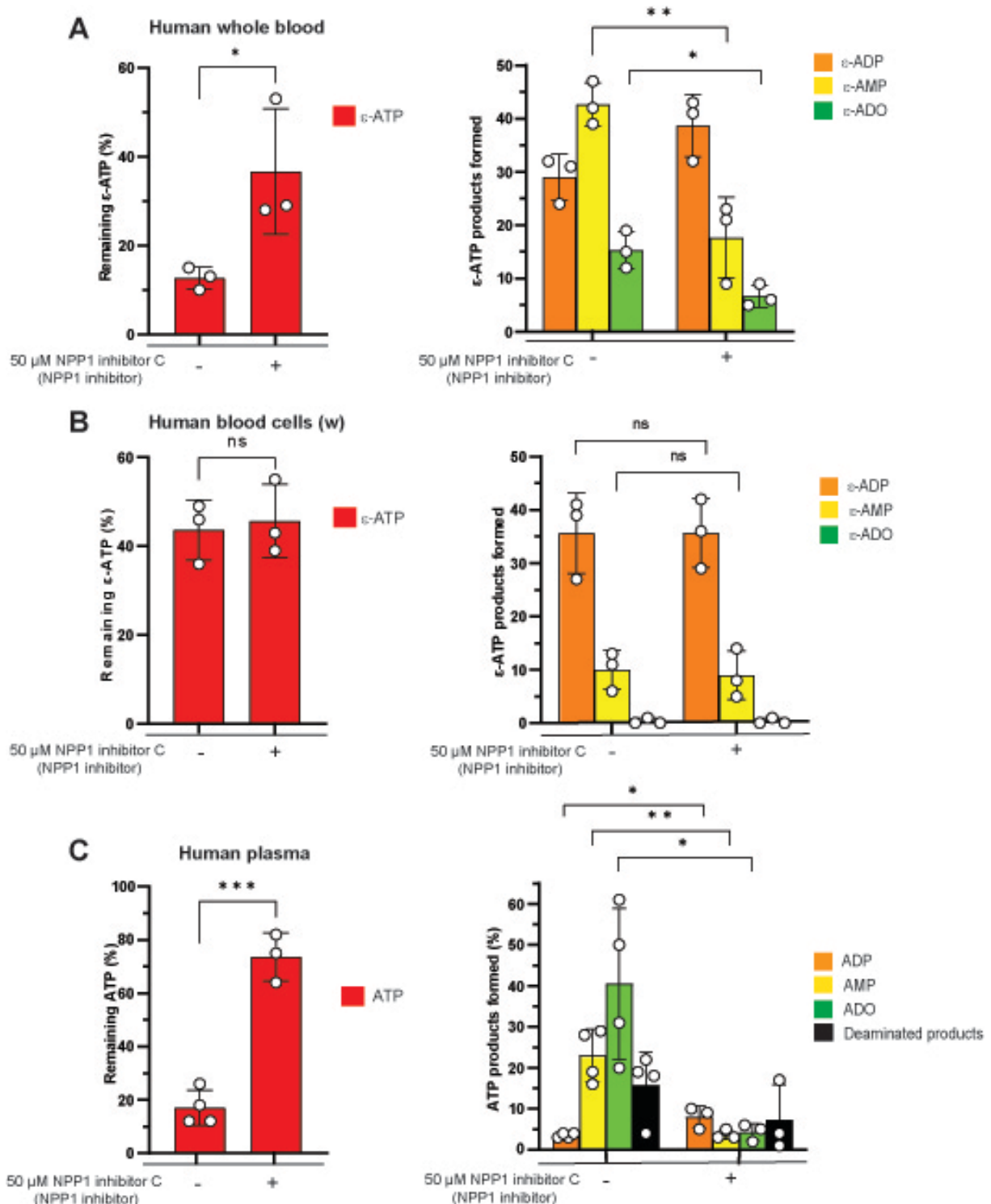


Figure 18: **Only soluble ENPP1 in plasma breaks down ATP in human blood. (A) Human whole Blood:** Blood from healthy volunteer was drawn and preincubated with 50 μ M NPP1 inhibitor C concentration for 10 min. 2 μ M ϵ -ATP was pipetted into the blood and incubated for 5 min. Reaction was ceased by transferring whole blood on ice and two centrifugation steps (1st run: 400 x g, 10min, 0°C; 2nd run: 2,300 x g, 5 min, 0°C) were performed to obtain plasma. Then plasma was treated with PCA and prepared for the HPLC analysis. (B) **Human blood cells:** Blood, drawn from healthy donor, were washed with HBSS to remove the plasma. Blood cells were then flicked on the bottom of Eppendorf

tube and gently resuspended with 50 μM NPP1 inhibitor C. These samples were preincubated for 10 min on 37 $^{\circ}\text{C}$, then incubated with 2 μM ϵ -ATP for 5 min at 37 $^{\circ}\text{C}$. To cease the reaction, washed blood cells were transferred on ice and processed, similar to whole blood. (C) **Human plasma:** Blood, drawn from healthy donor, were immediately cooled down and centrifuged, as described in (A) with the whole blood. The resulting plasma were preincubated with 50 μM NPP1 inhibitor C concentration, then with 2 μM ATP for another 10min, both at 37 $^{\circ}\text{C}$. PCA was added to cease the reaction and prepared for HPLC analysis. Purinergic compounds were measured in all three distinct blood compartments and normalized to the input ϵ -ATP or ATP, respectively. Bar graphs were shown as mean \pm SD; with error bars as SD. $n \geq 3$. Statistically significant differences are indicated with asterisks (* $p < 0.05$ vs. control with HBSS/without NPP1 inhibitor C; unpaired t-test)

3.2.3 CD73 and other mechanisms regulate AMP levels in human blood

CD73 plays a role in purinergic signaling as it is considered as a checkpoint control for adenosine, which exerts mostly anti-inflammatory functions on immune cells [75]. To investigate whether cell- bound or soluble CD73 activity is more pronounced in human blood, we used PSB12379 as inhibitor. The latter hinders this enzyme from utilizing AMP as substrate. Similar to POM-1 and NPP1 inhibitor C, we performed pilot experiments to determine a specific PSB12379 concentration that shows the maximum of inhibitory effect. Therefore, we used the same experimental design from our previous preliminary ATP breakdown experiment (3.2.1 and 3.2.2) with POM-1 and NPP1 inhibitor C (human plasma, preincubation with CD73 inhibitor and 10 min incubation with ATP). ATP leftover as well as breakdown products (Figure 19) were determined and illustrated as scatter plots.

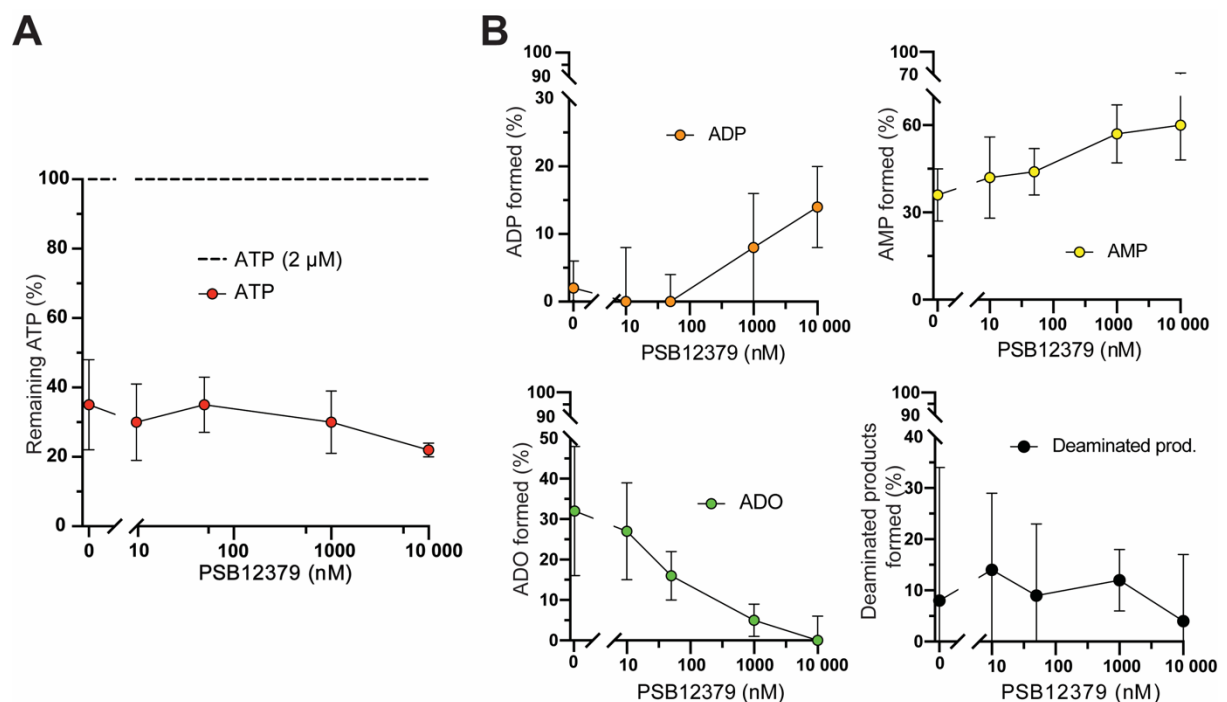


Figure 19: **The CD73 inhibitor PSB12379 dose-dependently reduces AMP breakdown in human plasma.** Blood from healthy donor was drawn and processed to plasma via centrifugation (1st run: 400 x g, 10min, 0°C; 2nd run: 2,300 x g, 5 min, 0°C). Plasma was then preincubated with dose-dependent concentrations of PSB12379 (10 nM, 50 nM 1 μ M and 10 μ M were used). Then, 2 μ M ATP was pipetted into the plasma and incubated for 10 min at 37°C. Plasma was treated with PCA to stop the reaction and further processed to HPLC analysis. Concentration of ATP remaining, ADP, AMP, ADO and deaminated products were assessed and normalized to added ATP. Scatterplot showed logarithmic mean \pm SD with error bars as SD (n = 3).

As expected, AMP production increased, and ADO decreased with increasing CD73 inhibitor concentration. At the highest concentration (10 μ M), about 60% of the added ATP was converted to AMP while the production of ADO was completely prevented. The percentage of remaining ATP was mostly independent from the inhibitor concentration but slightly decreased at the highest concentration. ADP production was low reaching a maximum of 15% at the highest PSB12379 concentration. Based on our results, we chose 10 μ M of CD73 inhibitor to examine the presence of CD73 on blood cells and whole blood.

We studied subsequently how CD73 is present in whole blood and blood cells. We applied the same experimental design on blood cells and whole blood when studying CD39 and NPP1 inhibitor. Blood cells (washed) or whole blood was preincubated with 10 μ M PSB12379 for 10 min. Then, ϵ -ATP (blood, blood cells) or ATP (plasma) were added, and ATP, ADP, AMP and ADO were assessed after 10 min, respectively (Figure 20A-C). No significant differences were observed in whole blood. Interestingly, applying CD73 inhibitor induced ATP degradation and ADP accumulation in washed blood cells, resulting in 13% ATP and 76% ADP, respectively. In human plasma, AMP accumulation (60%) was observed while ADO production was completely suppressed. Taken together, CD73 as cell-bound enzyme and soluble enzyme are present in both blood cells and plasma and other mechanisms regulate the loss of CD73 in human blood cells.

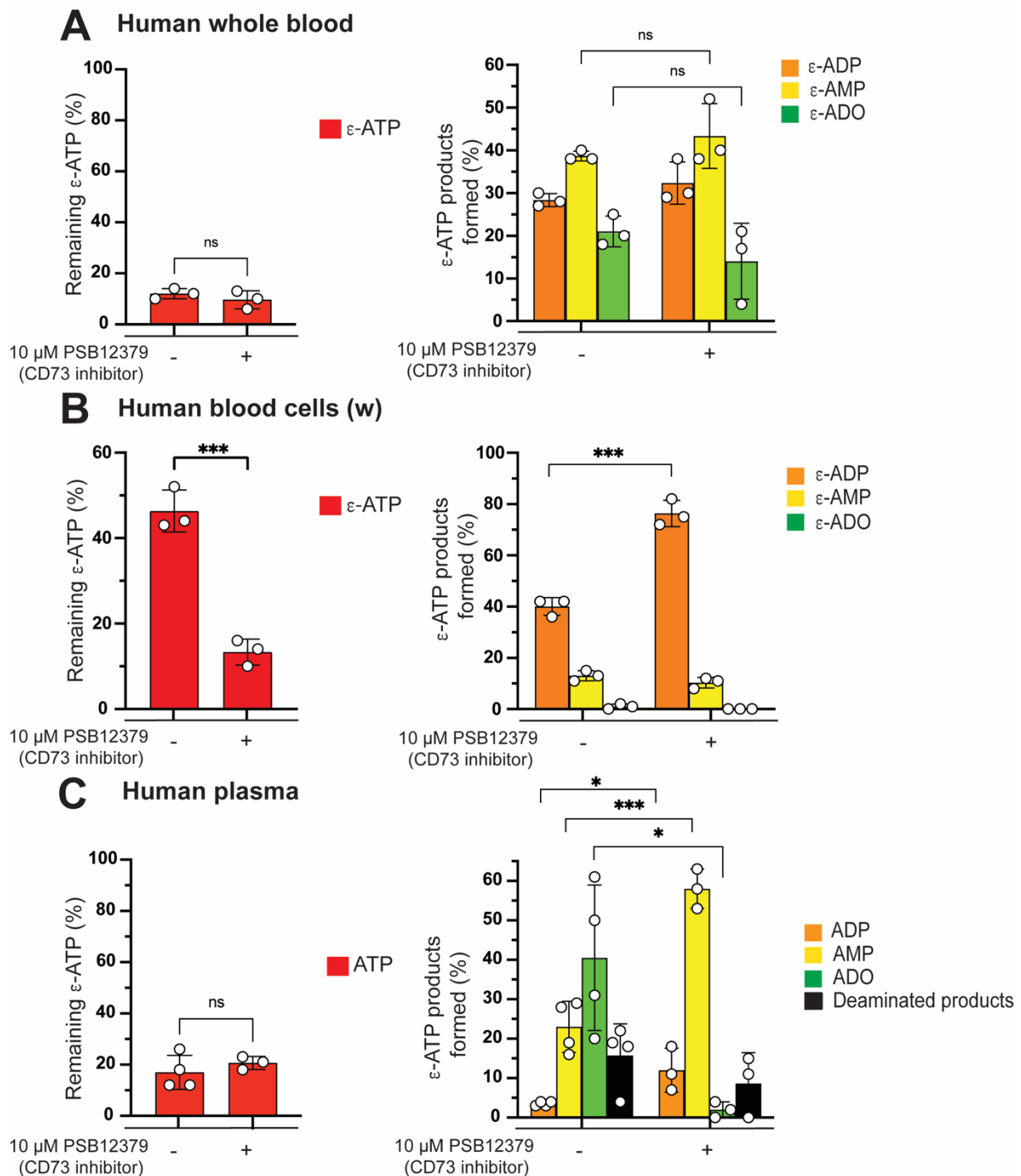


Figure 20: **Effect of CD73 inhibition on ATP hydrolysis in human blood.** (A) **Human whole blood:** Blood from healthy volunteer was drawn and pre-incubated with 10 μ M PSB12379 (CD73 inhibitor) or HBSS. 2 μ M ϵ -ATP was pipetted into the blood and incubated for 5 min. Reaction was ceased by transferring whole blood on ice and two centrifugation steps (1st run: 400 x g, 10min, 0 $^{\circ}$ C; 2nd run: 2,300 x g, 5 min, 0 $^{\circ}$ C) were performed to obtain plasma. Then plasma was treated with PCA and prepared for the HPLC analysis. (B) **Human blood cells:** Blood, drawn from healthy donor, were washed with HBSS to remove the plasma. Blood cells were then flicked on the bottom of Eppendorf tube and gently resuspended with HBSS or 10 μ M PSB12379. These samples were preincubated for 10 min on 37 $^{\circ}$ C,

then incubated with 2 μM ϵ -ATP for 5 min at 37 °C. To cease the reaction, washed blood cells were transferred on ice and processed, similar to whole blood. (C) **Human plasma:** Blood, drawn from healthy donor, were immediately cooled down and centrifuged, as described in (A) with the whole blood. The resulting plasma was pre-incubated with 10 μM PSB12379 or HBSS (control), then with 2 μM ATP for another 10min, both at 37 °C. PCA was added to cease the reaction and prepared for HPLC analysis. Purinergic compounds were measured in all three distinct blood compartments and normalized to the input ϵ -ATP or ATP, respectively. Bar graphs were shown as mean \pm SD; with error bars as SD. $n \geq 3$. Statistically significant differences are indicated with asterisks ($*p < 0.05$ vs. control with HBSS/without PSB12379; unpaired t-test)

3.3 The role of co-enzymes in ATP breakdown in human blood

Ectonucleotidases such as CD39 or ENPP1 require metal-ions like calcium (Ca^{2+}) or zinc (Zn^{2+}) to perform catalytic activity on ATP, ADP, and AMP as substrate. By contrast, EDTA and EGTA are chelating agents that scavenge such metal-ions. EGTA tends to exhibit more affinity to Ca^{2+} metal ions, whereas EDTA to Mg^{2+} and Zn^{2+} [132]. Moreover, EDTA is commonly used to prevent blood clotting in clinical samples. As EDTA induced ATP accumulation in whole blood [125], we studied how changes in metal-ions influence ectonucleotidase activity and the corresponding ATP breakdown profile.

3.3.1 Ca^{2+} and other metal-ions are crucial for ATP hydrolysis

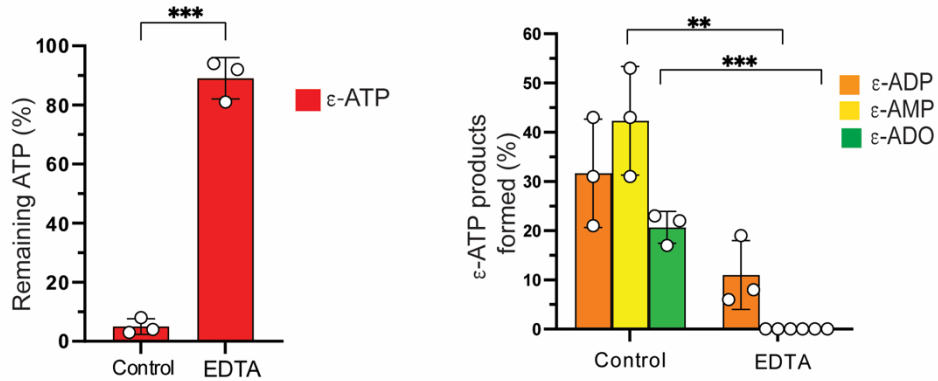
Firstly, we investigated how EDTA and EGTA influence ATP levels and the levels of its breakdown products in plasma. According to the concentration used in EDTA vacutainer tubes (6.15 mM), 5 mM should be sufficient to chelate all free metal ions in blood. Whole blood from a healthy donor was drawn in heparin tubes and plasma was obtained from whole blood via centrifugation. Then, plasma was preincubated with EDTA or EGTA. ATP was added to the plasma and the latter was incubated for 10 min. After that, ATP levels and its breakdown products were measured and illustrated as bar graphs (Figure 21C).

We observed a significant accumulation of ATP in EDTA- or EGTA-treated human plasma, compared to control plasma that was treated only with HBSS. Interestingly, EDTA blocked AMP and ADO production completely whereas in EGTA-treated plasma, ectonucleotidases could produce a low amount of AMP and ADO (3%). Deaminated products are slightly elevated in both chelating agents.

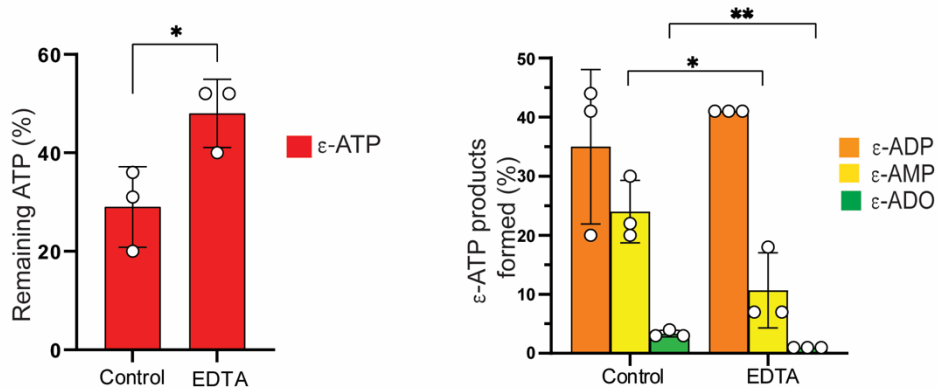
To gain an overall understanding, we further investigated how chelating agents alter ectonucleotidase activity in blood cells and whole blood and whether there are differences between cells and plasma. Therefore, whole blood or washed blood cells, drawn in an EDTA vacutainer were diluted with HBSS, and ϵ -ATP was added. ATP levels and its purinergic derivatives were measured and depicted as bar graphs (Figure 21A, B). Like in plasma, ATP

accumulation was observed in human whole blood treated with EDTA while the production of its breakdown products, in particular AMP and ADO, was inhibited. By contrast, ATP breakdown was also significantly reduced in EDTA-treated blood cells but to a lesser extent. This could explain that restoring physiological concentrations of ionized calcium (Ca^{2+}) by washing out EDTA and resuspending cells in HBSS is sufficient to restore the majority of cell-bound ectonucleotidase activity. Our results demonstrate the importance of Ca^{2+} and other metal ions for ATP breakdown by ectonucleotidase.

A Human whole blood



B Human blood cells (w)



C Human plasma

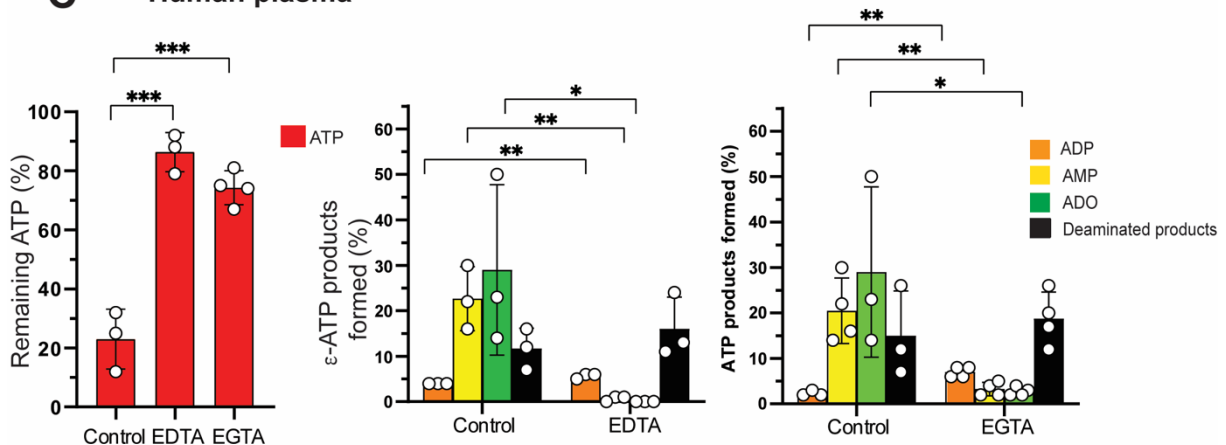


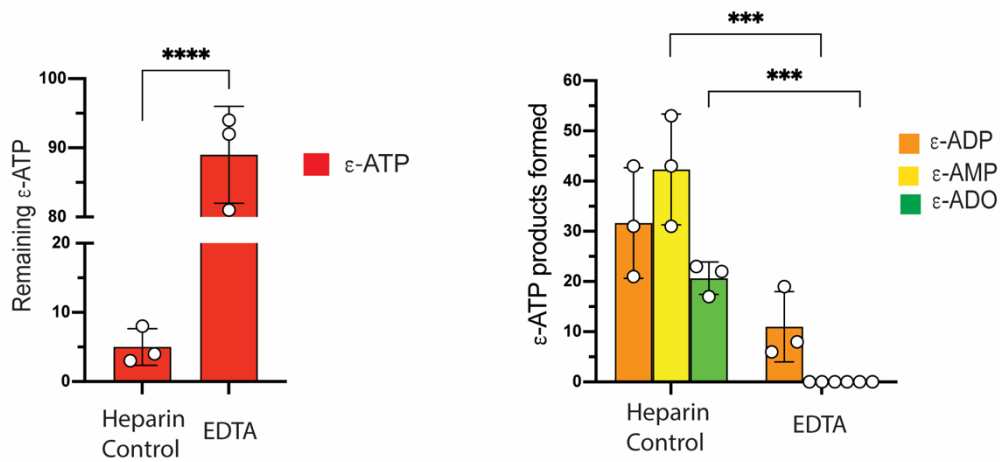
Figure 21: **Coenzymes play a major role in supporting ATP breakdown by soluble enzymes in human plasma.** (C) **Human plasma:** Blood, drawn from healthy donor in lithium-heparin vacutainer, were immediately cooled down and centrifuged twice (1st run: 400 x g, 10 min, 0°C; 2nd run: 2,300 x g, 5 min, 0°C). The resulting plasma was preincubated with 5 mM EGTA, EDTA or HBSS (control), then with 2 μM ATP for another 10min, both at 37 °C. Plasma was treated with PCA to cease the reaction and prepared for HPLC analysis. (A) **Human whole Blood (WB):** Blood from healthy volunteer was drawn in either heparin (here named as “control”) or EDTA vacutainer. Both heparin and EDTA blood

were diluted with HBSS and then subjected with ϵ -ATP for 5min at 37 °C. Reaction was ceased by transferring whole blood on ice and two centrifugation steps (1st run: 400 x g, 10min, 0°C; 2nd run: 2,300 x g, 5 min, 0°C) were performed to obtain plasma. Then plasma was treated with PCA and prepared for the HPLC analysis. (B) **Human blood cells (washed)**: Whole blood, drawn from healthy donor in heparin (“control”) or EDTA vacutainer, was washed with HBSS to remove the plasma. Blood cells were then flicked on the bottom of Eppendorf tube and gently resuspended with equal amount of HBSS. Washed blood cells were preincubated for 10 min, then incubated with 2 μ M ϵ -ATP for 10 min at 37 °C. To cease the reaction, washed blood cells were transferred on ice and processed, similar to whole blood to obtain the culture medium. Purinergic compounds were measured in all three distinct blood compartments and normalized to the input ϵ -ATP or ATP, respectively. Bar graphs were shown as mean \pm SD; with error bars as SD. n = 3. Statistically significant differences are indicated with asterisks (*p<0.05 vs. heparin control; unpaired t-test)

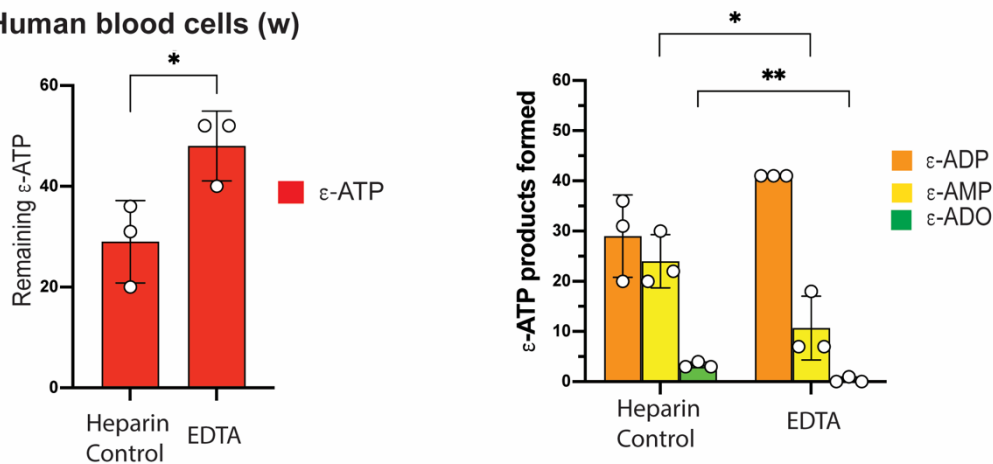
3.3.2 Calcium cannot restore ATP breakdown in EDTA-treated human plasma but in blood cells

As Ca^{2+} partially restore ATP breakdown in EDTA treated human blood cells (washed), we would like to know whether similar findings occur in EDTA treated plasma and whole blood, as control. Therefore, we apply physiological Ca^{2+} to resemble *in vivo* situation in human. Whole blood or plasma from healthy volunteer, drawn in EDTA vacutainer was preincubated with HBSS (1.2 mM Ca^{2+}), then with ϵ -ATP for 5 min. Remaining ATP and its breakdown products of human whole blood and plasma were assessed with HPLC (Figure 22A, C). As comparison, we depicted the outcome of our previous experiment with blood cells (Figure 22B). In whole blood and plasma, we could identify some similar breakdown pattern. ATP accumulation occurs significantly by 4.5-fold and low amount of AMP and adenosine level was detected. Our results show that physiological ionized Ca^{2+} does not induce replenishment of ATP breakdown in cell-free plasma, compared to blood cells (washed).

A Human whole blood



B Human blood cells (w)



C Human plasma

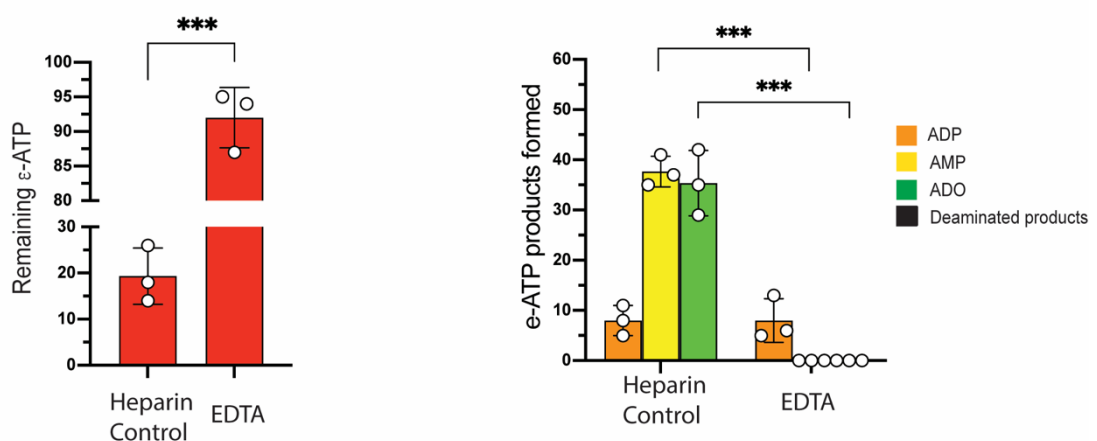


Figure 22: **Physiological Ca^{2+} did not induce replenishment of ATP breakdown in human whole blood and plasma, but so did human blood cells (washed).** (A) **Human whole Blood:** Blood from healthy volunteer was drawn in either heparin or EDTA vacutainer. Both heparin and EDTA blood were preincubated and diluted 1:2 with HBSS for 10 min at 37 °C. Then, 2 μM ϵ -ATP was subjected into whole blood for 5 min at 37 °C. Reaction was ceased by transferring whole blood on ice and two centrifugation steps (1st run: 400 x g, 10 min, 0°C; 2nd run: 2,300 x g, 5 min, 0°C) were performed to obtain plasma.

Then plasma was treated with PCA and prepared for the HPLC analysis. (B) **Human blood cells (washed)**: For comparison, we included the results from our previous experiment. (C) **Human plasma**: Blood, drawn from healthy donor in heparin and EDTA vacutainer, were immediately chilled down and centrifuged twice (1st run: 400 x g, 10min, 0°C; 2nd run: 2,300 x g, 5 min, 0°C). The resulting plasma was preincubated with 5 mM EGTA, EDTA or HBSS (control), then with 2 μM ATP for another 10 min, both at 37 °C. Plasma was treated with 8M PCA to cease the reaction and prepared for HPLC analysis. Bar graphs were shown as mean ± SD; with error bars as SD. n ≥ 3. Statistically significant differences are indicated with asterisks (*p<0.05 vs. heparin control; unpaired t-test).

It could be that more Ca²⁺ was required to restore ATP breakdown in EDTA treated plasma. To test this assumption, we applied more Ca²⁺ in a dose dependent manner. EDTA plasma from previous donor was taken and diluted 50-fold with increased Ca²⁺ concentration. Natural ATP was introduced into the plasma and ATP remain as well as its breakdown products were analyzed and depicted as scatter plot (Figure 23). No further changes in ATP breakdown were observed. Little or no AMP and adenosine was formed with increased Ca²⁺ concentration. Despite fluctuation, ATP and ADP level remain constant. Taken together with our previous findings, Ca²⁺ did not lead to replenishment of ATP breakdown in EDTA human plasma. However, this was achieved with human blood cells (washed).

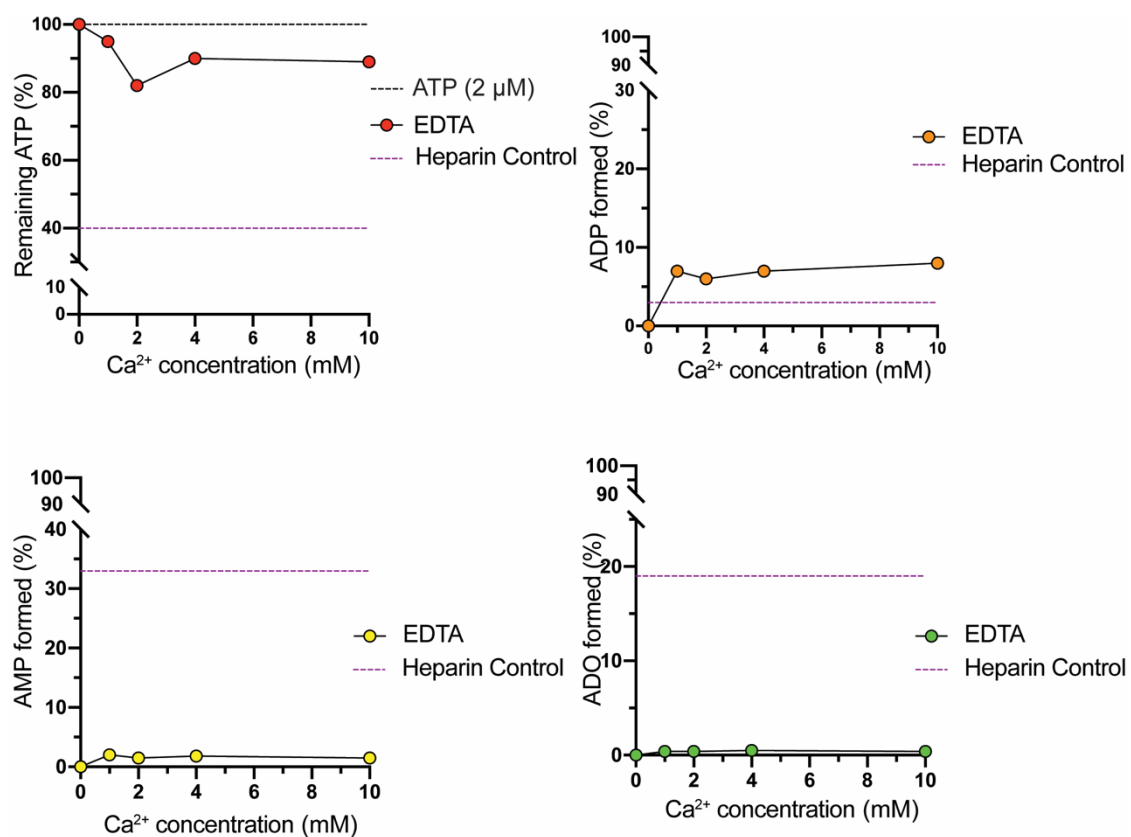


Figure 23: **Ca²⁺ dose-dependently does not restore ATP breakdown in EDTA treated plasma.** EDTA and heparin control plasma from previous donor was taken and preincubated in increased Ca²⁺ concentration (1,2, 4 and 10 mM CaCl₂) for 10 min at 37°C. Then, 2 μM ATP was applied into the plasma and incubated for 60 min at 37°C. To cease the reaction, plasma was treated with 8 M PCA and

processed for HPLC analysis. Concentration of ATP remaining, ADP, AMP, ADO and deaminated products were assessed and normalized to added ATP. Scatterplot were shown (n = 1).

3.3.3 Zinc can partially restore ATP breakdown in human plasma

Our results above (3.3.2.) show that EDTA completely suppresses ATP breakdown activity in both whole blood and plasma. As replenishing calcium (Ca^{2+}) alone did not restore enzymatic activity in EDTA treated plasma, we investigated whether Zn^{2+} was the missing “puzzle” needed by ectonucleotidases for ATP hydrolysis. To “eliminate” the effect of EDTA and give enzymes sufficient time to reconstitute, we diluted the EDTA treated plasma 1:50 with HBSS containing physiological concentrations of Ca^{2+} and Mg^{2+} and preincubated it with 10-fold Zn^{2+} concentration in the range of 1-1000 μM for 30 min. We added ATP into the plasma and measured the level of ATP and its derivatives via HPLC (Figure 24).

Notably, more Zn^{2+} input restored catalytic enzyme activity in EDTA plasma. Moreover, AMP production was increased steadily, yielding 17% at the highest Zn^{2+} concentration. Corresponding to AMP, a small amount of ADO was also observed at the two highest Zn^{2+} concentrations. ADP production remained unchanged. However, even at the highest Zn^{2+} concentration, ATP breakdown did not reach the same level as in heparin-treated control plasma. To conclude, we could demonstrate partial replenishment of ATPase in EDTA treated plasma by adding Zn^{2+} . According to the illustrated ATP breakdown profile, we could also identify ENPP1 or ENPP3 as these proteins require Zn^{2+} for their functionality.

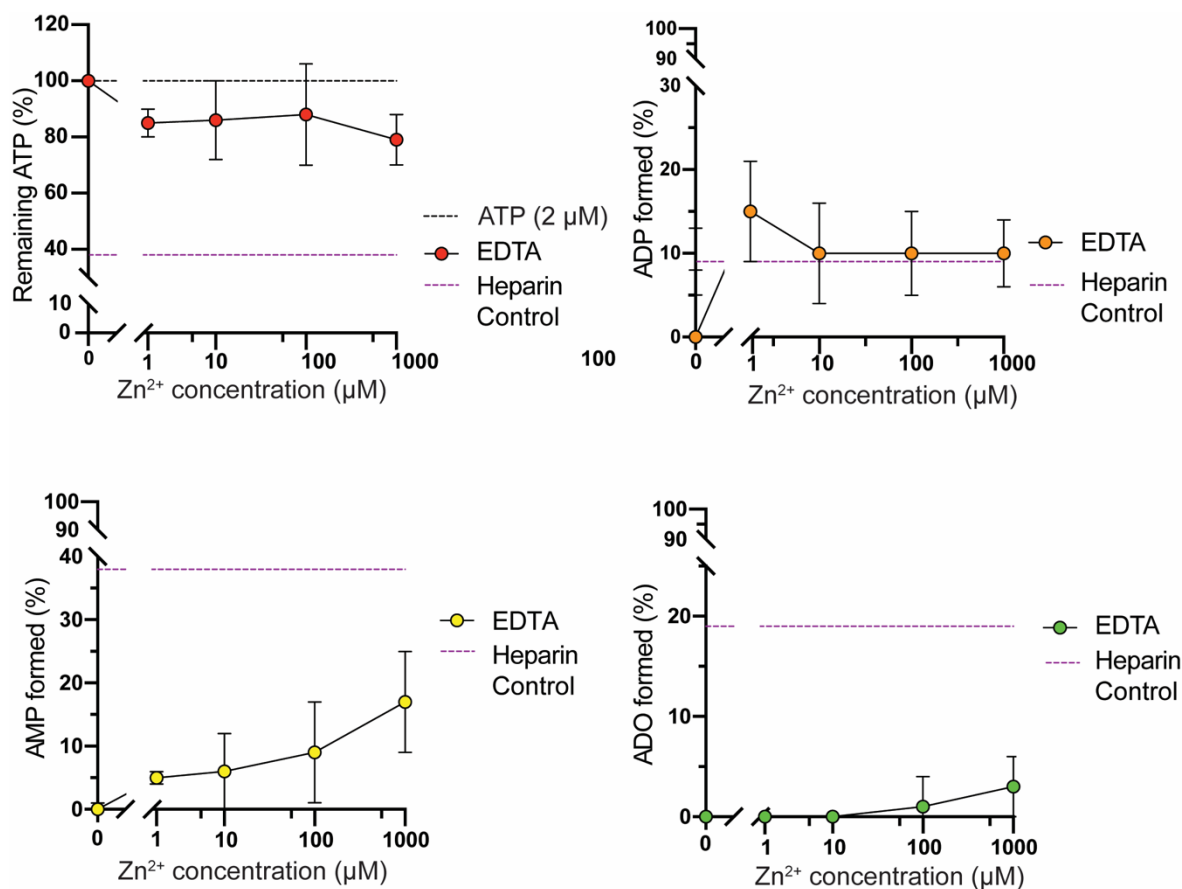


Figure 24: **Zinc can partially restore ATP breakdown in EDTA-treated human plasma.** Blood, drawn from healthy donor in heparin or EDTA vacutainer, were immediately cooled down and centrifuged twice (1st run: 400 x g, 10 min, 0°C; 2nd run: 2,300 x g, 5 min, 0°C). To neutralize EDTA effect, we diluted the plasma 1:50 and pre-incubated it with 10-fold Zn²⁺ concentration (1-1000 µM) for 30 min at 37 °C. Then, 2 µM ATP was introduced into the plasma and incubated for another 60 min at 37 °C. Reaction was ceased by treating the plasma with PCA and cool it on ice. Samples were further processed to analyze on HPLC. ATP, ADP, AMP and ADO levels were determined and normalized to added ATP. 10-fold Zn²⁺ concentration (1, 10, 100 and 1000 µM) were here shown logarithmic. Scatter plots were shown as mean ± SD, with error bars as SD. n = 3.

3.3.4 Zinc induces minor changes in ATP breakdown in blood cells

We studied subsequently whether Zn²⁺ increased ATP hydrolysis in EDTA-treated blood cells. Previously, we could reveal that Ca²⁺ is sufficient to restore breakdown activities of ATP in blood cells (washed). Therefore, washed blood cells were resuspended and preincubated with 10-fold Zn²⁺ concentration in the range of 1-1000 µM and ε-ATP was introduced into the washed blood cells. The remaining ATP as well as ADP, AMP and ADO were assessed and analyzed via HPLC (Figure 25). We found that only 1 mM of Zn²⁺ induced a minor effect on washed blood cells (more ATP degradation, more ADP and AMP production). Our results show that blood cells (washed) do not necessarily need zinc to further ATP degradation.

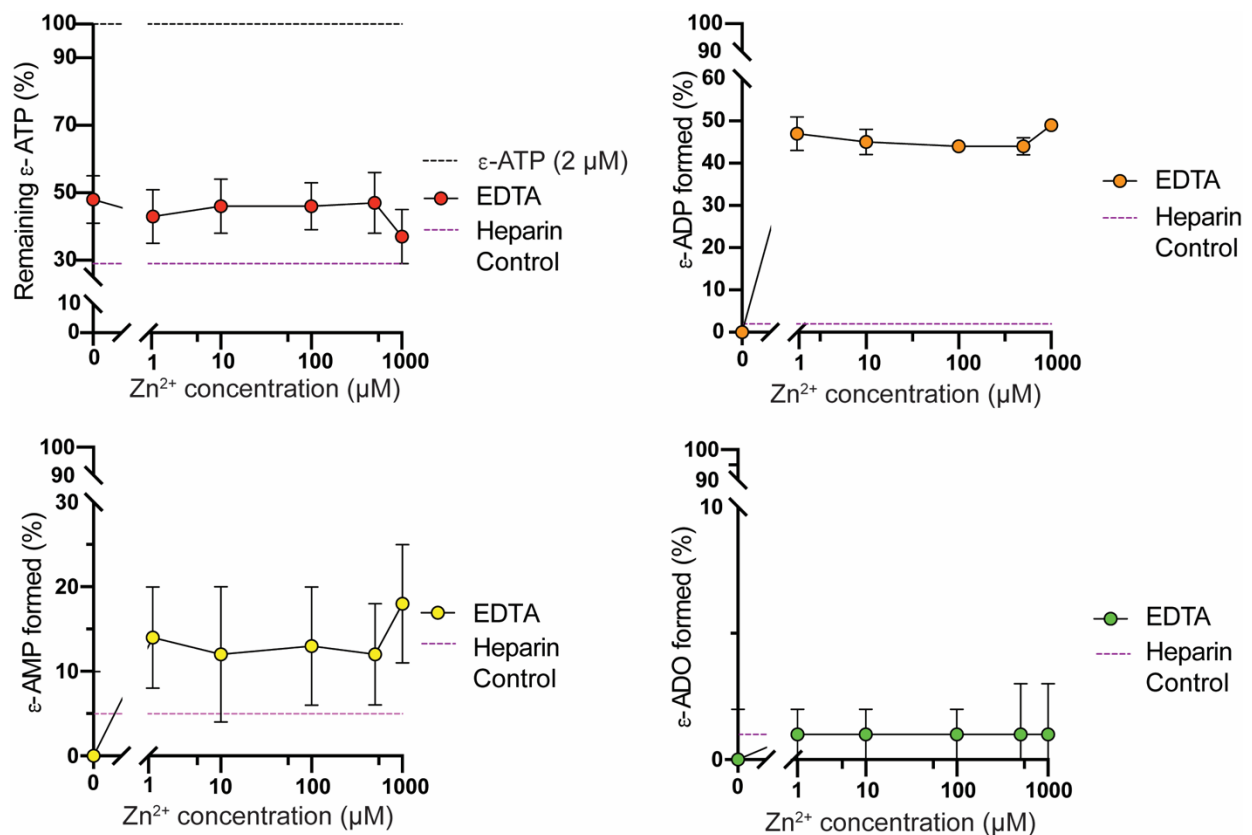


Figure 25: Substitution of **Zinc barely restores ATP breakdown in EDTA-treated blood cells**. Blood, drawn from healthy donor in lithium-heparin or EDTA vacutainer, were diluted 1:15 with HBSS and centrifuged 400 x g, 10 min, for 25°C. HBSS and plasma were discarded. Blood cells were then flicked on Eppendorf tube side and resuspended with 10-fold Zn²⁺ concentration. Samples were then pre-incubated for 30 min at 37°C. 2μM ε-ATP was subjected to the blood cells and incubated for another 10 min at 37°C. Reaction was stopped by transferring on ice and two sequential centrifugations (1st run: 400 x g, 10 min, 0°C; 2nd run: 2,300 x g, 5 min, 0°C) were performed to obtain the plasma. The latter was treated with PCA and prepared to analyze on HPLC. ATP, ADP, AMP and ADO levels were determined and normalized to added ATP. 10-fold Zn²⁺ concentration (1, 10, 100 and 1000 μM) were here shown logarithmic mean ± SD, with error bars as SD (n = 3).

3.4 Mice vs Human blood

3.4.1 ATP breakdown in mouse blood, but not plasma is more rapid than in human blood

In the previous section, we demonstrated that ectonucleotidases and their coenzymes are key regulators that degrade ATP and ADP to AMP and ADO in humans. It is known that mice and humans share functionalities on the genomic level. Therefore, we were wondering if we could observe similar findings in mice. We started by investigated whether overall ATP breakdown is different in mouse compared to human blood. As we found previously that human plasma

performed the majority of ATP breakdown, our focus was therefore more on the plasma and whole blood, as comparison.

To examine the ATP breakdown profile, healthy C57BL/6J mice, aged 15 ± 1 week ($n = 4$), were anaesthetized and whole blood was drawn in heparin syringes via cardiac puncture. We split mice whole blood in two moieties one of which was processed to plasma. Both whole blood and plasma were subjected to ϵ -ATP or ATP, respectively. We measured ATP levels and its derivatives at different time points (0,5,15,30 and only in plasma, 60 min) and displayed the results as scatter plots (Figure 26A: whole blood, Figure 26B: mice plasma). The results from the ATP breakdown time-response experiment with human samples shown in Figure 11 and Figure 13B were included as comparison.

Compared to humans, ATPases in whole blood of mice metabolized extracellular ATP to ADP and other derivatives more expeditiously than enzymes in human whole blood. HPLC analysis revealed that 96% of the added ATP was degraded immediately after pipetting it into the whole blood and remained after that unchanged over the incubation time. Also, mice exhibited a rapid increase in ADP and AMP that slowly degraded over time afterwards. In comparison, human whole blood produced more ADP and AMP over time. Mice exhibited 4-fold (beginning, 0min) and 5-fold (after 30 min) higher ADO levels than humans (Figure 26A). It seems likely that ectonucleotidases in mouse whole blood metabolize extracellular ATP, ADP and AMP to ADO more rapidly than in human whole blood. By contrast, ATP metabolism in mouse plasma was significantly slower than in whole blood but displayed a similar ATP breakdown pattern as in human plasma (Figure 26B). ATPases in mouse plasma hydrolyzed 88% of added ATP within 15 min which was then decelerated. ADP and AMP production reached their peak at 22% and 29% at 5 min, respectively and were slowly degraded after that. ADO and deaminated products increased gradually over time, yielding 52% and 43% after 60 min, respectively.

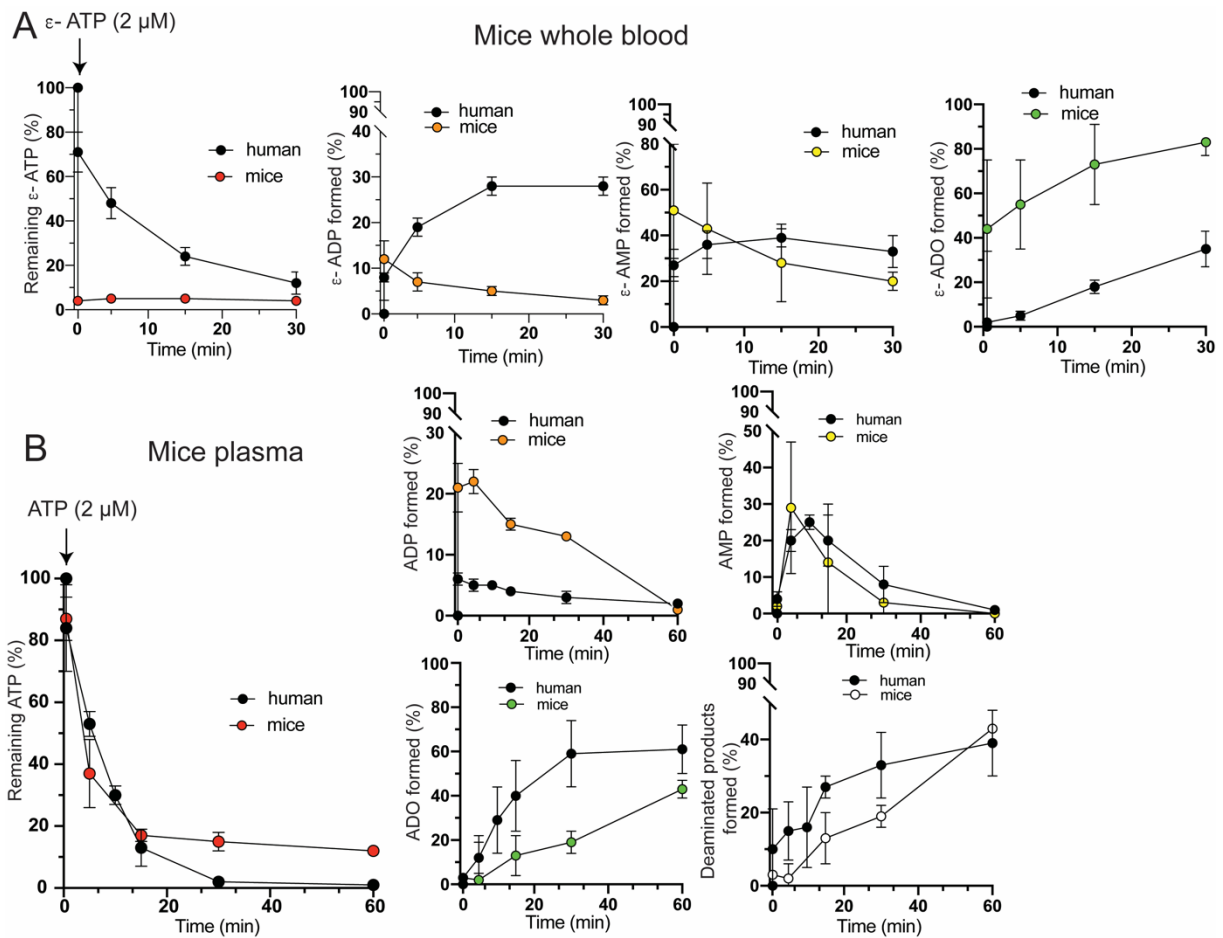


Figure 26: **ATP breakdown by blood cells, but not by plasma, is more rapid in mice than in humans.** Mice aged 15 ± 1 weeks were anaesthetized under isoflurane chamber and cardiac puncture method was applied to collect the blood via heparin syringe. Blood was split into two fractions. **(A) Mice whole Blood:** One fraction (Whole blood) was diluted 1:4 and pre-incubated for 10 min at 37°C . $2 \mu\text{M}$ ϵ -ATP was subjected into the whole blood and incubated up to 30 min. At each respective timepoints (0, 5, 15 and 30 min), whole blood was cooled on ice for 5 min to cease the metabolism. Two sequential centrifugations were applied (1st run: $400 \times g$, 10 min, 0°C ; 2nd run: $2,300 \times g$, 5 min, 0°C). Plasma was obtained and then treated with PCA to prevent further breakdown. **(B) Mice plasma:** The other fraction was immediately cooled on ice and processed to plasma with two centrifugation steps, as previously described in mice whole blood. Plasma was then diluted 1:4 with HBSS and pre-incubated for 10 min at 37°C . $2 \mu\text{M}$ ATP were pipetted into the plasma and incubated up to 60 min at 37°C . At each respective timepoints (0, 5, 15, 30 and 60 min), plasma was treated with PCA and cooled on ice. Samples from mice whole blood and mice plasma were then further processed for HPLC analysis. ATP levels and its metabolites- ADP, AMP, ADO and deaminated products were assessed and illustrated as scatterplots. The latter displayed mean \pm SD with error bars as SD ($n = 4$).

3.4.2 ATPase and CD73 inhibitors cause ATP accumulation and ADO decrease in mouse plasma

Our previous findings have demonstrated that CD39, ENPP1 and CD73 determine and fine-tune ATP hydrolysis in human plasma which plays a key role for immune cells and its endogenous feedback signaling. Interfering with these enzymes leads to impairment and therefore accumulation of ATP or AMP, as we could show in our ATP breakdown experiment by using inhibitors. Here, we focused again on the plasma as extracellular compartment and were wondering whether similar findings could be detected in mice.

Therefore, C57BL/6J mice, aged 17 ± 6 weeks, were anaesthetized and whole blood was collected in heparin syringes via cardiac puncture. We obtained the plasma from whole blood and preincubated it with inhibitors, either POM-1, NPP1 inhibitor C or PSB12379 against CD39, ENPP1 or CD73, respectively. Then, $2 \mu\text{M}$ ATP was introduced into the plasma and the ATP left as well as its breakdown products ADP, AMP, ADO and deaminated products were measured and depicted as bar graphs (Figure 27A-C).

We could clearly see that ATP accumulated significantly by 35-fold in mouse plasma in the presence of CD39 and ENPP1 inhibitors that influenced the breakdown products (Figure 27A, B). This correlates with our previous findings when studying ectonucleotidases in human plasma. HPLC analysis detected elevated ADO levels in mouse plasma under physiological conditions that dropped by 71% when blocking ENPP1 or CD39 activity. By contrast, when inhibiting CD73 activity, ADO levels decreased 4-fold while the amount of ADP and AMP increased. No differences occurred in ATP levels and deaminated products.

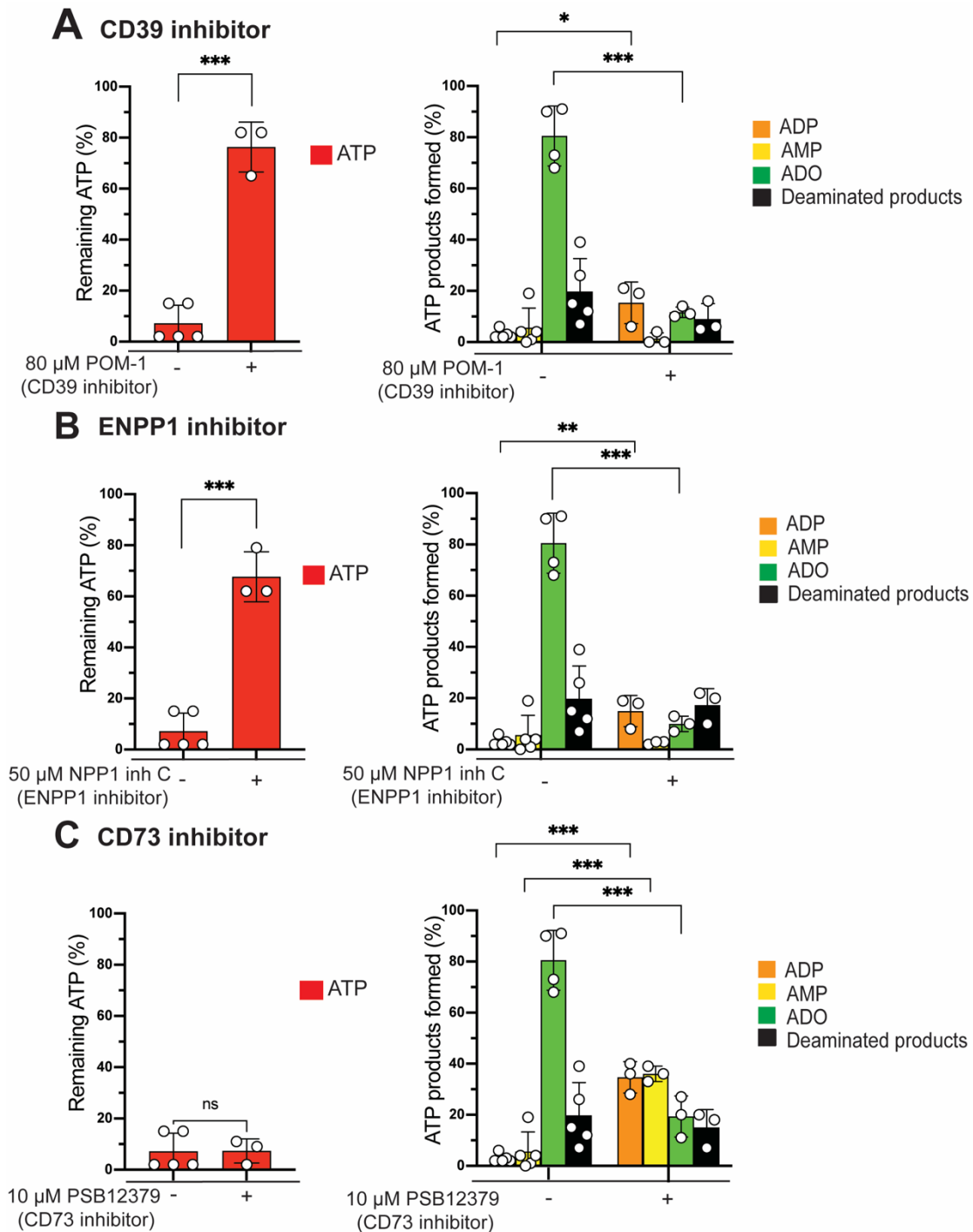


Figure 27: CD39, ENPP1, and CD73 all participate in ATP conversion in mouse plasma. Mice aged 17 ± 6 weeks were anaesthetized under isoflurane chamber and cardiac puncture method was used to collect the blood via heparin syringe. Mice whole blood was immediately cooled on ice and processed to plasma with two centrifugation steps (1st run: 400 x g, 10 min, 0°C; 2nd run: 2,300 x g, 5 min, 0°C). Plasma was then pre-incubated with HBSS, 80 μ M POM-1 (A, CD39 inhibitor), NPP1 inhibitor C (B, ENPP1 inhibitor) or PSB12379 (C, CD73 inhibitor) for 10 min at 37°C. 2 μ M ATP were pipetted into the plasma and incubated for another 10 min at 37°C. Plasma was treated with PCA and cooled on ice. Plasma samples were then further processed for HPLC analysis. ATP levels and its metabolites- ADP,

AMP, ADO and deaminated products were assessed and illustrated as bar graphs. The latter displayed mean \pm SD with error bars as SD. $n \geq 3$. Statistically significant differences are indicated with asterisks (* $p < 0.05$ vs. control without used inhibitors; unpaired t-test).

3.5 Clinical relevance of ATP breakdown

In the previous sections, we have characterized ATP hydrolysis in human and mouse blood studying both the cell-bound and soluble activity in the plasma. So far, we could show that ectonucleotidases such as CD39 or ENPP1 are key regulator that determine the rapidity of extracellular ATP degradation. Any manipulation on these enzymes causes ATP accumulation that can lead to shifts in the pro- and anti-inflammatory functions of immune cells. Using our previous findings, we translated the importance of ATP breakdown in clinical aspect. Because critical care patients with bacterial infections, sepsis or related complications show an elevation of basal ATP in plasma, we were wondering whether ATPase activity might also be impaired in these patients.

3.5.1 Patient demographics

14 male and 5 female sepsis patients ($n = 19$) aged 63 ± 15 participated in the ATP breakdown study (Table 3). They were critical care patients that had been diagnosed diseases, including cholecystitis, pneumonia, meningitis, urinary tract infection (UTI), cellulitis and gas gangrene. Additionally, pathogens were known that had been detected in sepsis patients, ranging from klebsiella to streptococcus. Correspondingly, pathogens like Klebsiella, streptococcus or Escherichia coli were detected.

Table 3: Sepsis patients participated in the ATP breakdown study. NK = not known, UTI = urinary tract infection

Sample No.	Age	Sex (m = 0, f = 1)	APACHE	Diagnosis	Pathogen
1	71	0	22	Cholecystitis	Klebsiella
2	64	0	21	Pneumonia	Group C Streptococcus
3	80	1	31	NK	NK
4	69	0	28	Pneumonia	S. pneumoniae
5	76	0	23	Cholecystitis	E.coli, Klebsiella
6	38	0	14	Meningitis	S.pneumoniae
7	76	0	20	UTI	E.coli
8	70	0	19	Pneumonia	S. pneumoniae
9	38	0	14	Cellulitis	Group A Streptococcus
10	57	1	25	Peritonitis	Group G Streptococcus
11	89	1	24	UTI	Klebsiella
12	65	1	32	NK	NK
13	61	1	25	UTI	E.coli
14	67	0	20	Pneumonia	Staphylococcus

15	79	0	33	Cellulitis	Group A Streptococcus
16	62	0	43	Pneumonia	Klebsiella
17	27	0	20	Cellulitis	NK
18	60	0	30	Gas ganrene	Streptococcus
19	51	0	16	Gas gangrene	Fusobacterium, Prevotella

3.5.2 Sepsis impair ATP breakdown in human plasma

To test this assumption, plasma from sepsis patients, which blood was drawn in Urayasu Hospital was firstly preincubated with HBSS, then subjected with ATP. After 25 min, we measured the quantity of ATP leftover as well as its breakdown products, ADP, AMP, ADO and deaminated products using HPLC (Figure 28). For comparison, we included healthy volunteers from both Urayasu and BIDMC hospital employees.

HPLC analysis showed 2.5-fold elevated ATP and 3.7-fold elevated ADP levels in sepsis patients, compared to healthy donors. Additionally, the production of AMP and deaminated products were impaired leading to a decrease in plasma of sepsis patient. These findings demonstrate the restricted activity of ATPases and ADA in sepsis plasma that might explain ATP accumulation.

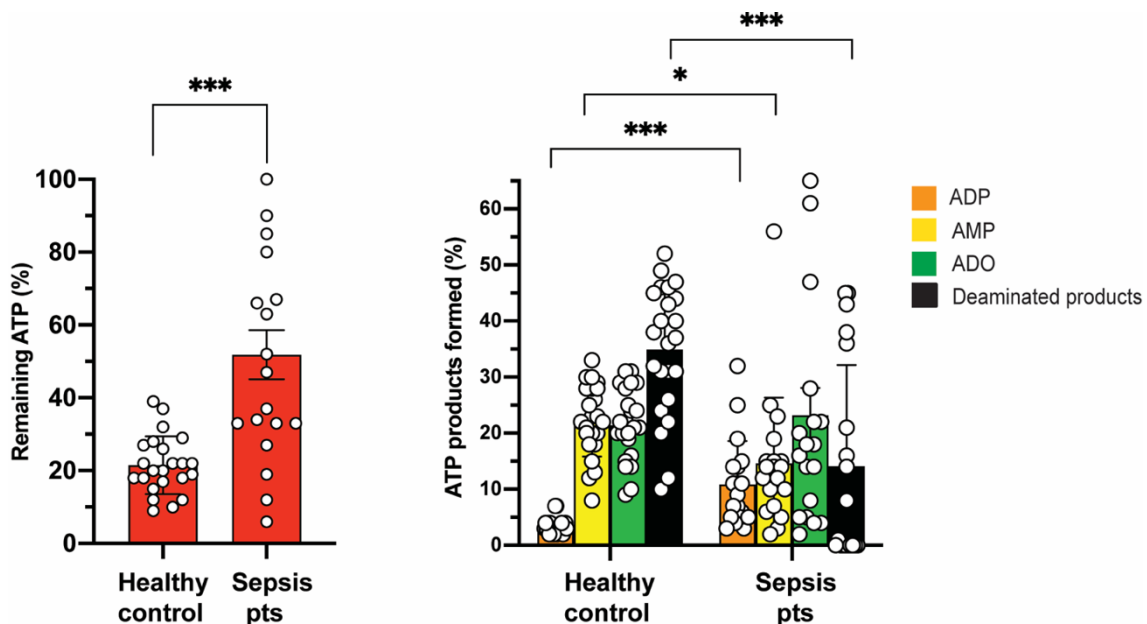


Figure 28: **Sepsis impaired ATP breakdown in human plasma.** We used sepsis and healthy volunteer plasma, drawn and prepared to plasma in Urayasu and BIDMC hospital for our ATP breakdown study, respectively. Plasma was diluted 1:10 with HBSS and pre-incubated for 10 min at 37°C. 2 μ M ATP was subjected to plasma and incubated for 25 min at 37°C. To stop further metabolism, plasma was treated with PCA and further processed for HPLC analysis. ATP levels and its metabolites- ADP, AMP, ADO and deaminated products were assessed, normalized to input ATP and illustrated as bar graphs. The latter displayed mean \pm standard error of mean (SEM) with error bars as SEM. n (healthy volunteer) =

23, n (sepsis patient) = 19. Statistically significant differences are indicated with asterisks (* $p < 0.05$ vs. healthy control; unpaired t-test).

3.5.3 Zinc can partially restore ATP breakdown in sepsis patient

We subsequently wanted to further elaborate by which mechanism ectonucleotidase functionality got impaired in sepsis patients. As outlined in our results described above (Figure 25), zinc and calcium in combination showed partial replenishment of ATP breakdown in EDTA treated plasma, thereby generating steady AMP production from extracellular ATP. As it was shown that zinc deficiency leads to an enhancement of inflammatory response [133], we were wondering whether introducing zinc into plasma of sepsis patients might also induce replenishment of ATP hydrolysis.

Therefore, we used the same sepsis plasma of patients from our previous experiment (Table 3). Plasma of sepsis patients was preincubated with Zn^{2+} and then, ϵ -ATP was added. We selected $5 \mu M Zn^{2+}$ as it represents the normal physiological amount in healthy humans [133]. We measured the ATP levels as well as its breakdown products ADP, AMP and ADO of each sepsis patient and illustrated the remaining ATP of each patient as bar graphs (Figure 29A). Based on the outcome, we categorized sepsis patients into those who responded positively to Zn^{2+} and those where Zn^{2+} suppressed ATP breakdown activity. HPLC analysis revealed that in 12 sepsis patients, zinc had a positive effect; in six patients, it had the opposing effect and in one patient, no difference was observed. Interestingly, the patients who responded positively to zinc had 35% higher ATP levels than those where zinc had an inhibiting effect. We could help the plasma of these patients to restore the ATP breakdown activity by reducing 3% of ATP remain. By contrast, ATP level was raised by 3% in those patients with the suppressing effect of Zn^{2+} .

HPLC analysis also measured breakdown products of those two groups. At those patient groups responding positively to Zn^{2+} , AMP and ADO levels increased slightly when sepsis plasma was treated with Zn^{2+} (Figure 29B). We saw a fold change of AMP and ADO by 24% or 9%, respectively. Only AMP level exhibit a significant fold change. By contrast, those patients having a suppressing effect on Zn^{2+} , we observed a decrease of ADP, AMP and ADO by 7%, 1% and 4%, respectively (Figure 29C). Our results above demonstrate the impairment of ENPP1 in plasma of sepsis patients that benefitted from Zn^{2+} replacement.

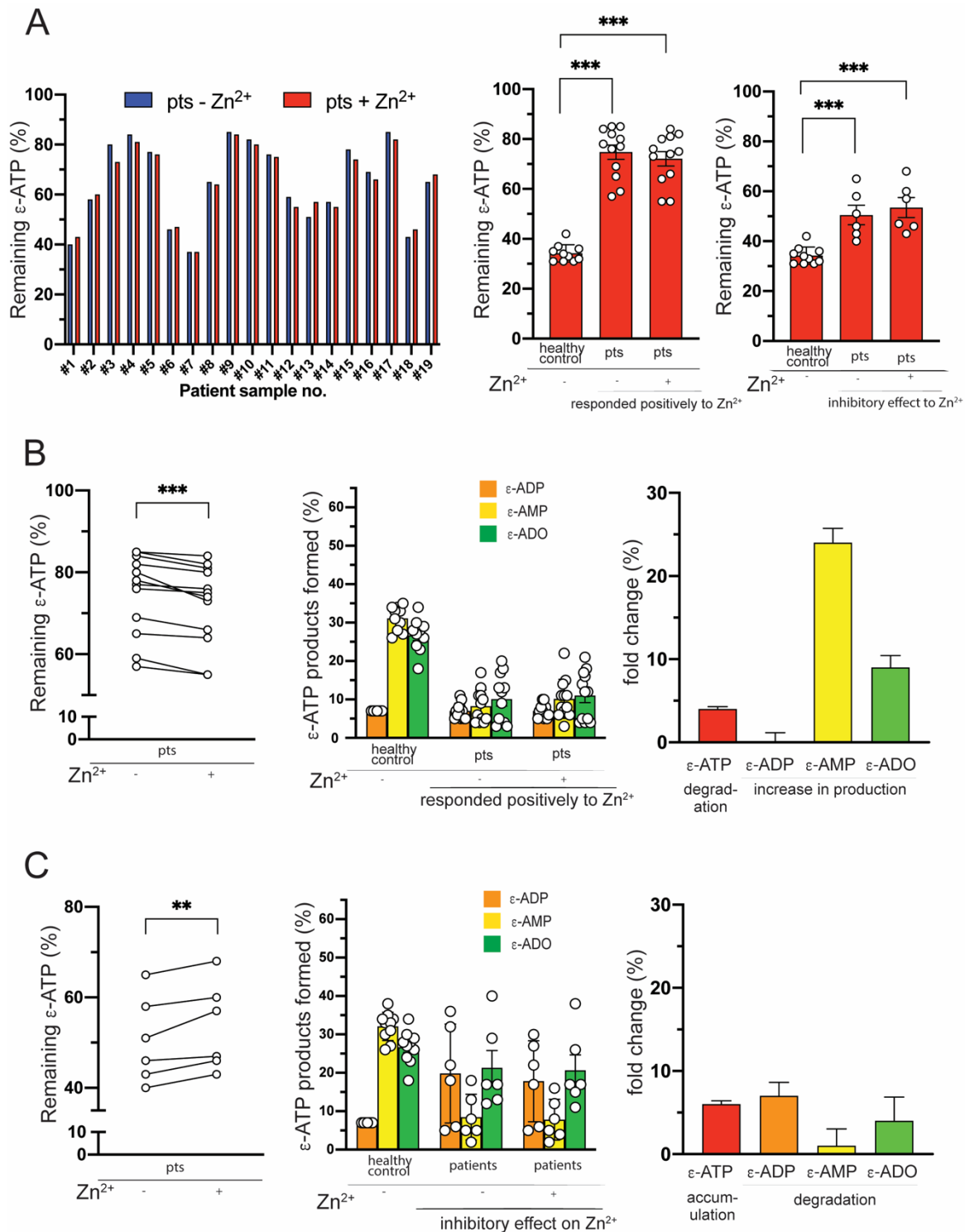


Figure 29: **ATP breakdown in some patients could be partially restored by Zn^{2+} substitution.** Plasma from sepsis and healthy volunteer was diluted 1:10 with $5 \mu M$ $ZnCl_2$ and preincubated for 30 min at $37^\circ C$. $2 \mu M$ ϵ -ATP was subjected to plasma and incubated for 25 min at $37^\circ C$. To cease the reaction, plasma was treated with PCA and further processed for HPLC analysis. (A) ATP levels from each patient ($n = 19$) were measured. Patients were then divided into two categories: those responded positively to zinc ($n = 12$) and those with an inhibitory effect ($n = 6$), showing as bar graphs in comparison to healthy control (SD indicate error bars). Patient #7 showed no difference with or without Zn^{2+} and

could not assigned to one of those categories. (B) **Zn²⁺ responded positively on sepsis patients:** ATP level before and after Zn²⁺ treatment was shown as before-after plot. It was analyzed with paired t-test, statistically significant differences are indicated with asterisks; p=0.003 (left panel). We also showed breakdown products of ATP before and after zinc (middle panel) and the fold change of increased ATP breakdown products (right panel). (C) **Zn²⁺ having inhibitory effect on sepsis patient:** ATP level before and after zinc treatment were shown as before-after plot analyzed with paired t-test, statistically significant differences are indicated with asterisks; p = 0.001. pts = patient

3.5.4 Sepsis impairs ATP hydrolysis in mouse plasma

Previously, we could demonstrate that sepsis does not only lead to elevated plasma ATP, but also the enzyme responsible for breaking down ATP is impaired leading to improper function of catalytic activities in sepsis patients. Therefore, we were wondering whether this finding occurs also in mice when inducing sepsis.

We selected adolescent C57/BL6J mice (n =12), aged 10 ± 0 weeks and weighted 23.06 ± 4.18 g for our sepsis induction model. Equal amounts of cecal slurry (0.3mg/g body weight) were injected intraperitoneally into those mice and animals were monitored after 10 hours, then every 2 hours. Except one mouse with an aggravated condition, all mice survived the sepsis procedure and lost $5.8 \pm 5.9\%$ of weight after 16-18 hours. Septic mice (n = 12) and healthy control mice (9 ± 1 week old, n = 19) were euthanized by cardiac puncture and blood was drawn with a heparinized syringe. We centrifuged the blood to extract the plasma. Mice plasma was preincubated with HBSS, followed by 2 μ M ATP pipetting into the plasma. After 25 min, ATP remaining, and its breakdown products were measured via HPLC (Figure 30). Similar to humans, we observed significantly increased ATP as well as ADP, AMP and deaminated products in sepsis mice. ADO levels, which were elevated in healthy control mice, were decreased to 37%.

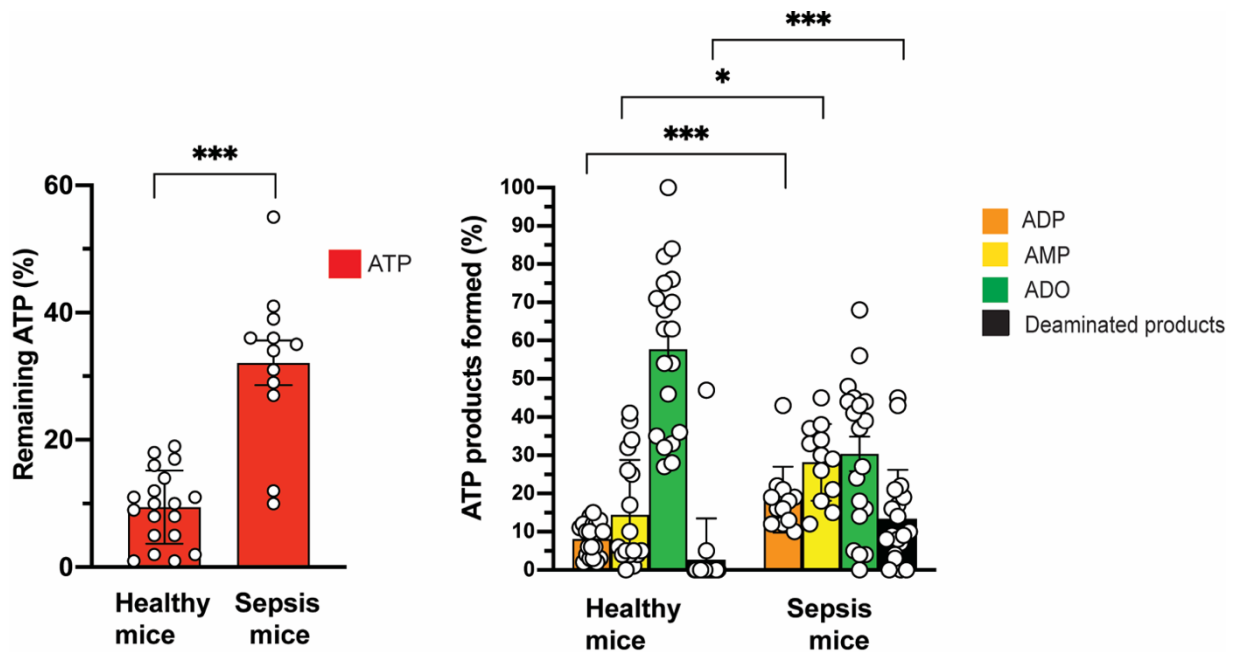


Figure 30: **Sepsis impairs ATPase activity in mice plasma.** C57/BL6J wildtype (n = 12) mice, aged 10 ± 0 weeks were selected for the sepsis induction. As comparison, we selected healthy control mice, aged 9 ± 1 (n = 19). 0.3 mg/g cecal slurry were administered intraperitoneally into the mice and evaluated after 10 hours and every 2 hours. After 18-20 hours, mice were euthanized by cardiac puncture and exsanguinated. Plasma was obtained by two centrifugation steps (1st run: 400 x g, 10 min, 0°C; 2nd run: 2,300 x g, 5 min, 0°C). Then, plasma was diluted and preincubated 1:10 with HBSS and 2 μ M ATP was subjected into the plasma. After 25 min, plasma was treated with PCA and processed for HPLC analysis. ATP levels and its metabolites- ADP, AMP, ADO and deaminated products were assessed, normalized to added ATP and illustrated as bar graphs. The latter displayed mean \pm SEM with error bars as SEM. Statistically significant differences are indicated with asterisks (* $p < 0.05$ vs. healthy mice; unpaired t-test).

We investigated on how plasma of sepsis mice responded to Zn^{2+} substitution. Previously, we could demonstrate partial replenishment of ATP breakdown activity in the plasma of human sepsis patients. Similar to the previous experimental design with sepsis patients, we repeated the ATP breakdown experiment with the sepsis mouse plasma, but pre-incubating it with 5 μ M Zn^{2+} . We assessed the ATP levels of each sepsis mouse and depicted it as bar graphs (Figure 31A). Interestingly, 9 out of 12 sepsis mice responded positively to Zn^{2+} substitution whereas 2 sepsis mice revealed the opposing effect and in one mouse, no effect was observed. Similar to sepsis patients, we categorized the sepsis mice into those that responded positively to Zn^{2+} and those with an inhibitory effect. Plasma of sepsis mice with a positive effect of Zn^{2+} showed a significant decrease of ATP levels by 32% before and after Zn^{2+} substitution (Figure 31B). We measured also ATP breakdown products of these sepsis mice group and could demonstrate an increase of ADO and deaminated products level by 36% and 12%-fold change,

respectively (Figure 31C). By contrast, ADO level is decreased in those mice subgroups with an inhibitory effect to Zn^{2+} , even though sample number is very low to make a statement (Figure 31D). These findings suggests that ENPP1 and CD73 might be impaired in sepsis mice and could benefit from Zn^{2+} substitution.

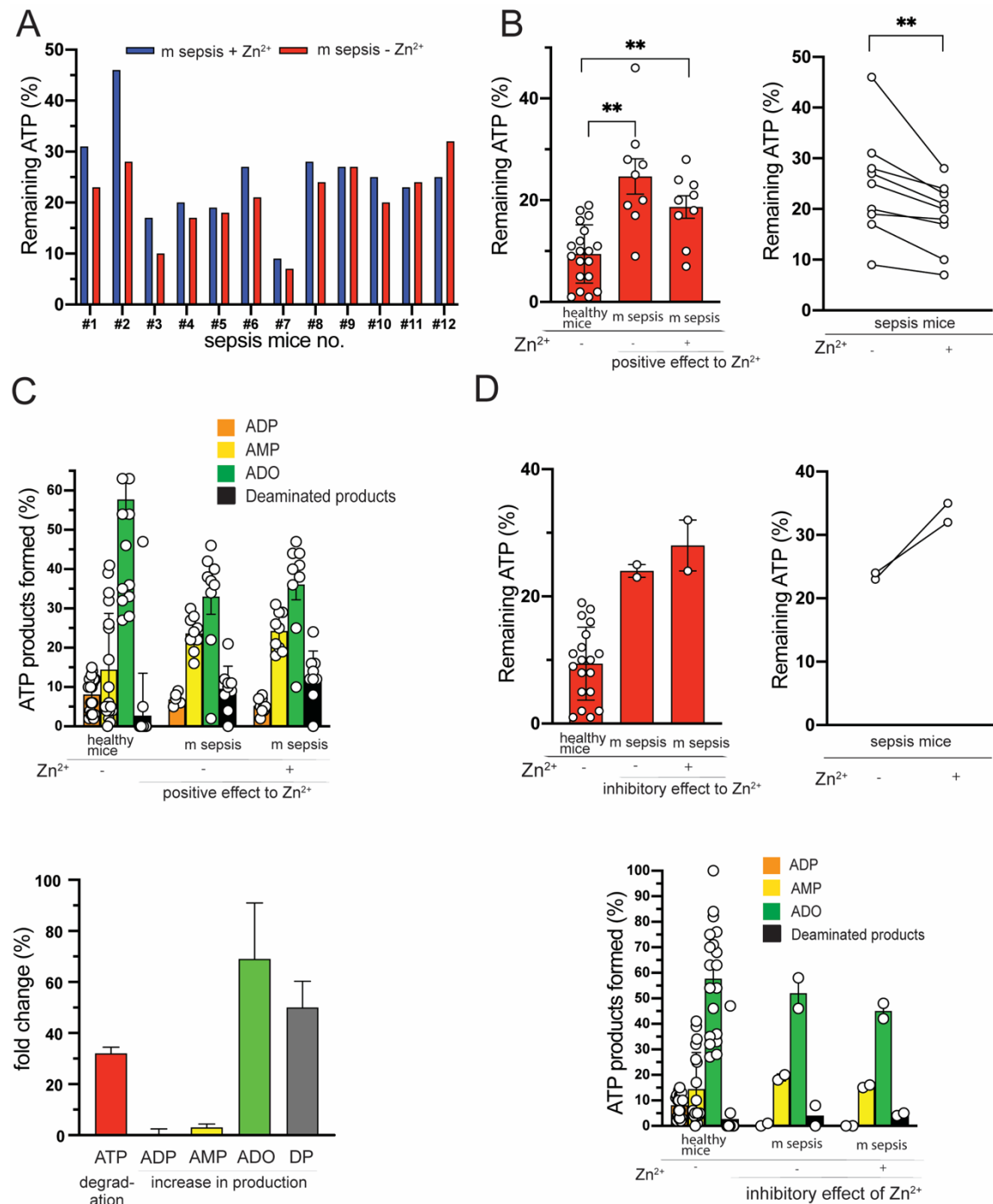


Figure 31: **75% of sepsis mice displayed a positive effect on Zn^{2+} .** (A) Sepsis mouse plasma from previous experiment (see 3.5.4; n = 12, aged 10 ± 0 weeks) were used for the Zn^{2+} study. Mice plasma was diluted and preincubated with $5 \mu M ZnCl_2$ or HBSS (control) for 10 min at $37^\circ C$. Then, $2 \mu M$ ATP

was subjected into the plasma and incubated for another 25 min at 37°C. Plasma was treated with 8 M PCA and processed for HPLC analysis. ATP remain its breakdown products as well were measured and normalized to added ATP. **(A)** ATP remain of each mouse in this study were illustrated and based on that, mice were separated into 2 categories, similar to sepsis patient from our previous study: those who responded positively to Zn²⁺ and those exhibiting an inhibitory effect. Mouse #12 showed no difference before and after Zn²⁺ and could not be assigned in one of the two categories. **Mice having a positive response on Zn²⁺** (n = 8): **(B)** ATP remains were illustrated as bar graphs (left panel) and before-after plot (right panel). Bar graphs showed as mean ± SEM with error bars as SEM. Here, one way ANOVA, followed by Dunnett's multiple comparisons test (relative to "control", left panel) as well as paired t-test (right panel) was performed. **(C)** ATP breakdown products (upper panel) as well as the fold change of ATP degradation and increase of ATP breakdown products (lower panel) were shown. **(D) Zn²⁺ responded negatively to ATP breakdown in sepsis mice** (n = 2): ATP remains were shown as bar graphs and before-after plot (upper panel). Breakdown products of ATP (lower panel) were illustrated as bar graphs. All statistically significant differences are indicated with asterisks (*p<0.05). DP = Deaminated products

3.5.5 Extracellular ATP and CD39 cause elevated PMN activation

Ectonucleotidases hydrolyze ATP, released into the extracellular space, step-wisely to adenosine, thereby regulating and fine-tuning PMN chemotaxis in an autocrine fashion[25]. Previously we could show in our study that impairment of those ectonucleotidases causes ATP accumulation. Our laboratory could also show that extracellular ATP sensitizes P2Y2 receptors, which improves PMN functions such as phagocytosis, degranulation or ROS production [108]. Based on these findings, we were keen interested on how ATP, together with ectonucleotidase inactivation, affects PMN function.

Human blood, drawn from healthy volunteers in heparin tubes, was preincubated with POM-1 (CD39 inhibitor), NPP1 inhibitor C (ENPP1 inhibitor) or PSB12379 (CD73 inhibitor). This procedure was followed by simultaneous activation of PMNs by fMLP and ATP. To investigate PMN function, we stained whole blood PMNs with antibodies against the early activation marker CD11b, CD66b (degranulation marker) and CD62L- (shedding of L-selectin) and analyzed the blood samples by flow cytometry (Figure 32A-D).

Stimulation with fMLP alone drives increase of CD11b+ stained neutrophils (Figure 32A). Together with extracellular ATP and fMLP in combination induced more PMN activation than fMLP alone. The response was even more elevated when additional CD39 activity was inhibited. Inhibition of CD73 led also to more PMN activation, but this increase was not statistically significant. By contrast, inactivation of ENPP1 did not have any effect on PMNs. A similar effect was shown in CD66b+ (Figure 32C) as well as in the shedding of L-selectin (CD62L-, Figure 32D) even though more flow cytometry experiments with CD62L- are required to verify our findings. We could specifically demonstrate that PMN function is regulated by CD39 and ATP in the extracellular space. Moreover, the fact that there was no effect of ENPP1 inhibitor C is in line with our previous findings that ENPP1 is a soluble enzyme in human blood.

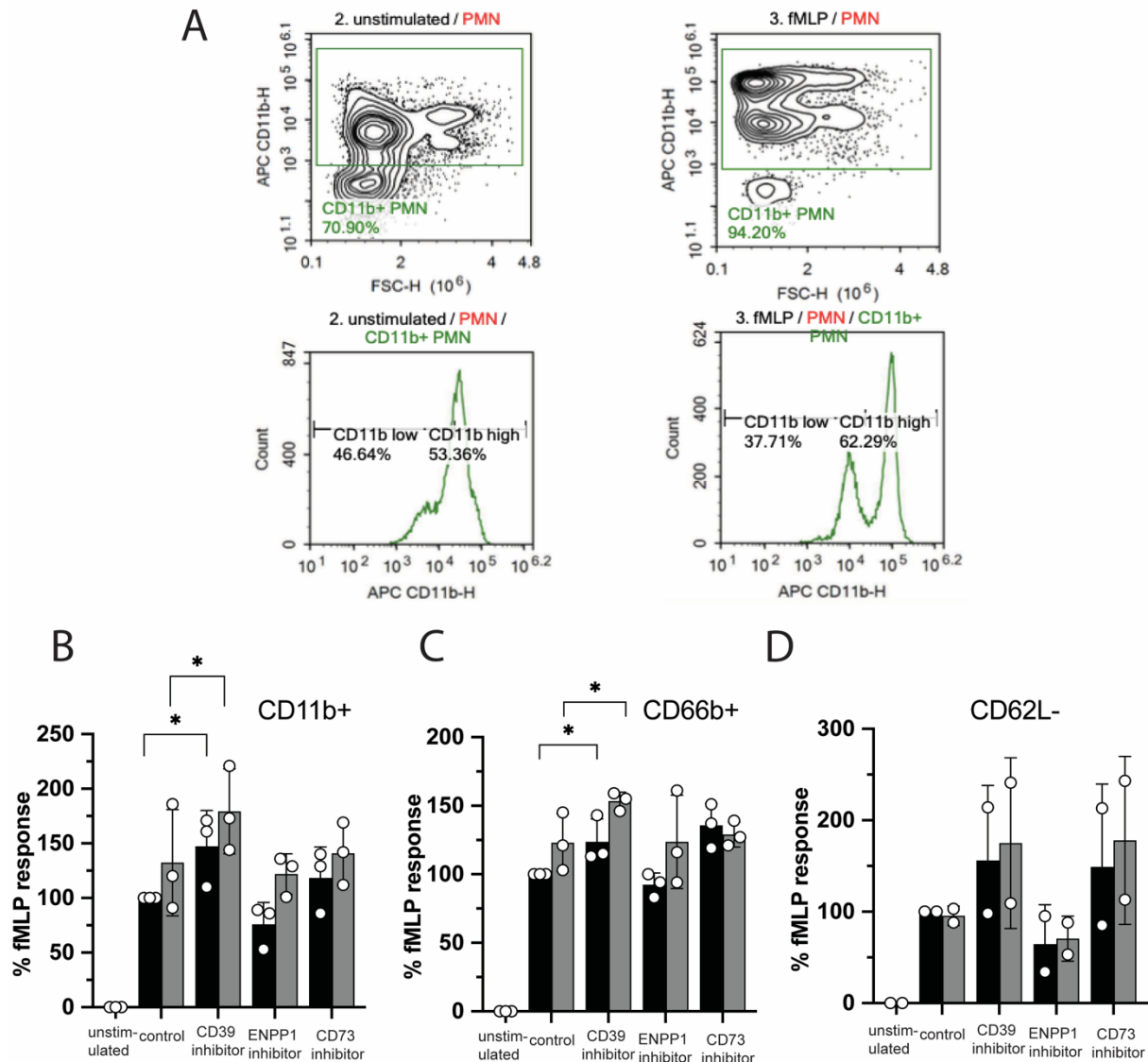


Figure 32: CD39 inhibition and extracellular ATP induce more PMN activation. Human blood, drawn in heparin tubes, was preincubated with either 80 μ M POM-1, 50 μ M NPP1 inhibitor C, 10 μ M PSM12379 or HBSS (control) for 10 min at 37°C. To stimulate the neutrophils, 40 nM fMLP and 1 μ M ATP were subjected simultaneously into the whole blood for 15 min at 37°C. Blood samples were then cooled on ice for 5 min and incubated with anti-CD11b expression, anti-CD66b expression and anti-CD62L shedding for 20 min under dark conditions. To lyse red blood cells, lysis buffer was used and incubated for another 10 min. Samples were then centrifuged at 400 x g, 5 min and most of supernatant containing the lysed cells were mostly removed. 30 μ l of FACs was analyzed in a flow cytometry. Bar graphs showed mean \pm SD with error bars as SD. Two-way ANOVA test, followed by Dunn's multiple comparison test as statistical analysis were performed. Statistically significant differences are indicated with asterisks (* p <0.05 vs. control without inhibitor).

4 Discussion

Neutrophils play a pivotal role as phagocytes circulating in the peripheral blood stream and perform antimicrobial host defense in the innate immune system [134]. Proper response to chemotactic cues as well as migration and chemotaxis serves neutrophil as orientation to migrate to the infection site in a chemotactic field. Rolling, adhesion and intraluminal crawling, supported by interactions of distinct selectins and integrins, and finally diapedesis process constitutes the neutrophil extravasation cascade that results in slow movement of neutrophils along the vascular wall and breaching the endothelium [86]. Subsequently, chemotaxis, the coordinated response to chemical stimuli, entails gradient sensing, cell polarization and forward movement within a chemotactic gradient [25].

Previous work from our laboratory could demonstrate the involvement of purinergic signaling system in regulating and fine-tuning neutrophil function [25]. Neutrophils possess primarily P2Y₂, A_{2a} and A₃ receptors. ATP release through PANX1 channel sensitizes nearby P2Y₂ receptors that further orchestrate neutrophil chemotaxis via intracellular signaling resulting in amplification of purinergic signal. Cell polarization and forward migration involves translocation of ATP to the forward edge of the cell, hydrolysis of ATP to adenosine by ectonucleotidase and activation of A₃ receptor that induce migration speed of neutrophils towards chemotactic source. By contrast, A_{2a} suppress neutrophil function at the back of the cell, also elicited by adenosine as endogenous ligand.

ATP and adenosine are opposing signaling molecules that regulate shifting between pro-inflammatory and anti-inflammatory functions in neutrophils [67]. However, pathological conditions like cancer or sepsis interfere with “push-pull” mechanism. Sepsis is a complex disease that induces severe systemic infection and inflammation, concomitant with manifestations such as tissue damage and/or organ failure [117]. The severity of outcome in septic individuals depends on many factors, including causative microorganisms, site of infection, health status, severity of tissue damage [135]. Several studies have shown that neutrophils, associated with sepsis, alter immune functionality that provides collateral damage in tissue and multiorgan failure instead of bacterial clearance [86].

Taken together, the balance between ATP and adenosine plays an important role to obviate such neutrophil-mediated manifestations in pathological conditions. Aim of the study was to gain a deeper understanding on how ATP and adenosine are regulated and the concomitant ectonucleotidase responsible for regulating immune function.

Added ATP results in breaking down rapidly and time-dependently by soluble ATPase in cell-free human plasma to ADP, AMP and adenosine, similar to human whole blood. This is in line with the ATP metabolism study from Coade *et al.* [136] in human blood. Despite of using Tritium (³H) adenine nucleotides, they could show similar rapid ATP breakdown in cell-free plasma. What intrigues more is that soluble ectonucleotidase in human plasma hydrolyze more added ATP than cell-bound enzymes. Therefore, we conclude that ATP breakdown plays an

even more crucial role in human plasma than in blood cells. This is in contrast to traditional paradigm focusing more on the cell-bound enzyme and little attention was drawn on soluble enzymes [65], [137]. Heptinstall *et al.* [138] studied isolated leukocytes and erythrocytes from human blood, stating the crucial roles of them in human whole blood and without leukocytes, breakdown of ATP is decelerated. Similar, ATP breakdown was observed in blood cells in our study. Moreover, we compared ATP hydrolysis among the compartments in human blood and could therefore contradict with their statements by revealing the importance of ATP breakdown in plasma.

In addition to that, we investigated further on ectonucleotidase responsible for ATP breakdown in different blood compartments. Our focus lies on ectoenzymes that are required to fine-tune ATP and ADO in an autocrine fashion. Among ectonucleotidase, two ways have been described of possessing scavenging effect on ATP. Ectonucleoside triphosphate diphosphohydrolase (ENTPDase) 1, also known as CD39, has been widely studied that converts step-wisely ATP to ADP, then to AMP [65], [75]. We identified the prevalence of CD39 as soluble and cell-bound form that plays a role in breaking down ATP. CD39 were abundantly found on the surface of many blood cells, but the existence as soluble form has been reported recently. Our findings suggest that soluble CD39 has been cleaved from blood cells and maintains its functionality in deactivating pericellular ATP. Benz *et al.* could show CD39 maintaining the regulation of inflammatory responses and thrombogenesis upon subjection into plasma microparticles.

By contrast, ENPP1 is another ectonucleotidase family that contributes to the regulation of ATP in the extracellular space. HPLC analysis showed that only ENPP1 as soluble form, but not cell-bound enzyme was prevalent in ATP hydrolysis. Even though ENPP1 has been widely studied, little is known about the role of ENPP1 in purinergic signaling. ENPP1, a membrane-bound glycoprotein, is known for converting i.a. extracellular ATP to AMP and inorganic pyrophosphate and the latter regulates many functions, e.g., mineralization in bone and cartilage development [72], [75]. Enyoji *et al.* [139] could demonstrate no difference in plasma ATP and ADP level between wildtype mice and CD39 depletion mice which could be explained by the fact that ENPP1 might substitute the loss of CD39 in CD39 depletion mice. As it is known that many immune cells, in particular neutrophils express ENPP1, we suggest that this enzyme in cell-bound form does not primarily perform its catalytic activity in breaking down ATP but other important functions in human body. By contrast, soluble ENPP1 is involved in ATP hydrolysis and hence, in regulating immune functions.

AMP production, derived from ATP or ADP is further dephosphorylated to adenosine by CD73. The latter appears as an immune checkpoint in adenosinergic signaling bound on the surface of the cell via GPI, but it has been reported to exist also as soluble form. We could reveal that added ATP, together with depletion of soluble CD73 activity results in significant accumulation of ADP and AMP and decrease of adenosine [48]. Thus, we could demonstrate the importance of CD73 activity regarding ATP breakdown in human plasma which coincide with the study

from Kuleskaya *et al.* They could show decreased activity in AMP breakdown when inhibiting CD/3 activity in murine brain. By contrast, added ATP and suppression of cell- bound CD73 activity, surprisingly, induce more ATP hydrolysis and ADP accumulation. We speculate that adenylate kinase might replace the loss of CD73 in human blood cells. Adenylate kinase (AK) is known for preserving energy homeostasis by regulating adenine nucleotides[140], [141]. Specifically, it performs the reversible interconversion $AMP + ATP \leftrightarrow 2 ADP$ [142]. Our current study demonstrated the presence of soluble and cell- bound CD73 in human blood and mouse plasma.

Based on our findings which ectonucleotidase regulated ATP breakdown in human blood, we were also keen interested in whether similar findings occurred in mice. Prior to that, we studied firstly on the ATP breakdown in mouse blood and compared the outcome with human blood. As previously, we demonstrated the major contribution of cell-free plasma in human whole blood, our focus laid therefore only on the mouse plasma. Our current study demonstrated that mouse blood hydrolyzed ATP more rapidly than human blood. However, mouse plasma broke down ATP more slowly than mouse whole blood and exhibit similar pattern as observed in human plasma. It seems that ectonucleotidase catalyzed ATP and ADP more rapidly than in human once released into the extracellular space that regulates the immune function. Over exceeded amount of adenosine level in mouse whole blood can be explained by the loss of binding site in adenosine ADA possibly grabbed to convert to inosine. We also examined types of ectonucleotidase prevalent in mouse plasma. Our findings reveal that CD39, ENPP1 and CD73 are present as soluble form in mouse plasma. This finding coincides with our previous results with the ectonucleotidase in human plasma.

Subsequently, we evaluated the importance of coenzymes ectonucleotidase requires to fulfill its catalytic activity in human blood. Therefore, we used EDTA and EGTA as chelating agent to scavenge Ca^{2+} and other metal ions in human blood. These two chelating agents also prevent blood clotting in vacutainers. Our findings show that EDTA and EGTA blocks ATP breakdown in both compartments, with a stronger effect on the human plasma and whole blood. Ledderose *et al.* [143] showed that the use of EDTA drives ATP elevation in human blood. It seems likely that deprivation of metal-ions in human blood additionally may drive disassembly of its ectoenzymes impairing its functionality and therefore, explaining the elevation of plasma ATP in EDTA blood.

Due to the fact that coenzymes are crucial for driving functionality in ectonucleotidase we wanted to examine whether replenishment of ATP breakdown with physiological Ca^{2+} and Mg^{2+} could be observed in EDTA- containing human blood. Our findings show that ATP breakdown in blood cells, but not in human plasma could be replenished with physiological Ca^{2+} and Mg^{2+} . It seems that 1.2 mM Ca^{2+} and Mg^{2+} was sufficient in blood cells, which contemplate possibly for CD39 that benefit from restoring the activity. CD39 requires Ca^{2+} and Mg^{2+} to perform functionality on extracellular ATP [65], [68].

By contrast, physiological Ca^{2+} and Mg^{2+} did not help ATP breakdown in EDTA containing plasma. As we could previously show the prevalence of CD39 in human plasma, we were wondering if 1.2 mM Ca^{2+} and Mg^{2+} was not sufficient for restoring ATP breakdown. Surprisingly, adding Ca^{2+} dose dependently did not induce replenishment in cell-free plasma, but so did in combination with Zn^{2+} . We could observe partial replenishment when adding Zn^{2+} dose dependently. The fact that AMP level increased by adding increasing Zn^{2+} advocate possibly for ENPP1 or ENPP3 that benefit from Zn^{2+} . It has been known that ENPP1 are Zn^{2+} and Ca^{2+} dependent for catalyzing extracellular ATP to AMP [71]. Therefore, Zn^{2+} seemed to induce re-assembly of ENPP1 dimer that might have cleaved in the presence of EDTA.

However, replenishment of ATP breakdown did not reach heparin control in human plasma and can be explained by the fact that some ENPP1s were still damaged from EDTA effect. By contrast, Zn^{2+} induced minor changes in ATP breakdown in EDTA containing blood cells, meaning that blood cells did not necessarily require Zn^{2+} . This would support our findings that CD39 is more prevalent as cell-bound enzyme as mentioned above, CD39 requires only Ca^{2+} and Mg^{2+} for its functionality [65].

Taken together with our findings, we translated the relevance of ATP breakdown mechanism in clinics and were wondering if ectonucleotidase activity were impaired in sepsis patient. Our findings could demonstrate the perturbation of ATP breakdown activity in sepsis patients as well as in sepsis mice. Recent animal studies have pointed out the accumulation of extracellular ATP released by tissue upon certain inflammatory events. Moreover, Sumi *et al.* [122] could show in her study that plasma ATP and ADP were elevated upon subjection of sepsis in mouse. It seemed likely that ectonucleotidase activity is impaired, probably because of the loss of functionality or as a result of damage. This could explain the elevation of ATP and ADP in CLP-sepsis mice.

We investigated further and elaborated by which mechanism induced impairment of ectonucleotidase activity in ATP breakdown. One possible reason could be that low amount of Zn^{2+} contribute to the irregular performance of breakdown activity. It has been known that zinc deficiency distorts immune function [133]. Our findings reveal that in 12 out of 19 (63%) enrolled patients as well as in 9 out of 12 (75%) sepsis mice, ATP breakdown was partially replenished by putting Zn^{2+} . Interestingly, we could support in restoring ATP breakdown in those sepsis patients exhibiting the highest ATP accumulation. Hereby, we could demonstrate that Zn^{2+} was apparently imbalanced in those sepsis patients. Thus, hypozincemia has been identified in sepsis patients. Hoeger *et al.* [133] demonstrated the deprivation of serum Zn^{2+} level in majority of sepsis patient. Another study of Takeda *et al.* [144] revealed that zinc insufficiency impaired ATP hydrolysis in rat plasma. However, limitation in our sepsis study is the comparably low amount of number of patient subjects which needs to be increased. Our next experiment would be to examine Zn^{2+} in sepsis-subjected mice in vivo to verify the Zn^{2+} dysregulation in sepsis.

Our study provided a deeper understanding in regulating ATP and purinergic signaling system that maintains cell metabolism and cell function. To summarize, we could identify the prevalence of CD39 in blood cells and ENPP1 in plasma that regulates the ATP breakdown and dysregulation might facilitate ATP elevation in human blood (Figure 33). Previous studies have shown that purinergic signaling in an autocrine/paracrine fashion regulates the PMN activation [25]. Also, extracellular ATP sensitizes PMN functions such as phagocytosis, degranulation and ROS production by engaging P2Y2 receptor [145]. We could show that extracellular ATP, in combination with fMLP drives more PMN activation than fMLP alone. This coincides with the study of Sumi *et al.* [122] that plasma ATP in mouse, caused by sepsis correlates with neutrophil activation. The fact that CD39 regulates neutrophil chemotaxis, we could show by flow cytometry analysis that inhibiting CD39 activity, together with subjecting extracellular ATP and stimulation by fMLP induce more PMN activation than fMLP and ATP alone. Inhibiting CD73 activity was also shown to drive more activation of PMNs, however, our findings were not significant to verify this statement.

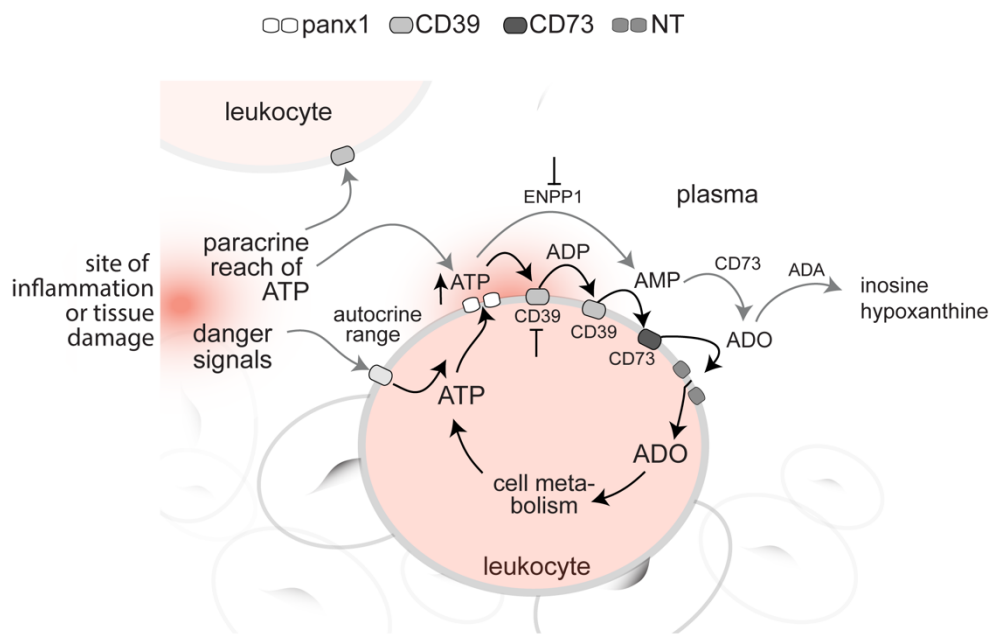


Figure 33: **Proposed model of ATP release, ATP hydrolysis into its metabolites and cell metabolism in blood cells and plasma.** ATP release, either resulting from inflammation and damaged tissue or from blood cells through pannexin (PANX) determine extracellular ATP concentration in the extracellular space. Cell-bound CD39 and soluble ENPP1 are regulator of ATP levels generating ADP and AMP. Cell-bound and soluble CD73 catalyze AMP further to adenosine. The latter is subsequently degraded to inosine and other deaminated products by adenosine deaminase (ADA) or uptaken by cells via nucleoside transporter (NT). Image was taken from [125] and modified to our findings.

5 Conclusion

To conclude, this study provides CD39 as key ectonucleotidase that controls ATP level and PMN activation. However, more research is needed to develop pharmaceutical agents to target ATP by CD39. Modulating CD39 activity could be one possible way to diminish excessive PMN function in sepsis patients. We believe that our study contributes to the development of novel immunomodulatory concepts for therapeutic strategies to avoid immune dysfunction in patients with bacterial and viral infection.

Bibliography

- [1] A. N. Drury *et al.*, "The physiological activity of adenine compounds with especial reference to their action upon the mammalian heart¹," *J. Physiol.*, vol. 68, no. 3, pp. 213–237, Nov. 1929, doi: 10.1113/jphysiol.1929.sp002608.
- [2] P. Holton, "The liberation of adenosine triphosphate on antidromic stimulation of sensory nerves," *J. Physiol.*, vol. 145, no. 3, pp. 494–504, Mar. 1959, doi: 10.1113/jphysiol.1959.sp006157.
- [3] G. Burnstock, "Discovery of purinergic signalling, the initial resistance and current explosion of interest: Discovery of purinergic signalling," *Br. J. Pharmacol.*, vol. 167, no. 2, pp. 238–255, Sep. 2012, doi: 10.1111/j.1476-5381.2012.02008.x.
- [4] G. Burnstock, "Evidence that adenosine triphosphate or are later nucleotide is the transmitter substance released by non-adrenergic inhibitory nerves in the gut," p. 21, Jun. 1970.
- [5] G. Burnstock *et al.*, "Purinergic signalling and immune cells," *Purinergic Signal.*, vol. 10, no. 4, pp. 529–564, Dec. 2014, doi: 10.1007/s11302-014-9427-2.
- [6] G. Burnstock *et al.*, "Is there a basis for distinguishing two types of P2-purinoceptor?," *Gen. Pharmacol. Vasc. Syst.*, vol. 16, no. 5, pp. 433–440, Jan. 1985, doi: 10.1016/0306-3623(85)90001-1.
- [7] M. P. Abbracchio *et al.*, "Purinoceptors: Are there families of P2X and P2Y purinoceptors?," *Pharmacol. Ther.*, vol. 64, no. 3, pp. 445–475, Jan. 1994, doi: 10.1016/0163-7258(94)00048-4.
- [8] M. Idzko *et al.*, "Nucleotide signalling during inflammation," *Nature*, vol. 509, no. 7500, pp. 310–317, May 2014, doi: 10.1038/nature13085.
- [9] G. G. Yegutkin, "Adenosine metabolism in the vascular system," *Biochem. Pharmacol.*, vol. 187, p. 114373, May 2021, doi: 10.1016/j.bcp.2020.114373.
- [10] W. Kühlbrandt, "Structure and function of mitochondrial membrane protein complexes," *BMC Biol.*, vol. 13, no. 1, p. 89, Dec. 2015, doi: 10.1186/s12915-015-0201-x.
- [11] P. Dimroth *et al.*, "ATP Synthesis by Decarboxylation Phosphorylation," in *Bioenergetics*, vol. 45, G. Schäfer and H. S. Penefsky, Eds. Berlin, Heidelberg: Springer Berlin Heidelberg, 2007, pp. 153–184. doi: 10.1007/400_2007_045.
- [12] L. Durnin *et al.*, "A commonly used ecto-ATPase inhibitor, ARL-67156, blocks degradation of ADP more than the degradation of ATP in murine colon," *Neurogastroenterol. Motil.*, vol. 28, no. 9, pp. 1370–1381, Sep. 2016, doi: 10.1111/nmo.12836.
- [13] C. M. Joyce *et al.*, "Polymerase structures and function: variations on a theme?," *J. Bacteriol.*, vol. 177, no. 22, pp. 6321–6329, Nov. 1995, doi: 10.1128/jb.177.22.6321-6329.1995.
- [14] C. J. Barclay, "Energetics of Contraction," in *Comprehensive Physiology*, 1st ed., R. Terjung, Ed. Wiley, 2015, pp. 961–995. doi: 10.1002/cphy.c140038.
- [15] M. Bonora *et al.*, "ATP synthesis and storage," *Purinergic Signal.*, vol. 8, no. 3, pp. 343–357, Sep. 2012, doi: 10.1007/s11302-012-9305-8.
- [16] Z. Wang *et al.*, "Glycolysis and Oxidative Phosphorylation Play Critical Roles in Natural Killer Cell Receptor-Mediated Natural Killer Cell Functions," *Front. Immunol.*, vol. 11, p. 202, Feb. 2020, doi: 10.3389/fimmu.2020.00202.
- [17] J. Zheng, "Energy metabolism of cancer: Glycolysis versus oxidative phosphorylation (Review)," *Oncol. Lett.*, vol. 4, no. 6, pp. 1151–1157, 2012, doi: 10.3892/ol.2012.928.
- [18] A. E. Senior *et al.*, "The molecular mechanism of ATP synthesis by F1F0-ATP synthase," *Biochim. Biophys. Acta BBA - Bioenerg.*, vol. 1553, no. 3, pp. 188–211, Feb. 2002, doi: 10.1016/S0005-2728(02)00185-8.
- [19] Z. Huang *et al.*, "From purines to purinergic signalling: molecular functions and human diseases," *Signal Transduct. Target. Ther.*, vol. 6, no. 1, p. 162, Dec. 2021, doi: 10.1038/s41392-021-00553-z.

- [20] C. Ledderose *et al.*, "Purinergic Signaling and the Immune Response in Sepsis: A Review," *Clin. Ther.*, vol. 38, no. 5, pp. 1054–1065, May 2016, doi: 10.1016/j.clinthera.2016.04.002.
- [21] P. Pelegrín, Ed., *Purinergic Signaling: Methods and Protocols*, vol. 2041. New York, NY: Springer New York, 2020. doi: 10.1007/978-1-4939-9717-6.
- [22] L. Dou, Y.-F. Chen, P. J. Cowan, and X.-P. Chen, "Extracellular ATP signaling and clinical relevance," *Clin. Immunol.*, vol. 188, pp. 67–73, Mar. 2018, doi: 10.1016/j.clim.2017.12.006.
- [23] R. Corriden *et al.*, "Basal Release of ATP: An Autocrine-Paracrine Mechanism for Cell Regulation," *Sci. Signal.*, vol. 3, no. 104, Jan. 2010, doi: 10.1126/scisignal.3104re1.
- [24] G. Burnstock, "Purinergic Signaling in the Cardiovascular System," *Circ. Res.*, vol. 120, no. 1, pp. 207–228, Jan. 2017, doi: 10.1161/CIRCRESAHA.116.309726.
- [25] W. G. Junger, "Immune cell regulation by autocrine purinergic signalling," *Nat. Rev. Immunol.*, vol. 11, no. 3, pp. 201–212, Mar. 2011, doi: 10.1038/nri2938.
- [26] G. Burnstock, "Physiology and Pathophysiology of Purinergic Neurotransmission," *Physiol. Rev.*, vol. 87, no. 2, pp. 659–797, Apr. 2007, doi: 10.1152/physrev.00043.2006.
- [27] E. R. Lazarowski, "Vesicular and conductive mechanisms of nucleotide release," *Purinergic Signal.*, p. 15, 2012.
- [28] Y. Moriyama *et al.*, "Vesicular nucleotide transporter (VNUT): appearance of an actress on the stage of purinergic signaling," *Purinergic Signal.*, vol. 13, no. 3, pp. 387–404, Sep. 2017, doi: 10.1007/s11302-017-9568-1.
- [29] A. Taruno, "ATP Release Channels," *Int. J. Mol. Sci.*, vol. 19, no. 3, p. 808, Mar. 2018, doi: 10.3390/ijms19030808.
- [30] M. Dosch *et al.*, "Mechanisms of ATP Release by Inflammatory Cells," *Int. J. Mol. Sci.*, vol. 19, no. 4, p. 1222, Apr. 2018, doi: 10.3390/ijms19041222.
- [31] Y. Harada *et al.*, "Vesicular nucleotide transporter mediates ATP release and migration in neutrophils," *J. Biol. Chem.*, vol. 293, no. 10, pp. 3770–3779, Mar. 2018, doi: 10.1074/jbc.M117.810168.
- [32] Z. Ma *et al.*, "Calcium homeostasis modulator 1 (CALHM1) is the pore-forming subunit of an ion channel that mediates extracellular Ca²⁺ regulation of neuronal excitability," *Proc. Natl. Acad. Sci.*, vol. 109, no. 28, Jul. 2012, doi: 10.1073/pnas.1204023109.
- [33] A. D. Workman *et al.*, "CALHM1-Mediated ATP Release and Ciliary Beat Frequency Modulation in Nasal Epithelial Cells," *Sci. Rep.*, vol. 7, no. 1, p. 6687, Dec. 2017, doi: 10.1038/s41598-017-07221-9.
- [34] T. Liu *et al.*, "The Volume-Regulated Anion Channel LRRC8/VRAC Is Dispensable for Cell Proliferation and Migration," *Int. J. Mol. Sci.*, vol. 20, no. 11, p. 2663, May 2019, doi: 10.3390/ijms20112663.
- [35] R. Z. Sabirov *et al.*, "The properties, functions, and pathophysiology of maxi-anion channels," *Pflüg. Arch. - Eur. J. Physiol.*, vol. 468, no. 3, pp. 405–420, Mar. 2016, doi: 10.1007/s00424-015-1774-5.
- [36] R. Z. Sabirov *et al.*, "The maxi-anion channel: a classical channel playing novel roles through an unidentified molecular entity," *J. Physiol. Sci.*, vol. 59, no. 1, pp. 3–21, Jan. 2009, doi: 10.1007/s12576-008-0008-4.
- [37] H.-J. Lee *et al.*, "Cryo-EM structure of human Cx31.3/GJC3 connexin hemichannel," *Sci. Adv.*, vol. 6, no. 35, p. eaba4996, Aug. 2020, doi: 10.1126/sciadv.aba4996.
- [38] M. F. Muñoz, T. N. Griffith, and J. E. Contreras, "Mechanisms of ATP release in pain: role of pannexin and connexin channels," *Purinergic Signal.*, vol. 17, no. 4, pp. 549–561, Dec. 2021, doi: 10.1007/s11302-021-09822-6.
- [39] E. De Vuyst *et al.*, "Connexin Hemichannels and Gap Junction Channels Are Differentially Influenced by Lipopolysaccharide and Basic Fibroblast Growth Factor," *Mol. Biol. Cell*, vol. 18, no. 1, pp. 34–46, Jan. 2007, doi: 10.1091/mbc.e06-03-0182.
- [40] G. Dahl, "ATP release through pannexon channels," *Philos. Trans. R. Soc. B Biol. Sci.*, vol. 370, no. 1672, p. 20140191, Jul. 2015, doi: 10.1098/rstb.2014.0191.

- [41]X. Wang *et al.*, “Purinergic Regulation of Neutrophil Function,” *Front. Immunol.*, vol. 9, p. 399, Mar. 2018, doi: 10.3389/fimmu.2018.00399.
- [42]M. R. Elliott *et al.*, “Nucleotides released by apoptotic cells act as a find-me signal to promote phagocytic clearance,” *Nature*, vol. 461, no. 7261, pp. 282–286, Sep. 2009, doi: 10.1038/nature08296.
- [43]J. Amores-Iniesta *et al.*, “Extracellular ATP Activates the NLRP3 Inflammasome and Is an Early Danger Signal of Skin Allograft Rejection,” *Cell Rep.*, vol. 21, no. 12, pp. 3414–3426, Dec. 2017, doi: 10.1016/j.celrep.2017.11.079.
- [44]W. Wang *et al.*, “Paxillin mediates ATP-induced activation of P2X7 receptor and NLRP3 inflammasome,” *BMC Biol.*, vol. 18, no. 1, p. 182, Dec. 2020, doi: 10.1186/s12915-020-00918-w.
- [45]H. A. Praetorius *et al.*, “ATP release from non-excitabile cells,” *Purinergic Signal.*, vol. 5, no. 4, pp. 433–446, Dec. 2009, doi: 10.1007/s11302-009-9146-2.
- [46]G. Burnstock, “Purine and purinergic receptors,” *Brain Neurosci. Adv.*, vol. 2, p. 239821281881749, Jan. 2018, doi: 10.1177/2398212818817494.
- [47]S. Sheth *et al.*, “Adenosine Receptors: Expression, Function and Regulation,” *Int. J. Mol. Sci.*, vol. 15, no. 2, pp. 2024–2052, Jan. 2014, doi: 10.3390/ijms15022024.
- [48]L. Antonioli *et al.*, “Immunity, inflammation and cancer: a leading role for adenosine,” *Nat. Rev. Cancer*, vol. 13, no. 12, pp. 842–857, Dec. 2013, doi: 10.1038/nrc3613.
- [49]K. A. Jacobson *et al.*, “G protein-coupled adenosine (P1) and P2Y receptors: ligand design and receptor interactions,” *Purinergic Signal.*, vol. 8, no. 3, pp. 419–436, Sep. 2012, doi: 10.1007/s11302-012-9294-7.
- [50]G. Kasuya *et al.*, “Structural insights into the competitive inhibition of the ATP-gated P2X receptor channel,” *Nat. Commun.*, vol. 8, no. 1, p. 876, Dec. 2017, doi: 10.1038/s41467-017-00887-9.
- [51]M. Li *et al.*, “Subtype-specific control of P2X receptor channel signaling by ATP and Mg²⁺,” *Proc. Natl. Acad. Sci.*, vol. 110, no. 36, Sep. 2013, doi: 10.1073/pnas.1308088110.
- [52]L. Stokes *et al.*, “P2X4 Receptor Function in the Nervous System and Current Breakthroughs in Pharmacology,” *Front. Pharmacol.*, vol. 8, p. 291, May 2017, doi: 10.3389/fphar.2017.00291.
- [53]E. Richler *et al.*, “Neuronal P2X2 Receptors Are Mobile ATP Sensors That Explore the Plasma Membrane When Activated,” *J. Neurosci.*, vol. 31, no. 46, pp. 16716–16730, Nov. 2011, doi: 10.1523/JNEUROSCI.3362-11.2011.
- [54]T. Kawate, “P2X Receptor Activation,” in *Protein Reviews*, vol. 1051, M. Z. Atassi, Ed. Singapore: Springer Singapore, 2017, pp. 55–69. doi: 10.1007/5584_2017_55.
- [55]R. A. North, “P2X receptors,” *Philos. Trans. R. Soc. B Biol. Sci.*, vol. 371, no. 1700, p. 20150427, Aug. 2016, doi: 10.1098/rstb.2015.0427.
- [56]K. A. Jacobson *et al.*, “Update of P2Y receptor pharmacology: IUPHAR Review 27,” *Br. J. Pharmacol.*, vol. 177, no. 11, pp. 2413–2433, Jun. 2020, doi: 10.1111/bph.15005.
- [57]M. Alves *et al.*, “The Metabotropic Purinergic P2Y Receptor Family as Novel Drug Target in Epilepsy,” *Front. Pharmacol.*, vol. 9, p. 193, Mar. 2018, doi: 10.3389/fphar.2018.00193.
- [58]C. Dillard *et al.*, “Expression Pattern of Purinergic Signaling Components in Colorectal Cancer Cells and Differential Cellular Outcomes Induced by Extracellular ATP and Adenosine,” *Int. J. Mol. Sci.*, vol. 22, no. 21, p. 11472, Oct. 2021, doi: 10.3390/ijms222111472.
- [59]H. Zimmermann *et al.*, “Cellular function and molecular structure of ecto-nucleotidases,” *Purinergic Signal.*, vol. 8, no. 3, pp. 437–502, Sep. 2012, doi: 10.1007/s11302-012-9309-4.
- [60]A. L. Giuliani *et al.*, “Ectonucleotidases in Acute and Chronic Inflammation,” *Front. Pharmacol.*, vol. 11, p. 619458, Feb. 2021, doi: 10.3389/fphar.2020.619458.
- [61]E. H. Zhong *et al.*, “Structural and functional characterization of engineered bifunctional fusion proteins of CD39 and CD73 ectonucleotidases,” *Am. J. Physiol.-Cell Physiol.*, vol. 320, no. 1, pp. C15–C29, Jan. 2021, doi: 10.1152/ajpcell.00430.2020.

- [62]H. Zhao *et al.*, “What Else Can CD39 Tell Us?,” *Front. Immunol.*, vol. 8, p. 727, Jun. 2017, doi: 10.3389/fimmu.2017.00727.
- [63]S.-Y. Lee *et al.*, “Development of a selective and highly sensitive fluorescence assay for nucleoside triphosphate diphosphohydrolase1 (NTPDase1, CD39),” *The Analyst*, vol. 143, no. 22, pp. 5417–5430, 2018, doi: 10.1039/C8AN01108G.
- [64]K. I. Onyedibe *et al.*, “ENPP1, an Old Enzyme with New Functions, and Small Molecule Inhibitors—A STING in the Tale of ENPP1,” *Molecules*, vol. 24, no. 22, p. 4192, Nov. 2019, doi: 10.3390/molecules24224192.
- [65]H. Zimmermann *et al.*, “Cellular function and molecular structure of ecto-nucleotidases,” *Purinergic Signal.*, vol. 8, no. 3, pp. 437–502, Sep. 2012, doi: 10.1007/s11302-012-9309-4.
- [66]M. S. Longhi *et al.*, “Targeting ectonucleotidases to treat inflammation and halt cancer development in the gut,” *Biochem. Pharmacol.*, vol. 187, p. 114417, May 2021, doi: 10.1016/j.bcp.2021.114417.
- [67]L. Antonioli *et al.*, “CD39 and CD73 in immunity and inflammation,” *Trends Mol. Med.*, vol. 19, no. 6, pp. 355–367, Jun. 2013, doi: 10.1016/j.molmed.2013.03.005.
- [68]V. S. Nunes *et al.*, “Structural Comparative Analysis of Ecto- NTPDase Models from S. Mansoni and H. Sapiens,” in *Bioinformatics Research and Applications*, vol. 9096, R. Harrison, Y. Li, and I. Măndoiu, Eds. Cham: Springer International Publishing, 2015, pp. 247–259. doi: 10.1007/978-3-319-19048-8_21.
- [69]R. Resta *et al.*, “Ecto-enzyme and signaling functions of lymphocyte CD 73,” *Immunol. Rev.*, vol. 161, no. 1, pp. 95–109, Feb. 1998, doi: 10.1111/j.1600-065X.1998.tb01574.x.
- [70]L. R. Beckenkamp *et al.*, “Characterization of soluble CD39 (SolCD39/NTPDase1) from PiggyBac nonviral system as a tool to control the nucleotides level,” *Biochem. J.*, vol. 476, no. 11, pp. 1637–1651, Jun. 2019, doi: 10.1042/BCJ20190040.
- [71]R. Borza, “Structure and function of the ecto-nucleotide pyrophosphatase/phosphodiesterase (ENPP) family: Tidying up diversity,” p. 12, 2021.
- [72]T. Takahashi *et al.*, “SURFACE ALLOANTIGENS OF PLASMA CELLS,” *J. Exp. Med.*, vol. 131, no. 6, pp. 1325–1341, Jun. 1970, doi: 10.1084/jem.131.6.1325.
- [73]J. W. Goding *et al.*, “Physiological and pathophysiological functions of the ecto-nucleotide pyrophosphatase/phosphodiesterase family,” *Biochim. Biophys. Acta BBA - Mol. Basis Dis.*, vol. 1638, no. 1, pp. 1–19, May 2003, doi: 10.1016/S0925-4439(03)00058-9.
- [74]K. Kato *et al.*, “Crystal structure of Enpp1, an extracellular glycoprotein involved in bone mineralization and insulin signaling,” *Proc. Natl. Acad. Sci.*, vol. 109, no. 42, pp. 16876–16881, Oct. 2012, doi: 10.1073/pnas.1208017109.
- [75]S. Chen *et al.*, “CD73: an emerging checkpoint for cancer immunotherapy,” *Immunotherapy*, vol. 11, no. 11, pp. 983–997, Aug. 2019, doi: 10.2217/imt-2018-0200.
- [76]E. Scaletti *et al.*, “Substrate binding modes of purine and pyrimidine nucleotides to human ecto-5'-nucleotidase (CD73) and inhibition by their bisphosphonic acid derivatives,” *Purinergic Signal.*, vol. 17, no. 4, pp. 693–704, Dec. 2021, doi: 10.1007/s11302-021-09802-w.
- [77]B. Zhang, “CD73 promotes tumor growth and metastasis,” *Oncolimmunology*, vol. 1, no. 1, pp. 67–70, Jan. 2012, doi: 10.4161/onci.1.1.18068.
- [78]D. P. H. M. Heuts *et al.*, “Crystal Structure of a Soluble Form of Human CD73 with Ecto-5'-Nucleotidase Activity,” *ChemBioChem*, vol. 13, no. 16, pp. 2384–2391, Nov. 2012, doi: 10.1002/cbic.201200426.
- [79]K. Knapp *et al.*, “Crystal Structure of the Human Ecto-5'-Nucleotidase (CD73): Insights into the Regulation of Purinergic Signaling,” *Structure*, vol. 20, no. 12, pp. 2161–2173, Dec. 2012, doi: 10.1016/j.str.2012.10.001.
- [80]R. Huizinga *et al.*, “Endotoxin- and ATP-neutralizing activity of alkaline phosphatase as a strategy to limit neuroinflammation,” *J. Neuroinflammation*, vol. 9, no. 1, p. 266, Dec. 2012, doi: 10.1186/1742-2094-9-266.

- [81] A. V. Sauer *et al.*, “Autoimmune Dysregulation and Purine Metabolism in Adenosine Deaminase Deficiency,” *Front. Immunol.*, vol. 3, 2012, doi: 10.3389/fimmu.2012.00265.
- [82] M. Löffler *et al.*, “Physiological Roles of Vascular Nucleoside Transporters,” *Arterioscler. Thromb. Vasc. Biol.*, vol. 27, no. 5, pp. 1004–1013, May 2007, doi: 10.1161/ATVBAHA.106.126714.
- [83] M. Pastor-Anglada *et al.*, “Emerging Roles of Nucleoside Transporters,” *Front. Pharmacol.*, vol. 9, p. 606, Jun. 2018, doi: 10.3389/fphar.2018.00606.
- [84] C. Rosales, “Neutrophil: A Cell with Many Roles in Inflammation or Several Cell Types?,” *Front. Physiol.*, vol. 9, p. 113, Feb. 2018, doi: 10.3389/fphys.2018.00113.
- [85] J. M. McCracken *et al.*, “Regulation of Human Neutrophil Apoptosis and Lifespan in Health and Disease,” *J. Cell Death*, vol. 7, p. JCD.S11038, Jan. 2014, doi: 10.4137/JCD.S11038.
- [86] T. Németh *et al.*, “Neutrophils as emerging therapeutic targets,” *Nat. Rev. Drug Discov.*, vol. 19, no. 4, pp. 253–275, Apr. 2020, doi: 10.1038/s41573-019-0054-z.
- [87] J. W. Leiding, “Neutrophil Evolution and Their Diseases in Humans,” *Front. Immunol.*, vol. 8, p. 1009, Aug. 2017, doi: 10.3389/fimmu.2017.01009.
- [88] S. Cheryedath, MSc, “What is Absolute Neutrophil Count and how is measured in blood test?” <https://www.news-medical.net/health/Absolute-Neutrophil-Count-%28ANC%29.aspx> (accessed Dec. 04, 2022).
- [89] P. X. Liew *et al.*, “The Neutrophil’s Role During Health and Disease,” *Physiol. Rev.*, vol. 99, no. 2, pp. 1223–1248, Apr. 2019, doi: 10.1152/physrev.00012.2018.
- [90] S. Nourshargh *et al.*, “Leukocyte Migration into Inflamed Tissues,” *Immunity*, vol. 41, no. 5, pp. 694–707, Nov. 2014, doi: 10.1016/j.immuni.2014.10.008.
- [91] D. Proebstl *et al.*, “Pericytes support neutrophil subendothelial cell crawling and breaching of venular walls in vivo,” *J. Exp. Med.*, vol. 209, no. 6, pp. 1219–1234, Jun. 2012, doi: 10.1084/jem.20111622.
- [92] M. Metzemaekers *et al.*, “Neutrophil chemoattractant receptors in health and disease: double-edged swords,” *Cell. Mol. Immunol.*, vol. 17, no. 5, pp. 433–450, May 2020, doi: 10.1038/s41423-020-0412-0.
- [93] D. M. Underhill *et al.*, “Information processing during phagocytosis,” *Nat. Rev. Immunol.*, vol. 12, no. 7, pp. 492–502, Jul. 2012, doi: 10.1038/nri3244.
- [94] C. Rosales *et al.*, “Phagocytosis: A Fundamental Process in Immunity,” *BioMed Res. Int.*, vol. 2017, pp. 1–18, 2017, doi: 10.1155/2017/9042851.
- [95] E. Uribe-Querol *et al.*, “Phagocytosis: Our Current Understanding of a Universal Biological Process,” *Front. Immunol.*, vol. 11, p. 1066, Jun. 2020, doi: 10.3389/fimmu.2020.01066.
- [96] C. C. Winterbourn *et al.*, “Reactive Oxygen Species and Neutrophil Function,” *Annu. Rev. Biochem.*, vol. 85, no. 1, pp. 765–792, Jun. 2016, doi: 10.1146/annurev-biochem-060815-014442.
- [97] G. T. Nguyen *et al.*, “Neutrophils to the ROScue: Mechanisms of NADPH Oxidase Activation and Bacterial Resistance,” *Front. Cell. Infect. Microbiol.*, vol. 7, p. 373, Aug. 2017, doi: 10.3389/fcimb.2017.00373.
- [98] Y. Chen *et al.*, “Measurement of Oxidative Burst in Neutrophils,” in *Leucocytes*, vol. 844, R. B. Ashman, Ed. Totowa, NJ: Humana Press, 2012, pp. 115–124. doi: 10.1007/978-1-61779-527-5_8.
- [99] A. Tarafdar *et al.*, “The Role of NADPH Oxidases and Oxidative Stress in Neurodegenerative Disorders,” *Int. J. Mol. Sci.*, vol. 19, no. 12, p. 3824, Nov. 2018, doi: 10.3390/ijms19123824.
- [100] K. R. Eichelberger *et al.*, “Manipulating neutrophil degranulation as a bacterial virulence strategy,” *PLOS Pathog.*, vol. 16, no. 12, p. e1009054, Dec. 2020, doi: 10.1371/journal.ppat.1009054.
- [101] E. Mortaz *et al.*, “Update on Neutrophil Function in Severe Inflammation,” *Front. Immunol.*, vol. 9, p. 2171, Oct. 2018, doi: 10.3389/fimmu.2018.02171.
- [102] H. Takei *et al.*, “Rapid killing of human neutrophils by the potent activator phorbol 12-myristate 13-acetate (PMA) accompanied by changes different from typical apoptosis or

- necrosis," *J. Leukoc. Biol.*, vol. 59, no. 2, pp. 229–240, Feb. 1996, doi: 10.1002/jlb.59.2.229.
- [103] M. J. Kaplan *et al.*, "Neutrophil Extracellular Traps: Double-Edged Swords of Innate Immunity," *J. Immunol.*, vol. 189, no. 6, pp. 2689–2695, Sep. 2012, doi: 10.4049/jimmunol.1201719.
- [104] C. M. de Bont *et al.*, "NETosis, complement, and coagulation: a triangular relationship," *Cell. Mol. Immunol.*, vol. 16, no. 1, pp. 19–27, Jan. 2019, doi: 10.1038/s41423-018-0024-0.
- [105] Z. Cahilog *et al.*, "The Role of Neutrophil NETosis in Organ Injury: Novel Inflammatory Cell Death Mechanisms," *Inflammation*, vol. 43, no. 6, pp. 2021–2032, Dec. 2020, doi: 10.1007/s10753-020-01294-x.
- [106] N. V. Vorobjeva *et al.*, "NETosis: Molecular Mechanisms, Role in Physiology and Pathology," *Biochem. Mosc.*, vol. 85, no. 10, pp. 1178–1190, Oct. 2020, doi: 10.1134/S0006297920100065.
- [107] C. Brostjan *et al.*, "The role of neutrophil death in chronic inflammation and cancer," *Cell Death Discov.*, vol. 6, no. 1, p. 26, Dec. 2020, doi: 10.1038/s41420-020-0255-6.
- [108] Y. Chen *et al.*, "Purinergic Signaling: A Fundamental Mechanism in Neutrophil Activation," *Sci. Signal.*, vol. 3, no. 125, Jun. 2010, doi: 10.1126/scisignal.2000549.
- [109] Y. Bao *et al.*, "mTOR and differential activation of mitochondria orchestrate neutrophil chemotaxis," *J. Cell Biol.*, vol. 210, no. 7, pp. 1153–1164, Sep. 2015, doi: 10.1083/jcb.201503066.
- [110] Y. Bao *et al.*, "Mitochondria Regulate Neutrophil Activation by Generating ATP for Autocrine Purinergic Signaling," *J. Biol. Chem.*, vol. 289, no. 39, pp. 26794–26803, Sep. 2014, doi: 10.1074/jbc.M114.572495.
- [111] Y. Chen *et al.*, "ATP Release Guides Neutrophil Chemotaxis via P2Y2 and A3 Receptors," *Science*, vol. 314, no. 5806, pp. 1792–1795, Dec. 2006, doi: 10.1126/science.1132559.
- [112] C. L. Alvarez *et al.*, "Extracellular ATP and adenosine in tumor microenvironment: Roles in epithelial–mesenchymal transition, cell migration, and invasion," *J. Cell. Physiol.*, vol. 237, no. 1, pp. 389–400, Jan. 2022, doi: 10.1002/jcp.30580.
- [113] A. del R. Campos-Contreras *et al.*, "Purinergic Signaling in the Hallmarks of Cancer," *Cells*, vol. 9, no. 7, p. 1612, Jul. 2020, doi: 10.3390/cells9071612.
- [114] F. Di Virgilio *et al.*, "Extracellular ATP and P2 purinergic signalling in the tumour microenvironment," *Nat. Rev. Cancer*, vol. 18, no. 10, pp. 601–618, Oct. 2018, doi: 10.1038/s41568-018-0037-0.
- [115] G. Burnstock *et al.*, "Purinergic signalling and cancer," *Purinergic Signal.*, vol. 9, no. 4, pp. 491–540, Dec. 2013, doi: 10.1007/s11302-013-9372-5.
- [116] H. I. Kim *et al.*, "Sepsis: Early Recognition and Optimized Treatment," *Tuberc. Respir. Dis.*, vol. 82, no. 1, p. 6, 2019, doi: 10.4046/trd.2018.0041.
- [117] F. Zhang *et al.*, "Neutrophil Dysfunction in Sepsis," *Chin. Med. J. (Engl.)*, vol. 129, no. 22, pp. 2741–2744, Nov. 2016, doi: 10.4103/0366-6999.193447.
- [118] L. Heubner *et al.*, "Characteristics and outcomes of sepsis patients with and without COVID-19," *J. Infect. Public Health*, vol. 15, no. 6, pp. 670–676, 2022, doi: <https://doi.org/10.1016/j.jiph.2022.05.008>.
- [119] C. Rhee *et al.*, "Prevalence, Underlying Causes, and Preventability of Sepsis-Associated Mortality in US Acute Care Hospitals," *JAMA Netw. Open*, vol. 2, no. 2, p. e187571, Feb. 2019, doi: 10.1001/jamanetworkopen.2018.7571.
- [120] J.-L. Vincent *et al.*, "Frequency and mortality of septic shock in Europe and North America: a systematic review and meta-analysis," *Crit. Care*, vol. 23, no. 1, p. 196, Dec. 2019, doi: 10.1186/s13054-019-2478-6.
- [121] J. C. Alves-Filho *et al.*, "THE ROLE OF NEUTROPHILS IN SEVERE SEPSIS," *Shock*, vol. 30, no. 7, pp. 3–9, Oct. 2008, doi: 10.1097/SHK.0b013e3181818466.

- [122] Y. Sumi *et al.*, “Plasma ATP is Required for Neutrophil Activation in a Mouse Sepsis Model,” *Shock*, vol. 42, no. 2, pp. 142–147, Aug. 2014, doi: 10.1097/SHK.000000000000180.
- [123] X. Li *et al.*, “Systemic Adenosine Triphosphate Impairs Neutrophil Chemotaxis and Host Defense in Sepsis:,” *Crit. Care Med.*, vol. 45, no. 1, pp. e97–e104, Jan. 2017, doi: 10.1097/CCM.0000000000002052.
- [124] M. E. Starr *et al.*, “A New Cecal Slurry Preparation Protocol with Improved Long-Term Reproducibility for Animal Models of Sepsis,” *PLoS ONE*, vol. 9, no. 12, p. e115705, Dec. 2014, doi: 10.1371/journal.pone.0115705.
- [125] C. Ledderose *et al.*, “Optimized HPLC method to elucidate the complex purinergic signaling dynamics that regulate ATP, ADP, AMP, and adenosine levels in human blood,” *Purinergic Signal.*, vol. 18, no. 2, pp. 223–239, Jun. 2022, doi: 10.1007/s11302-022-09842-w.
- [126] M. De Ita *et al.*, “ATP releases ATP or other nucleotides from human peripheral blood leukocytes through purinergic P2 receptors,” *Life Sci.*, vol. 145, pp. 85–92, Jan. 2016, doi: 10.1016/j.lfs.2015.12.013.
- [127] L. Durnin *et al.*, “A commonly used ecto-ATPase inhibitor, ARL-67156, blocks degradation of ADP more than the degradation of ATP in murine colon,” *Neurogastroenterol. Motil.*, vol. 28, no. 9, pp. 1370–1381, Sep. 2016, doi: 10.1111/nmo.12836.
- [128] n.a., “N6-Ethenoadenosine.” <https://www.biosynth.com/p/NE01669/39007-51-7-n6-ethenoadenosine> (accessed May 12, 2022).
- [129] M. J. Wall *et al.*, “The novel NTPDase inhibitor sodium polyoxotungstate (POM-1) inhibits ATP breakdown but also blocks central synaptic transmission, an action independent of NTPDase inhibition,” *Neuropharmacology*, vol. 55, no. 7, pp. 1251–1258, Dec. 2008, doi: 10.1016/j.neuropharm.2008.08.005.
- [130] C. E. Müller *et al.*, “Polyoxometalates—a new class of potent ecto-nucleoside triphosphate diphosphohydrolase (NTPDase) inhibitors,” *Bioorg. Med. Chem. Lett.*, vol. 16, no. 23, pp. 5943–5947, Dec. 2006, doi: 10.1016/j.bmcl.2006.09.003.
- [131] M. Kawaguchi *et al.*, “Development of an ENPP1 Fluorescence Probe for Inhibitor Screening, Cellular Imaging, and Prognostic Assessment of Malignant Breast Cancer,” *J. Med. Chem.*, vol. 62, no. 20, pp. 9254–9269, Oct. 2019, doi: 10.1021/acs.jmedchem.9b01213.
- [132] S. Corsello *et al.*, “The usefulness of chelation therapy for the remission of symptoms caused by previous treatment with mercury-containing pharmaceuticals: a case report,” *Cases J.*, vol. 2, no. 1, p. 199, Dec. 2009, doi: 10.1186/1757-1626-2-199.
- [133] J. Hoeger *et al.*, “Persistent low serum zinc is associated with recurrent sepsis in critically ill patients - A pilot study,” *PLOS ONE*, vol. 12, no. 5, p. e0176069, May 2017, doi: 10.1371/journal.pone.0176069.
- [134] X. Shen *et al.*, “Targeting Neutrophils in Sepsis: From Mechanism to Translation,” *Front. Pharmacol.*, vol. 12, p. 644270, Apr. 2021, doi: 10.3389/fphar.2021.644270.
- [135] D. C. Angus *et al.*, “Severe Sepsis and Septic Shock,” *N. Engl. J. Med.*, vol. 369, no. 9, pp. 840–851, Aug. 2013, doi: 10.1056/NEJMra1208623.
- [136] S. B. Coade and J. D. Pearson, “Metabolism of adenine nucleotides in human blood,” p. 7.
- [137] G. G. Yegutkin, “Nucleotide- and nucleoside-converting ectoenzymes: Important modulators of purinergic signalling cascade,” *Biochim. Biophys. Acta BBA - Mol. Cell Res.*, vol. 1783, no. 5, pp. 673–694, May 2008, doi: 10.1016/j.bbamcr.2008.01.024.
- [138] S. Heptinstall *et al.*, “Adenine nucleotide metabolism in human blood - important roles for leukocytes and erythrocytes: Adenine nucleotide metabolism in human blood,” *J. Thromb. Haemost.*, vol. 3, no. 10, pp. 2331–2339, Sep. 2005, doi: 10.1111/j.1538-7836.2005.01489.x.

- [139] K. Enyoji *et al.*, "Targeted disruption of cd39/ATP diphosphohydrolase results in disordered hemostasis and thromboregulation," *Nat. Med.*, vol. 5, no. 9, pp. 1010–1017, Sep. 1999, doi: 10.1038/12447.
- [140] P. Dzeja *et al.*, "Adenylate Kinase and AMP Signaling Networks: Metabolic Monitoring, Signal Communication and Body Energy Sensing," *Int. J. Mol. Sci.*, vol. 10, no. 4, pp. 1729–1772, Apr. 2009, doi: 10.3390/ijms10041729.
- [141] S. Zervou *et al.*, "Subtle Role for Adenylate Kinase 1 in Maintaining Normal Basal Contractile Function and Metabolism in the Murine Heart," *Front. Physiol.*, vol. 12, p. 13, 2021.
- [142] A. Klepinin *et al.*, "Adenylate Kinase and Metabolic Signaling in Cancer Cells," *Front. Oncol.*, vol. 10, p. 660, May 2020, doi: 10.3389/fonc.2020.00660.
- [143] C. Ledderose *et al.*, "Optimized HPLC method to elucidate the complex purinergic signaling dynamics that regulate ATP, ADP, AMP, and adenosine levels in human blood," *Purinergic Signal.*, vol. 18, no. 2, pp. 223–239, Jun. 2022, doi: 10.1007/s11302-022-09842-w.
- [144] T. Takeda *et al.*, "Zinc deficiency causes delayed ATP clearance and adenosine generation in rats and cell culture models," *Commun. Biol.*, vol. 1, no. 1, p. 113, Dec. 2018, doi: 10.1038/s42003-018-0118-3.
- [145] Y. Chen *et al.*, "ATP Release Guides Neutrophil Chemotaxis via P2Y2 and A3 Receptors," *Science*, vol. 314, no. 5806, pp. 1792–1795, Dec. 2006, doi: 10.1126/science.1132559.

List of Figures

Figure 1: Structure of Adenosine 5'-Triphosphate	8
Figure 2: ATP release from cells appears as autocrine or paracrine messenger.....	9
Figure 3: Purinergic signaling system in immune cells	13
Figure 4: (A) 3D model of CD39 :.....	15
Figure 5: Crystal structure of ENPP1	17
Figure 6: Crystal structure of CD73	17
Figure 7: Polymorphonuclear leukocytes (PMN) and red blood cells (RBC)	19
Figure 8: Neutrophil recruitment to the infection site (extravasation)	20
Figure 9: Purinergic signaling mechanism regulate chemotaxis of neutrophils	21
Figure 10: ATP added into human whole blood is rapidly hydrolyzed but can also cause ATP release from cells	35
Figure 11: ATP added to human plasma is rapidly converted to adenosine and adenosine breakdown products	37
Figure 12: ATPase and CD73, but not ADA catalyze ϵ-ATP and ϵ-ADP to ϵ-AMP and ϵ-ADO, in whole blood	39
Figure 13: ATPase and CD73, but not ADA catalyze ϵ-ATP to ϵ-ADP, ϵ-AMP and ϵ-ADO in plasma	40
Figure 14: Cell-free plasma breaks down added ATP more than blood cells (washed) . 41	
Figure 15: Blocking CD39 with POM-1 dose-dependently reduces ATP breakdown in human plasma	42
Figure 16: Soluble CD39 in plasma contributes more to ATP breakdown in human blood than cell- bound CD39	44
Figure 17: Blocking ENPP1 with ENPP1 inhibitor C dose-dependently reduces ATP breakdown in human plasma	46
Figure 18: Only soluble ENPP1 in plasma breaks down ATP in human blood. (A) Human whole Blood :.....	47
Figure 19: The CD73 inhibitor PSB12379 dose-dependently reduces AMP breakdown in human plasma	49
Figure 20: Effect of CD73 inhibition on ATP hydrolysis in human blood. (A) Human whole blood :.....	50
Figure 21: Coenzymes play a major role in supporting ATP breakdown by soluble enzymes in human plasma	53
Figure 22: Physiological Ca^{2+} did not induce replenishment of ATP breakdown in human whole blood and plasma, but so did human blood cells (washed)	55
Figure 23: Ca^{2+} dose-dependently does not restore ATP breakdown in EDTA treated plasma	56
Figure 24: Zinc can partially restore ATP breakdown in EDTA-treated human plasma . 58	
Figure 25: Substitution of Zinc barely restores ATP breakdown in EDTA-treated blood cells	59

Figure 26: **ATP breakdown by blood cells, but not by plasma, is more rapid in mice than in humans.**..... 61

Figure 27: **CD39, ENPP1, and CD73 all participate in ATP conversion in mouse plasma.** 63

Figure 28: **Sepsis impairs ATP breakdown in human plasma.**..... 65

Figure 29: **ATP breakdown in some patients could be partially restored by Zn²⁺ substitution.** 67

Figure 30: **Sepsis impairs ATPase activity in mice plasma.**..... 69

Figure 31: **75% of sepsis mice displayed a positive effect on Zn²⁺.** 70

Figure 32: **CD39 inhibition and extracellular ATP induce more PMN activation.** 72

Figure 33: **Proposed model of ATP release, ATP hydrolysis into its metabolites and cell metabolism in blood cells and plasma.** 77

List of Tables

Table 1: Overview purinergic receptor subtypes.....	11
Table 2: Sepsis severity score of mice.	29
Table 3: Sepsis patients participated in the ATP breakdown study.....	64
Table 4: CD11b+ to study neutrophil function in human whole blood.....	97
Table 5: CD62L- (shedding) to study neutrophil function in human whole blood	97
Table 6: CD66+ to study neutrophil function in human whole blood.....	98

List of Abbreviations

aa	Amino acid
AC	Adenylyl cyclase
Acetyl CoA	Acetyl coenzyme A
ADA	Adenosine deaminase
ADO	Adenosine
ADP	Adenosine 5'-diphosphate
AK	Adenylate kinase
AMP	Adenosine 5'-monophosphate
AMPCP	α , β -Methyleneadenosine 5'-diphosphate monosodium salt
ANOVA	Analysis of Variance
AP	Alkaline phosphatase
ATP	Adenosine 5'-triphosphate
ATX	Autaxin
BIDMC	Beth Israel Deaconess Medical Center
BSA	Bovine serum albumin
cAMP	Cyclic adenosine 5'-monophosphate
CALHM-1	Calcium homeostasis modulator- 1
CD	Cluster of differentiation
CLP	Cecal ligation puncture
CNS	Central nervous system
CNT	Concentrative nucleoside transporter
COVID-19	Coronavirus Disease 19
CS	Cecal Slurry
CTS	Cytosine triphosphate
C _x	Connexin
DAMP	Damage-associated molecular pattern
EAE	Encephalomyelitis
ϵ -ADO	Etheno- adenosine
ϵ -ADP	Etheno- adenosine 5'-diphosphate
ϵ -AMP	Etheno- adenosine 5'-monophosphate
ϵ -ATP	Etheno- adenosine 5'-triphosphate
EDTA	Ethylene diamine tetra acetic acid
EGTA	Ethylene glycol tetra acetic acid
EMT	Epithelial-to-mesenchymal transition
ENPP	Ectonucleotide pyrophosphatase/phosphodiesterase
ENT	Equilibrative nucleoside transporters
ENTPD	Ectonucleoside triphosphate diphosphohydrolase
ER	Endoplasmic reticulum
ERK	Extracellular signal-regulated kinase
fMLP	N-formyl-L-methionyl -L-leucyl-phenylalanine
FPR	Formyl peptide receptor
FSC	Forward- scattered light
G-CSF	Granulocyte colony stimulatory factor
GMP	Granulocyte-monocyte progenitor
GPCR	G protein- coupled receptors
GPI	Glycosylphosphatidylinositol (GPI)

GTP	Guanosine triphosphate
HBSS	Hank's Balanced Salt Solution
HPLC	High Performance Liquid Chromatography
HSC	Hematopoietic stem cells
IACUC	Institutional Animal Care & Use Committee
ICAM-1/2	Intracellular Adhesion Molecule-1/2
ICU	Intensive care unit
IL-8	Interleukin-8
IS	Immune system
K_m	Michaelis constant
LBT ₄	Leukotriene B ₄
LFA-1	Lymphocyte function-associated antigen-1
LMPP	Lymphoid-primed multipotent progenitors
LN	Liquid nitrogen
L1	Linker region 1
MAC	Maxi-anion channel
MAC1	Macrophage-1 antigen
MAPK	Mitogen-activated protein kinase
M-CASS	Mouse clinical assessment score
MCL	Macrophage C-type lectin
MPP	Multipotent progenitor cells
MPO	Myeloperoxidase
mTOR	Mammalian target of rapamycin
NAD ⁺	Nicotinamide adenine dinucleotide
NANC	Non-adrenergic, non-cholinergic
ND	Not detected
NET	Neutrophil extracellular traps
NIH	National Institutes of Health
NK	Natural Killer cells
NK	Not Known
NOX2	NADPH oxidase 2
NT	Nucleoside transporter
NT5E	Ecto- 5'- nucleotidase
NUC	Nuclease- like domain
OH•	Hydroxyl radicals
PAMP	Pathogen-associated molecular pattern
PANX	Pannexin
PBS	Phosphate buffered saline
PCA	Perchloric acid
PC-1	Cell-differentiation antigen
PDE	Phosphodiesterase
PECAM	Platelet endothelial cell adhesion molecule
p_i	Inorganic phosphate
PLC	Choline-specific phospholipase C
PMN	Polymorphonuclear neutrophils
POM-1	Sodium polyoxotungstate
PRR	Pattern recognition receptor
PTFE	Polytetrafluoroethylene

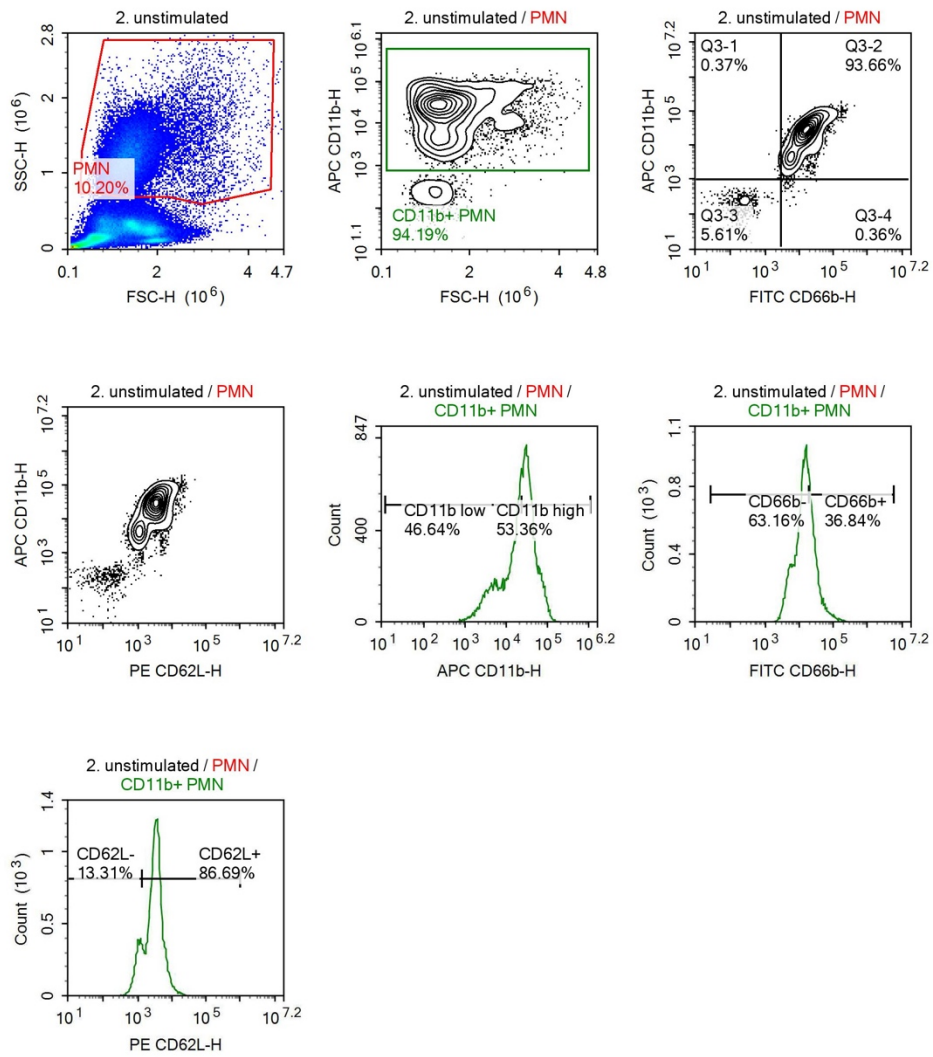
pts	Patients
RBC	Red blood cells
ROS	Reactive Oxygen Species
SD	Standard Deviation
SEM	Standard error of mean
SMB	Somatomedin B-like domain
SPE	Solid-phase extraction
SSC	Side-scattered light
TBA	Tetrabutylammonium
TCA	Tricarboxylic acid
TM	Transmembrane
TME	Tumor microenvironment
TNAP	Tissue nonspecific alkaline phosphatase
TNF- α	Tumor necrosis factor - alpha
UAS	University of Applied Science
UDP	Uridine diphosphate
UMP	Uridine monophosphate
U.S.	United States
UTI	Urinary tract infection
UTP	Uridine triphosphate
VNUT	Vesicular nucleotide transporter
VRAC	Volume-regulated anion channel
WB	Whole Blood
wt	Wildtype
^3H	Tritium

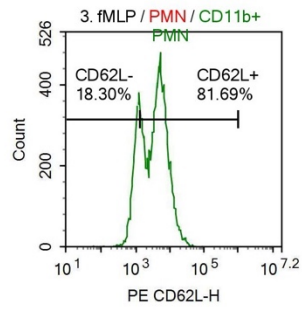
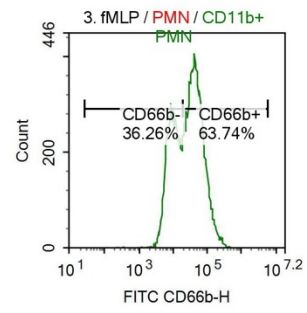
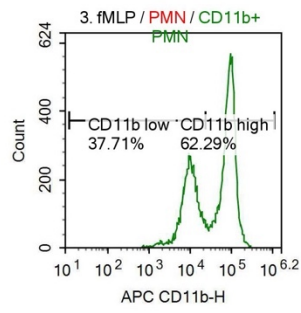
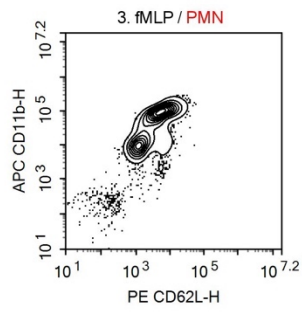
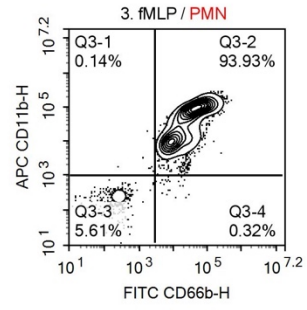
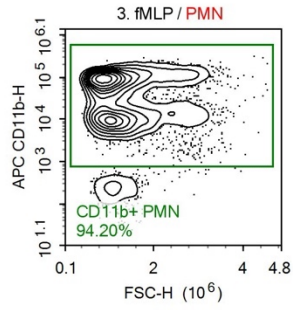
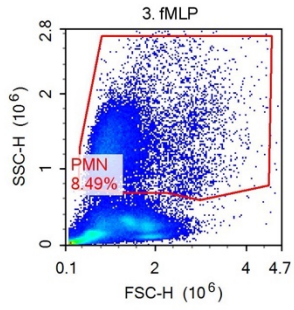
Data File C:\CHEM32\1\DATA\DIAGNOSE\DGNOISE 2022-02-15 15-34-21\DGNOISE000006.D
Sample Name: 3. POM1 0, h

=====

*** End of Report ***

B: Flow cytometry (unstimulated vs fMLP)





C: Flow cytometry (raw data)

Table 4: CD11b+ to study neutrophil function in human whole blood

Sample	PMN Median APC CD11b-H	CD11b+ PMN Median APC CD11b-H	CD11b high % Parent
1. unstained	207	855	0.01%
2. unstimulated	23638	24962	53.36%
3. fMLP	54027	61404	62.29%
4. fMLP+ATP	64546	68853	70.48%
5. fMLP+POM-1	79931	83569	75.62%
6. fMLP+POM-1,ATP	85564	87907	80.26%
7. fMLP+NPP1 inhC	51522	56447	63.24%
8. fMLP+NPP1 inh C,ATP	58561	61703	66.57%
9. fMLP+TNAP inh	75116	78024	70.75%
10. fMLP+TNAP inh,ATP	76373	79604	70.31%
11. fMLP+PSB12379	70748	76011	75.37%
12. fMLP+PSB12379,ATP	64562	69983	67.34%
13. fMLP+pentostatin	71111	76882	68.76%
14. fMLP+pentostatin,ATP	49301	58535	61.28%

Table 5: CD62L- (shedding) to study neutrophil function in human whole blood

Sample	PMN Median PE CD62L-H	CD11b+ PMN Median PE CD62L-H	CD62L- % Parent	CD62L+ % Parent
1. unstained	282	3505	88.79%	3.74%
2. unstimulated	3234	3356	13.31%	86.69%
3. fMLP	3577	3897	18.30%	81.69%
4. fMLP+ATP	3581	3833	14.74%	85.26%
5. fMLP+POM-1	4302	4515	12.06%	87.94%
6. fMLP+POM-1,ATP	4500	4662	9.59%	90.40%
7. fMLP+NPP1 inhC	3307	3539	16.02%	83.98%
8. fMLP+NPP1 inh C,ATP	3469	3642	16.17%	83.82%
9. fMLP+TNAP inh	4325	4510	9.90%	90.10%
10. fMLP+TNAP inh,ATP	4440	4672	10.09%	89.91%
11. fMLP+PSB12379	4279	4662	7.65%	92.33%
12. fMLP+PSB12379,ATP	3944	4231	11.00%	89.00%
13. fMLP+pentostatin	4292	4678	9.57%	90.43%

14. fMLP+pentostatin,ATP	3301	3651	15.17%	84.83%
-----------------------------	------	------	--------	--------

Table 6: CD66+ to study neutrophil function in human whole blood.

Sample	PMN Median FITC CD66b-H	CD11b+ PMN Median FITC CD66b-H	CD66b+ % Parent
1. unstained	1242	10979	0.03%
2. unstimulated	15298	15984	36.84%
3. fMLP	28025	30764	63.74%
4. fMLP+ATP	29244	31212	67.92%
5. fMLP+POM-1	35173	37064	76.09%
6. fMLP+POM-1,ATP	37433	38839	78.37%
7. fMLP+NPP1 inhC	26492	28234	64.93%
8. fMLP+NPP1 inh C,ATP	28342	29867	66.50%
9. fMLP+TNAP inh	35682	37199	74.29%
10. fMLP+TNAP inh,ATP	36869	39060	74.38%
11. fMLP+PSB12379	35306	38303	78.49%
12. fMLP+PSB12379,ATP	32421	34714	71.72%
13. fMLP+pentostatin	35984	39058	74.65%
14. fMLP+pentostatin,ATP	27165	29834	64.37%